AN EXPERIMENTAL STUDY OF IMPROVING THE PERFORMANCE OF PHOTOVOLTAIC SOLAR MODULE USING UPPER AND LOWER WATER COOLING: A CASE STUDY OF IRAQ

2022
MASTER THESIS
MECHANICAL ENGINEERING

AHMED KADHIM MOHAMMED AL-MAMOORI

Thesis Advisor

Asst.Prof.Dr. Mehmet BAKIRCI

AN EXPERIMENTAL STUDY OF IMPROVING THE PERFORMANCE OF PHOTOVOLTAIC SOLAR MODULE USING UPPER AND LOWER WATER COOLING: A CASE STUDY OF IRAQ

Ahmed Kadhim Mohammed AL-MAMOORI

T.C.
Karabük University
Institute of Graduate Programs
Department of Mechanical Engineering
Prepared as
Master Thesis

Asst.Prof.Dr. Mehmet BAKIRCI

KARABÜK
May 2022

I certify that in my opinion the thesis submitted by Ahmed Kadhim Mohammed AL-MAMOORI titled "AN EXPERIMENTAL STUDY OF IMPROVING THE PERFORMANCE OF PHOTOVOLTAIC SOLAR MODULE USING UPPER AND LOWER WATER COOLING: A CASE STUDY OF IRAQ" is fully adequate in scope and quality as a thesis for the degree of Master of Science.

Asst.Prof.Dr. Mehmet BAKIRCI ....
Thesis Advisor, Department of Mechanical Engineering

This thesis is accepted by the examining committee with a unanimous vote in the Department of Mechanical Engineering as a Master of Science thesis. 30 05, 2022

Examining Committee Members (Institutions)   Signature

Chairman   : Prof. Dr. Emrah Deniz   ....

Member   : Prof. Dr. Ahmed Kabul   ....

Member   : Asst.Prof.Dr. Mehmet BAKIRCI   ....

The degree of Master of Science by the thesis submitted is approved by the Administrative Board of the Institute of Graduate Programs, Karabük University.

Prof. Dr. Hasan SOLMAZ.................   ....
Director of the Institute of Graduate Programs

ii

Ahmed Kadhim Mohammed AL-MAMOORI

ABSTRACT

M. Sc. Thesis

AN EXPERIMENTAL STUDY OF IMPROVING THE PERFORMANCE OF PHOTOVOLTAIC SOLAR MODULE USING UPPER AND LOWER WATER COOLING: A CASE STUDY OF IRAQ

Ahmed Kadhim Mohammed AL-MAMOORI

Karabük University
Institute of Graduate Programs
The Department of Mechanical Engineering

Thesis Advisor:
Asst. Prof. Dr. Mehmet BAKIRCI
May 2022, 138 pages

Photovoltaic modules, which are based on the principle of converting falling sunlight into electrical or thermal energy, are regarded as one of the most important sources of renewable energy. The significant heat storage inside the PV panel as a result of the amount of absorbed radiation is still an impediment to obtaining the needed efficiency. The current study aims to increase efficiency and performance by developing a hybrid passive (PV/T) system, where the investigation was carried out in August 2021 in the outdoor. There were three monocrystalline photovoltaic panels with an output power of 100 W each. The first panel was treated with the upper water nozzle cooling technique, the second panel was fitted with lower cooling nozzles, and the last panel was left without cooling to serve as a reference for performance comparison. Both the two nozzle cooling techniques have demonstrated their efficacy in dispersing surface heat to half the temperature of the uncooled panel at the suggested maximum flow rate.

Infrared thermal imaging also demonstrated the efficacy of heat dissipation cooling, making this method equivalent to that of (CFD) simulation. Although its reference output power was 50.93 W before cooling, heat dissipation improved the electrical characteristics, including the output power, by 80.08% and 75.26% for upper and lower cooling, respectively. Improved performance was achieved by increasing output power. When spraying upper and lower water, the panel's efficiency improved by 14.31% and 13.57%, respectively, compared to the uncooled panel's efficiency of 9.7%. It should be noted that the upper nozzle cooling was more efficient than the lower nozzle cooling, with a rate of performance improvement of 7.6% at maximum flow. According to the statistics of our present investigation, the upper and lower cooling techniques were effective in enhancing the electrical and thermal characteristics of the photovoltaic panels to suit the harsh Iraqi summer and extend the life of the panels.

Science Code : 91408

ÖZET

Yüksek Lisans Tezi

ÜST VE ALT SU SOĞUTMA KULLANILARAK FOTOVOLTAIK GÜNEŞ MODÜLÜNÜN PERFORMANSININ İYİLEŞTİRİLMESİNE YÖNELİK DENEYSEL BİR ÇALIŞMA: IRAK ÖRNEĞİ

Ahmed Kadhim Mohammed AL-MAMOORI

Karabük Üniversitesi
Lisansüstü Eğitim Enstitüsü
Makina Mühendisliği Anabilim Dalı

Tez Danışmanı:
Dr. Öğr.Üyesi.Mehmet BAKIRCI
Mayis 2022, 138 sayfa

Düşen güneş ışığını elektrik veya termal enerjiye dönüştürme prensibine dayanan fotovoltaik modüller, yenilenebilir enerjinin en önemli kaynaklarından biri olarak kabul edilmektedir. Soğurulan radyasyon miktarının bir sonucu olarak PV panel içinde önemli ölçüde ısı depolaması, gerekli verimliliğin elde edilmesi için hala bir engeldir. Mevcut çalışma, araştırmanın Ağustos 2021'de açık havada gerçekleştirildiği bir hibrit pasif (PV/T) sistemi geliştirerek verimliliği ve performansı artırmayı hedefliyor. Her birinin çıkış gücü 100 W olan üç adet monokristal fotovoltaik panel vardı. Birinci panele üst su nozulu soğutma tekniği uygulanmış, ikinci panele alt soğutma nozülleri takılmış ve son panel, performans karşılaştırması için referans olması için soğutmadan bırakılmıştır. Her iki nozul soğutma tekniği de önerilen maksimum akış hızında soğutulmamış panelin sıcaklığının yarısına kadar yüzey ısısını dağıtmadaki etkinliklerini göstermiştir. Kızılötesi termal görüntüleme de ısı yayılımlı soğutmanın

etkinliğini göstererek bu yöntemi (CFD) simülasyonuna eşdeğer hale getirdi. Soğutmadan önce referans çıkış gücü 50,93 W olmasına rağmen, ısı dağılımı, çıkış gücü de dahil olmak üzere elektriksel özellikleri, üst ve alt soğutma için sırasıyla %80.08 ve %75.26 iyileştirdi. Çıkış gücü artırılarak iyileştirilmiş performans elde edildi. Üst ve alt su püskürtülürken, panelin verimliliği, soğutmasız panelin verimliliğine %9.7 kıyasla sırasıyla %14.31 ve 13.57 arttı. Üst nozul soğutmasının, maksimum akışta %7, 6 performans iyileştirme oranı ile alt nozul soğutmasından daha verimli olduğu belirtilmelidir. Mevcut araştırmamızın istatistiklerine göre, üst ve alt soğutma teknikleri, fotovoltaik panellerin elektriksel ve termal özelliklerini, sert Irak yazına uyacak ve panellerin ömrünü uzatacak şekilde geliştirmede etkiliydi.

ACKNOWLEDGMENT

In the name of Allah, the Merciful

Praise be to Allah, Lord of the Worlds, for his bounty and generosity, providing me with the strength and determination to finish this work. I also want to express my sincere gratitude to my direct supervisor "Asst. Prof. Dr. Mehmet Bakirci" for the support he provided me through his continuous guidance, useful advice, patience, and support throughout the writing of this thesis.

Thanks also to "Asst. Prof. Dr. Abdulrahman Th. Mohammad AL-Zuhayri," the instructor at the Technical Institute-Baquba, for his guidance and moral and scientific support throughout the duration of the experiment.

I'm also grateful for my mother's prayers for me and my family, especially my beloved wife and sons, as well as my brothers and friends, who have helped me overcome all of the obstacles I've faced. I also dedicate this effort to future scholars in order for them to profit from and improve the content as much as feasible.

CONTENTS

LIST OF FIGURES

LIST OF TABLES

SYMBOLS AND ABBREVIATIONS

SYMBOLS

%	: Percent Sign.
A_s	: Surface area of panel (m^2)
A_C	: Area of cell (m^2)
AM	: Air mass (kg)
R	: Solar radiation intensity (w/m^2)
T_{pv}	: Photovoltaic panel temperature (°C)
T_{amb}	: ambient temperature (°C)
T_{rise}	: The ambient temperature at sunrise (°C)
T_{ref}	: Temperature of reference panel (ºC)
T-Front	: Temperature of front surface (°C)
T-Rear	: Temperature of rear surface (ºC)
V_{pv}	: Photovoltaic panel voltage (V)
I_{pv}	: Photovoltaic panel current (A)
P_{pv}	: Photovoltaic panel power (W)
V_{mp}	: Photoelectric voltage at maximum power point (V)
I_{mp}	: Photoelectric current at maximum power point (A)
P_{max}	: Photoelectric power at maximum power point (W)
P_{wc}	: Panel Power with cooling technique (W)
P_{woc}	: Panel Power without cooling technique (W)
Isc	: Short circuit current (A)
Voc	: Open circuit voltage (V)
η_{el}	: Electrical efficiency (%)
η_{wc}	: Panel efficiency with cooling technique
$\eta_{woc:}$	: Panel efficiency without cooling technique
$\acute{\eta}$	: Improvement in electrical efficiency
$\acute{P}$	: Enhancement in maximal power output (W)
el	: Electrical

c   : Cell

amb   : Ambient

wc   : With cooling technique

woc   : Without cooling technique

mp   : Maximum power

^{o}C : Celsius degree

^{o}K : Kelvin

W   : Watt

L/m   : Litter per minute

hr   : Hour

ϵ : Emissivity

ABBREVIATIONS

PV   : Photovoltaic

PV/T   : Photovoltaic / Thermal

STC   : Standard Test Conditions

EVA   : Ethyl Vinyl Acetate

NOCT   : Nominal Operating Cell Temperature

DC   : Direct Current

AC   : Alternating Current

CFD   : Computational Fluid Dynamics

PCM   : Phase Change Material

IR   : Infrared Camera

AL_2O_3 : Alumina Oxide

USB   : Universal Serial Port

PC   : Personal Computer

ANSYS   : Analysis System

PVC   : Polyvinyl chloride (Plastic)

IS-100P   : I-Star Company for PV Module (100) Watt

PART 1

INTRODUCTION

1.1. OVERVIEW

The Earth's surface has huge energy sources that are well-known to everyone. Because it has the potential to accomplish most actions, all people have benefited from this energy for many years. This energy is turned into numerous forms, including mechanical, electrical, thermal, chemical, kinetic, and other so-called equipped energy.

Energy consumption has become one of the aspects of life and its most important component, and all efforts have been made to achieve this goal. The most widespread primary source of conventional energy is fossil fuels. Due to the huge amounts of carbon that it releases and the generation of global warming, it is expected that its amount will decrease and the risks will increase when burning in the future. The entire world is facing great difficulties and enormous fears due to the increase in demand for energy and its consumption as a result of population increase and industrial development, which has led to the deterioration of the global economy and an increase in expenditures [1].

To improve the economic reality and provide energy free from health and physical harm while maintaining a risk-free environment, all countries have to face this massive economic and environmental disaster and search for alternatives, including solar energy, wind energy, hydropower, and other forms of safe, sustainable and friendly energy for the environment [2].

Solar energy is the most popular energy source due to its ease of investment as thermal energy through specialized collectors or as electrical energy through photovoltaic

cells, of which solar radiation is the primary source and plays an important role in the abundance of cell energy. The amount of incident solar radiation determines the efficiency of solar cells. Figure 1.1 illustrates that nations on the Asian continent receive the largest percentage of solar radiation compared to other countries [3]. Iraq was selected as a unique case study. It has a hot and dry climate in summer, and is characterized by abundant solar energy and a high percentage of radiation, and the daily radiation energy ranges between (2000-2500kWh/m^2) from the global average of solar radiation, as shown in Figure 1.2 direct normal irradiance, and global horizontal irradiance [4,5].
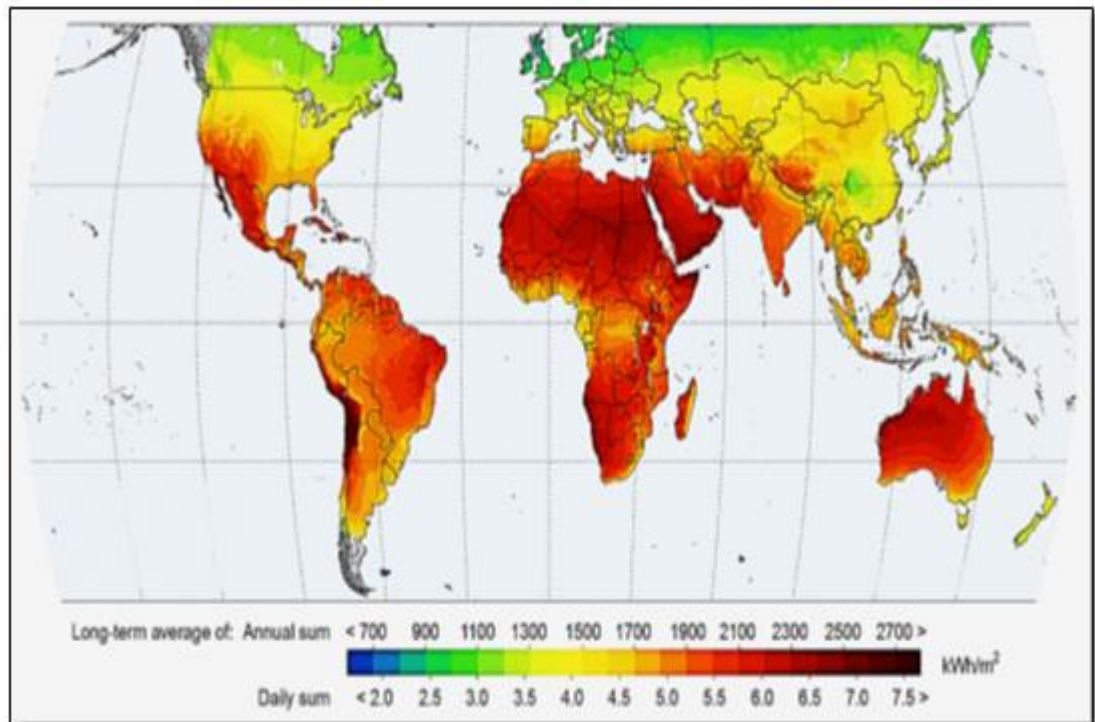
Figure 1.1. Maps of global horizontal irradiation [4].
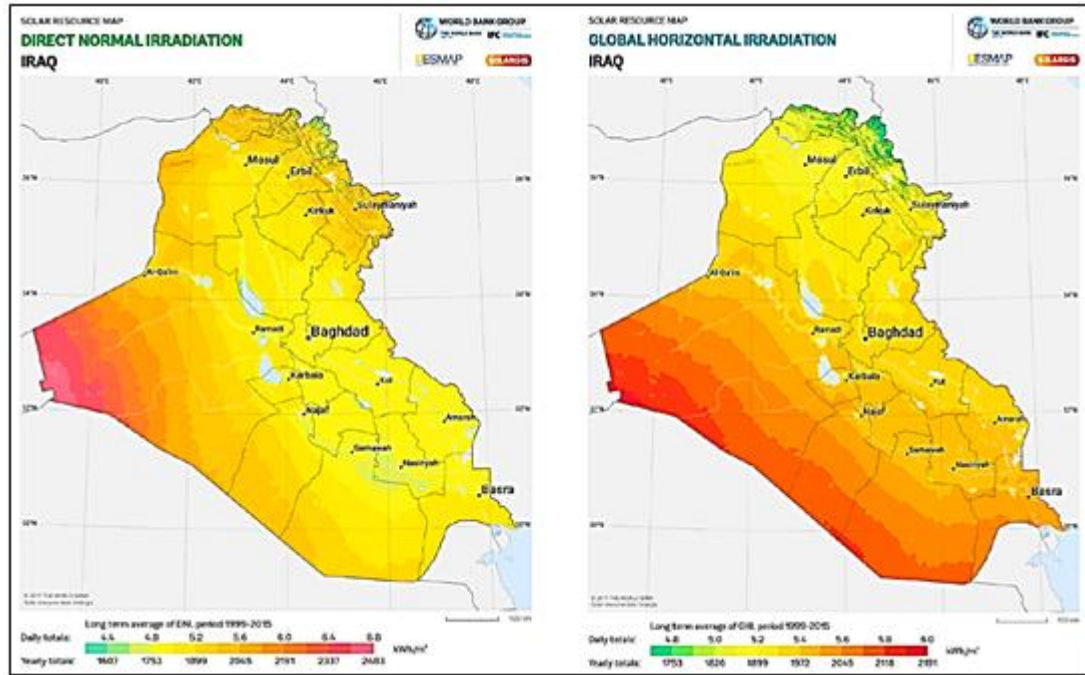
Figure 1.2. Percentage of solar, direct and global radiation (Case of Iraq) [5].

1.2. PHOTOVOLTAIC (PV) SOLAR CELL

The science of photovoltaic cells piqued the interest of the French, as "Charles Fritts" offered the first cell design in 1883, with an efficiency with 1-2 %, based on the scientist Edmund's discovery of cells in 1839.

A photovoltaic cell is a solid electrical device that may come in many different forms and sizes. Monocrystalline cells are one of the most popular semiconductor-based cells, with silicon as the basis material. Voltage and electric current are generated through the photoelectric effect, which is defined as a physical and chemical phenomenon [6].

Aluminum, glass, polymer and ethylene vinyl acetate (EVA), EVA are the basic materials for the installation of the PV module as showed in Figure 1.3, and the outer frame and metal grid protect the sensitive parts and the wiring chamber from external strikes, moisture and corrosive agents because they are very thin. Photovoltaic cells make up the solar module, as shown in Figure 1.4. Some tests need to assemble a set of modules to create an array, referred to as a "solar farm" when many arrays are

combined. Different types of solar cells are connected in parallel, or in series, or two links together, in a series connection, the voltage will increase, as the current will be constant, and vice versa is achieved in parallel, so that we can know the current and voltage rate of the matrix, as well as its electrical efficiency [7].
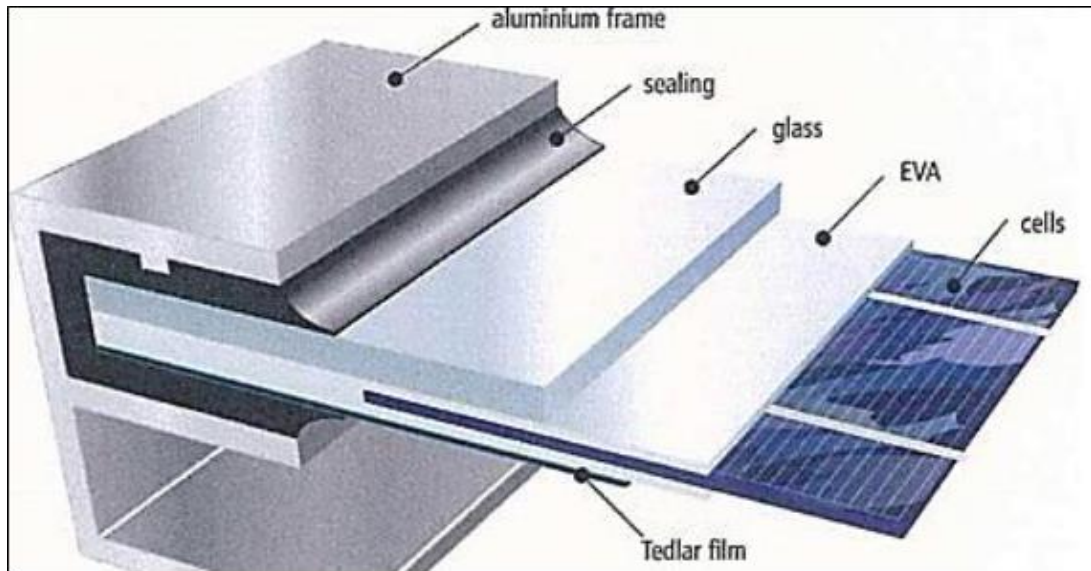
Figure 1.3. PV module layers [7].
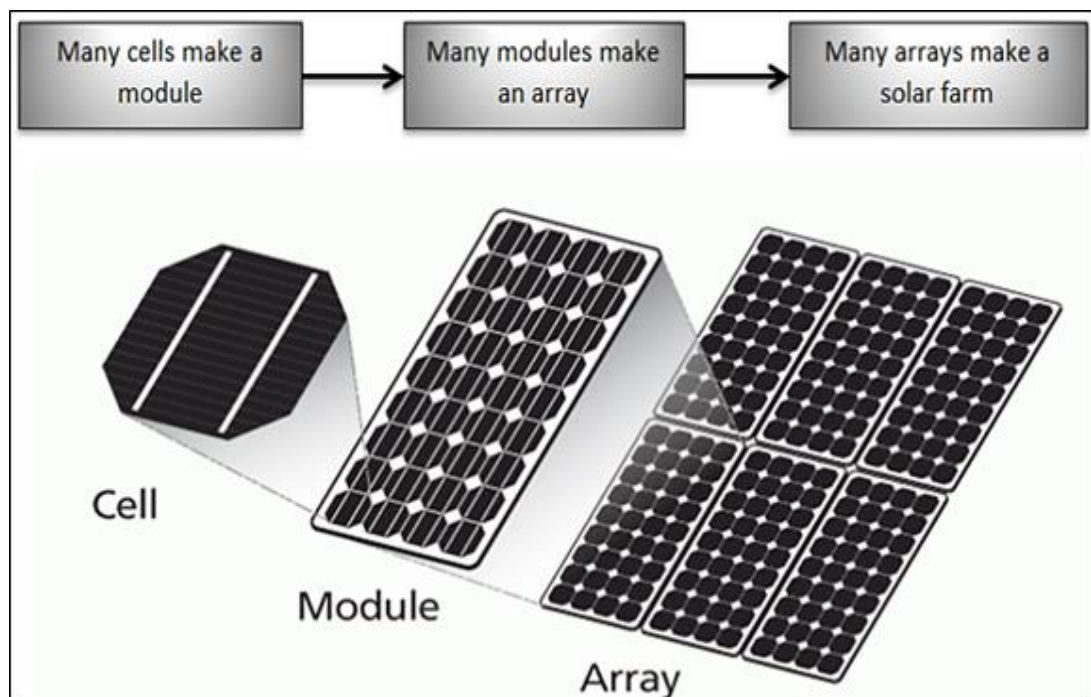
Figure 1.4. Typical view of a photovoltaic system [7].

4

1.3. PHOTOVOLTAIC SOLAR CELL OPERATION PRINCIPLE

The basic idea of a photovoltaic cell is to transform part of the incident light into electricity. The two layers (p-n) intersect to promote the transmission and absorption of electrons for photons from the greatest concentration level (N-Type semiconductor), which is very thin to the lowest concentration level (p-Type semiconductor), thereby boosting the electron's energy. Because the photon's energy is insufficient in comparison to the band gap, it cannot leap across the conduction band. As a result, the electron is unable to pass through. In the meantime, energy is turned into kinetic energy, therefor; the cell is heat up. Figures 1.5 and 1.6 depict the working principle as well as the structure, it should be noted that if the photon's energy surpasses the band gap, the electron could freely flow within the conduction limitations, resulting in generated a DC current [8].
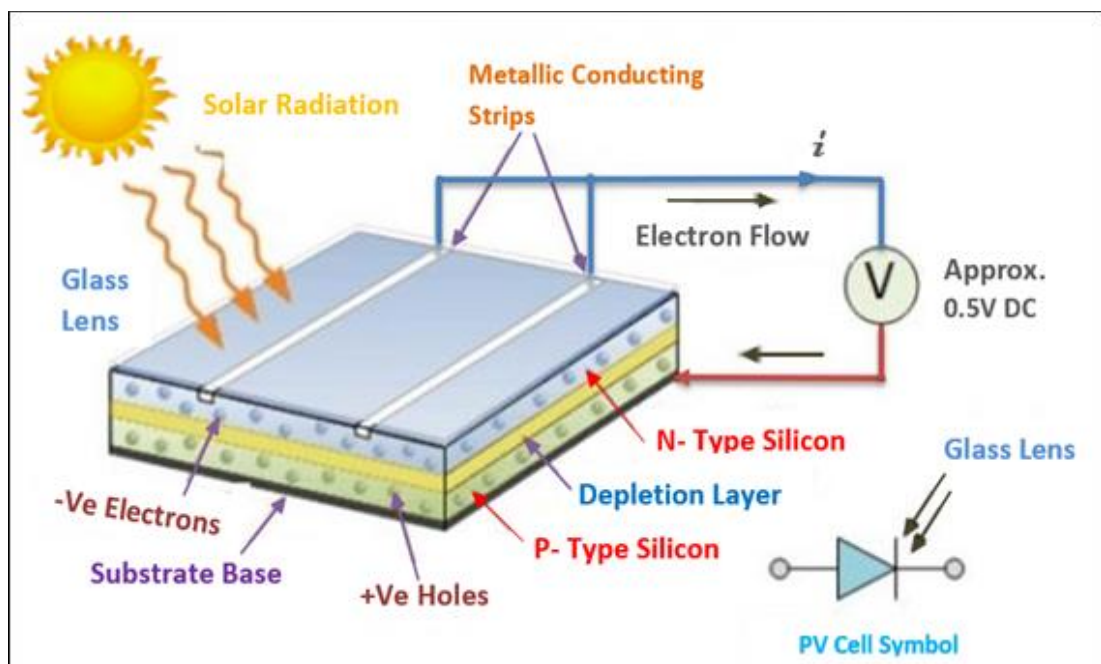
Figure 1.5. Practical concept of photovoltaic cells [8].
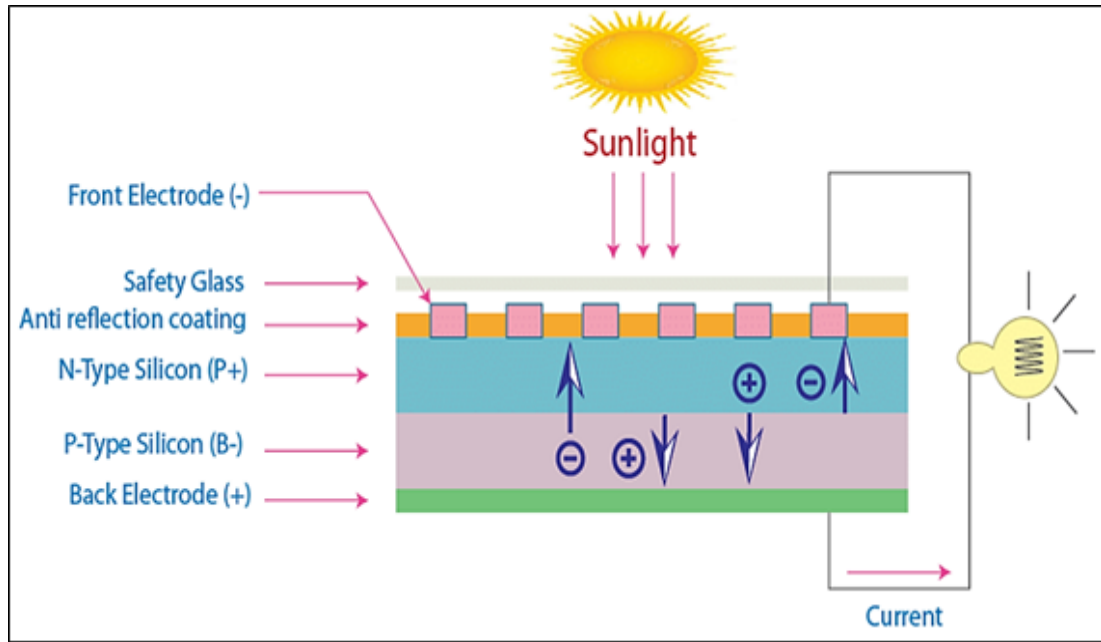
Figure 1.6. Photovoltaic cell structure [8].

1.4. TEMPERATURE'S IMPACT ON PHOTOVOLTAIC CELLS

The operation of a photovoltaic system is based on the conversion of solar radiation (or sunlight in general) into electric current and voltage using semiconductor cells. Only about 15% of the radiation is utilized, with the remainder being dispersed as heat to cell surfaces [9].

The temperature factor of a photovoltaic solar panel has a considerable influence on its efficiency, and we find that it dominates the atoms of the material at the moment the radiation falls, causing them to vibrate and thus reduce conductivity. The effect of heat on cell capacity can be represented in numbers. The maximum power decreases 19.5-20% when the temperature increases to between 20 and 50 ⁰C. Meanwhile, the open circuit voltage (Voc) decreases linearly by (-0.5%/⁰C). This behavior can be seen in Figure 1.7, which also shows that at higher temperatures, the ratio of (Isc) increases by (+0.05%/⁰C) [10].

In the same context, Kncay (2012), explained in his experimental investigation that increasing temperatures, along with changing levels of wind gusts, made convection ineffective comparable to the air temperature, as shown in Figure 1.8, the voltage

decline on the panel with the current according to the degrees of the indicator. The panel recorded the highest voltage at (T4) with constant radiation at 80 W/m², as well as the amount of energy generated at (T1). Recent studies indicate an inverse proportion when the temperature increases by 1°C and the level of performance decreases by 0.5 to 0.8%, so we conclude that this parameter is inversely proportional to temperature [11].
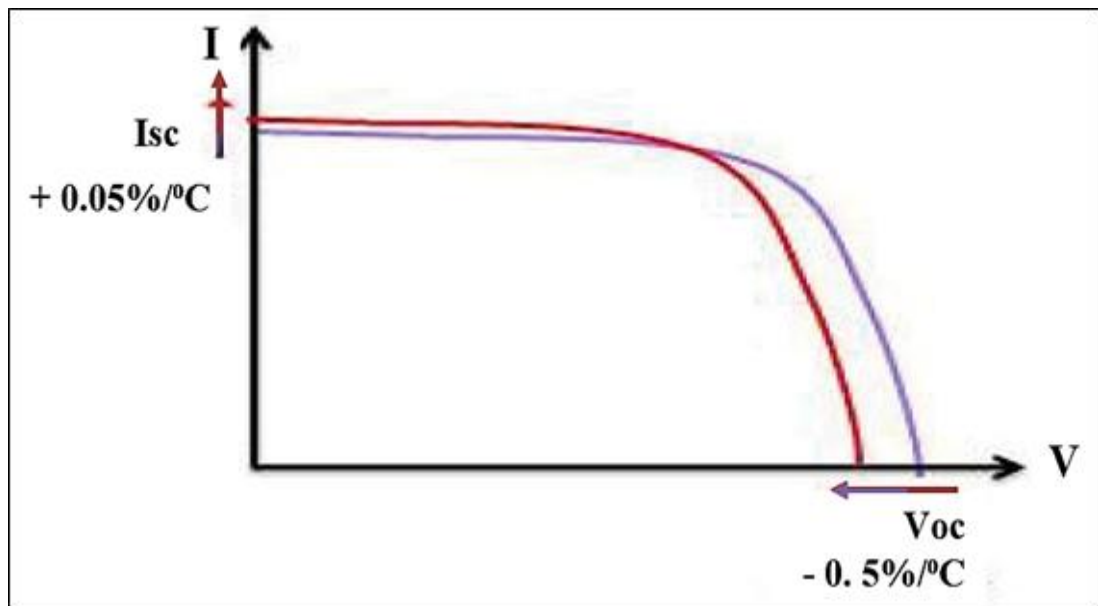
Figure 1.7. Effect temperature on (Isc) and (Voc) characteristics [10].
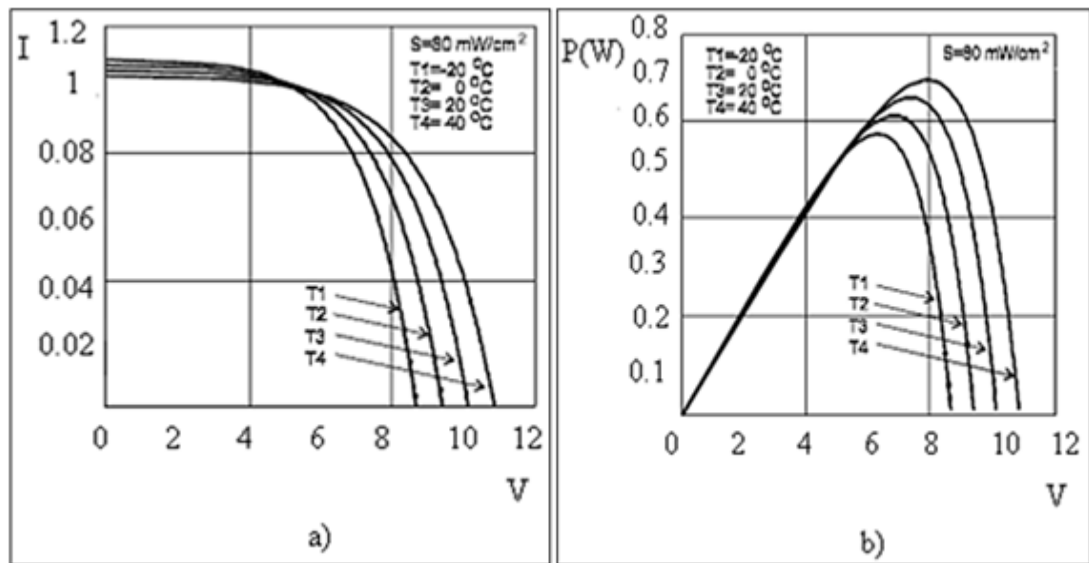
Figure 1.8. Impact of heat coefficient on the characteristics of the PV module [11].

As for high temperatures swept the series and shunt resistances, as most research has demonstrated that heating the solar panel's surfaces raises the high resistance of the series while lowering the convert resistance, as indicated in Figure 1.9. Intuitively, higher electrical PV module surface temperatures lead to a decrease in panel voltage, causing lower power output and eventually decreased solar module performance. Depending on the temperature coefficient of the cell component, extensive investigations indicated an efficiency decrease of 0.1 to 0.5% per 1 °C [12].
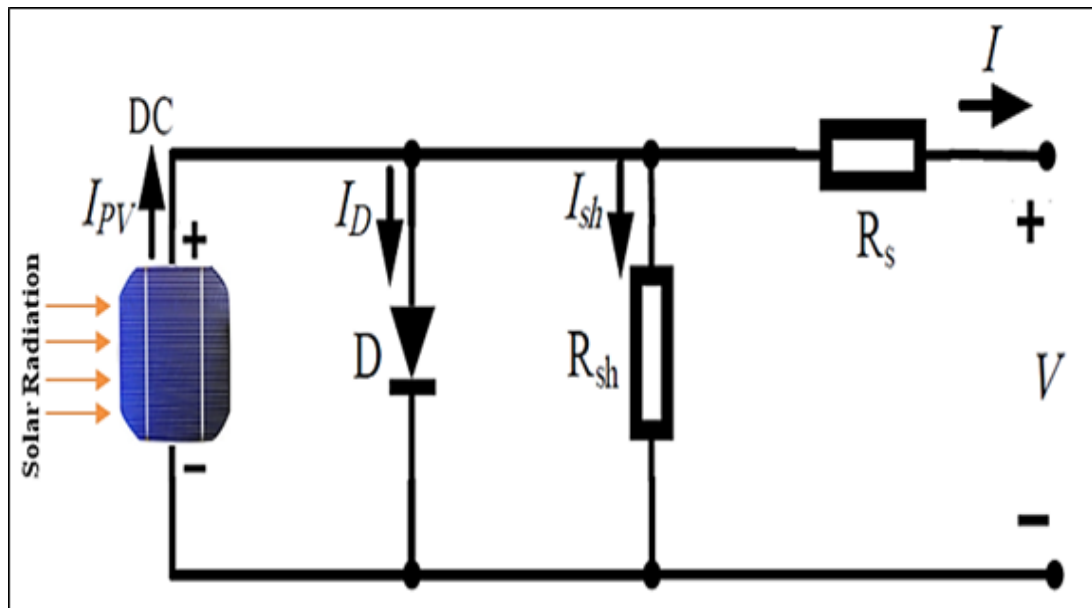
Figure 1.9. PV module of equivalent circuit [12].

Figure 1.10 describes how transparent tempered glass dominates the panel design and has a high absorbent quality based on the amount of emissivity dissipated by absorbing direct sunlight and heat, whereas reflection determines the amount of heat transmitted to the front and rear surfaces of the photovoltaic cell, as well as its sides. It is worth noting that a panel's electrical efficiency is inversely related to its temperature while it is working; therefor, the temperature of the panel becomes higher than the ambient temperature. Despite the accumulation of dust and dirt on the front surface, the researchers confirmed that heat is concentrated on the rear surface of the panel more than it is on the front surface, increasing the opacity of the surface and reducing the amount of radiation [13].

Regrettably, the surface heat of the panels, particularly the rear surface, may reach more than 70 ºC, particularly in July and August, while using photovoltaic cells and the closest illustration of this is Iraq's atmosphere. PV/T technique must be used to disperse cell heat and enhance efficiency, since it is used for two purposes: the first is to try to dissipate heat and clean the surface from pollutants, and the second is to utilize heat out by heating and cooking applications, among other things [14].
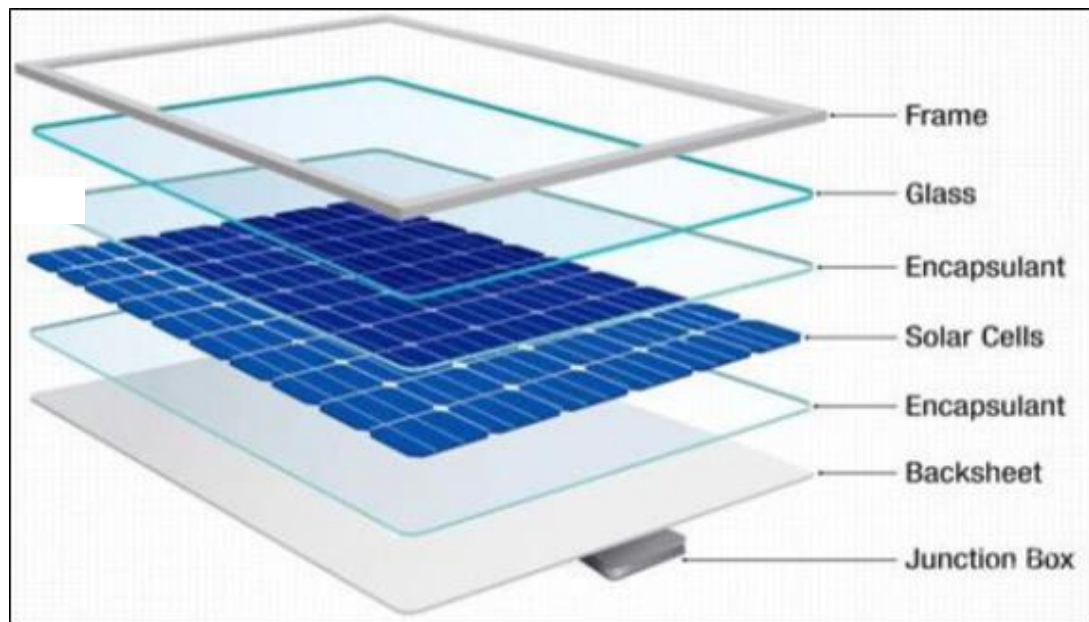
Figure 1.10. Distribution the layers of the PV module.

1.5. PROBLEM STATEMENT

Photovoltaic techniques (PVs) have grown in the past two centuries, and their most important advantages are converting solar photovoltaic energy into electrical energy as well as thermal energy to be exploited in various fields of life, workmanship and productivity. However, when this module is exposed to direct sunshine and heat, it quickly loses its efficiency and longevity, especially in nations with severe climates like Iraq. When compared to the rest of the systems, heat is a negative parameter and an intrinsic flaw that cells suffer from, since their efficiency does not exceed 20% under typical circumstances (STC) at temperature 25 ºC and radiation 1000 W/m². The loss of efficiency and consumer discontent with this phenomenon are caused by the

high temperature of the cell surface while connecting loads in a hot, dry environment, causing the voltage to decrease with a little increase in the electric current.

To alleviate resentment caused by decreased efficiency, heat must be dissipated by a variety of methods, including air and water cooling of various types, phase material changes, physical changes such as adding nanomaterials to the coolant, direct conductive cooling, and other techniques. The optimization of performance depends on the effect of the cooling method employed, as well as the size of the solar panel, the material it is constructed of, and the angle it is set at. We add to that, the most critical factors are the season of use and the system's geographic location.

To achieve the improvement goal, we created a photovoltaic system with a passive cooling system that cleans the module in addition to its main task, as well as investigated the module's characteristics with extreme precision and in a way that manages the necessary parameters that affect the panel's performance. Thus, documentation over time, including the rate of irradiation, wind speed, and ambient temperature, as well as measuring the electrical characteristics before and after the improvement, using smart and programmed instruments with a graphic interface built exclusively for this purpose. We would like to point out that, in comparison to active energy systems that function with pumps, this technology requires no energy expenditure; nonetheless, it is no secret that the latter systems are more effective than other systems.

1.6. THE CURRENT EXPERIMENT'S AIM

The objective of our current technique development is to investigate the effectiveness enhancement of solar modules by dissipating as much heat as possible while also cleaning the panel's surfaces. Three panels were designed, each made of monocrystalline semiconductor material and placed outdoor in direct sunlight, in response to the climate of Diyala city and which is known for high temperatures and dry and dusty air. The following procedures reflect an experimental assessment to increase the performance of the photovoltaic module as below:

1. A design that featured three photovoltaic panels, first of which was represented by the reference, which devoid of any cooling technique, the other two by a sprinkler cooling system. The experimental test was carried out in Iraq, notably in the city of Diyala, during August 2021, with meteorological conditions that matched with that month.

2. The cooling systems consisted of installing upper and lower nozzles particularly designed to spray water on the two surfaces of the solar module at varying flow rates in each test at a set angle appropriate to the size of the panel to cover it with water completely.

3. All the needs for the experimental procedure in which the cooling platform is accomplished, as embodied by test and measurement instruments, are being prepared.

4. Studying the effect of the cooling technology applied to the solar system, identifying the temperature of the PV system's front and back surfaces, as well as the effect on the electrical characteristics before and after the application of flow rates through water spray nozzles.

5. The data was collected using programs to obtain graphs that depicted the reality of the experimental process and allowed for analysis and comparison of its various curves, as well as interpretation, in order to determine which was the most efficient, its level of acceptability, and suggest future ideas.

1.7. COMPREHENSIVE STRUCTURE FOR THESIS

Our present research thesis has five major chapters interspersed with secondary branches, in addition to the abstract at the opening. The following is a full summary of what was covered in each chapter:

Chapter 1 (General Introduction). It serves as an introduction to the technique utilized in our present research, as well as a discussion of the fundamentals of panels, the factors they affected and how to enhance their qualities, as well as a roadmap for the chapters that follow.

Chapter 2 (Literature Review). It illuminates ancient researchers' investigations, contributions, and work, as well as what they discovered about the negatives and positives of all photovoltaic panel cooling systems, as it was discovered that there are few articles about the various passive flows feeding the upper and lower spraying nozzles.

Chapter 3 (Experimental Work and Instruments). During the month of August, this chapter is concerned with the topographical depiction of the work site, as well as describing everything related to the experimental practical side of measuring devices and equipment, as well as explaining and clarifying the method of installing and preparing the systems for daily examination using upper and lower cooling techniques with plastic nozzles water.

Chapter 4 (Results and Discussion). The results of our daily tests on photovoltaic modules with specified specifications utilizing various flow scenarios of upper and lower passive cooling systems are discussed in this chapter, and they are compared to the non-cooled panel. The major aim of this section is to determine how well the cooling systems are being used, as well as to assess their performance and efficacy in dispersing heat and increasing power and efficiency. As a point of comparison, the chapter concluded with a summary of some previous studies that used the same current cooling technology but with some differences, such as panel dimensions, flow rate, type of cooling or nozzle type, to determine the extent to which panel efficiency has improved and the causes of its degradation.

Chapter 5 (Conclusions and Recommendations). This chapter provides an overview of the practical aspect and outcomes of boosting solar panel efficiency, as well as guiding advice of interest to researchers and plans for the future based on the extracted results supported by references.

PART 2

SURVEY OF LITERATURE

2.1. GENERAL BACKGROUND

The application of the principle of environmentally friendly photovoltaic cells is economically feasible, particularly in terms of reducing the cost of electricity bills for consumers, and most importantly, the elimination of pollution by reducing the level of carbon emissions and other pollutants, despite the consequences of expensive purchase, installation and subsequent processing of equipment. The heat problem is still one of solar cells' drawbacks, and the benefits will not be complete until this bad phenomenon is solved with modern cooling methods by dispersing and expelling the maximum amount of surface heat, hence enhancing power output and electrical efficiency. Researchers have not stood by passively by the problem of heat during the last two decades, instead focusing on several studies on how to manage the problem with different current cooling systems.

The researchers were interested in putting cooling technology to use; some were interested in active cooling and passive cooling, while others focused their testing on the indoor environment, that is, in a closed environment while controlling the room temperature and radiation percentage. Other researchers concentrated on putting it to the test by putting the cell outdoor to study the reality of its behavior under real weather conditions. We would like to emphasize that the purpose of all of the strategies outlined is to achieve the maximum degree of efficiency; an overview of previous research and attempts can be found below.

2.2. HIGH TEMPERATURES IMPACT ON PV MODULE PERFORMANCE

This section will include several experimental and analytical investigations that demonstrate the impact of high temperatures on solar module performance when outdoors in real-world climatic circumstances or indoor. The required percentage of electrical efficiency is possible to reach by taking interest in two main factors, according to an article Dubey system design and equipment, as well as temperature dispersion on the cell surface [15] .

According to Chow (2010), the greatest proportion of the radiation landing on the cell's surface is reflected, resulting in operational heat that surrounds all sections of the panel by absorption, resulting in a PV module efficiency of 4% to 7%. He also proved that the cell temperature climbs to 60 ⁰C and exceeds the ambient temperature, reducing the panel's efficiency by 4% per 1 ⁰C, in addition to the cell's damage and shortening its life span if heat continues to dominate during the operational duration [16].

Kandil, et al. (2011), and his research group in Kuwait presented an in-depth inquiry into the topic of the influence of heat on outdoor solar modules, which lasted from 2009 to 2010. He emphasized that the harmful effect of heat was not limited to a single type of cell, but could be seen in a (STC) panel that he employed in his research. Based on his experiment, specifically in August, the experiment was subjected to identifying the electrical characteristics. If the temperature rises by 20%, the value of the open circuit voltage decreases by roughly 8.8%. The output power was reduced by around 6.3% due to lowering all of the parameters [17].

Researchers are still studying the impact of most weather conditions, particularly high temperatures, on photovoltaic cell efficiency, which is a significant negative component on the cell's output power. In the same vein, John et al. (2014), stated that the cell's temperature caused by absorption obstructs the progression of the cell voltage, which reduces as soon as the temperature begins to rise somewhat along with the current. He also mentioned that the efficiency of standard cells is determined according to the nominal temperature (NOCT), when firms design the cell. He found that the surface temperature of the cell reached 35 ⁰C when he erected a solar array

above the building, but that it worsened when he continued to operate until the temperature reached 70 ⁰C during the summer owing to the absence of cooling conditions at the top of the building [18].

Aish (2015), conducted a realistic experimental investigation in September and November into the disadvantages of high cell temperature. The study specialized in distinct types of cells, according to a study conducted on the characteristics of the mono-crystalline cell and its low power and performance. The panels were put through their paces at three different temperatures 25, 35, and 45 ⁰C under steady radiation. The solar module's efficiency values at three different temperatures were 6.9%, 6.56% and 6.02%, respectively, according to the findings analyzer. It was discovered that when the cell temperature rose, the efficiency dropped. The researcher also focused on the low power percentage. Monocrystalline cells had the greatest drop in energy when the temperature was elevated among the species investigated, with a rate of decrease of (0.54%/⁰C), unless they were cooled by various cooling techniques [19].

Zaini, et al. (2015), used a monocrystalline solar module with a rated output power of 50 W according to standards (STC) in Malaysia, where the weather is pleasant, with summer temperatures varying between 31 ⁰C to 35 ⁰C. The panel in a closed container received 458 W/m^2 of steady and direct irradiation from a halogen light source. Their sample was given a temperature of 27.7 °C as a reference. The impacts of high temperatures on solar panel performance, notably the open voltage (V_{oc}) and maximum power (P_{max}) as shown in Figure 2.1, are supported by experimental data and numerical analysis, as they began to drop together gradually as the temperature climbed, with only a minor rise in the current that was almost negligible. The researcher, at the end of his discussion, recommended choosing a distinct location in cold or slightly warm areas to install photovoltaic modules, or finding a solution to the overheating of the panel, such as using different cooling methods such as water, air, nanomaterials, or all together to achieve the best performance of the photovoltaic module [20].
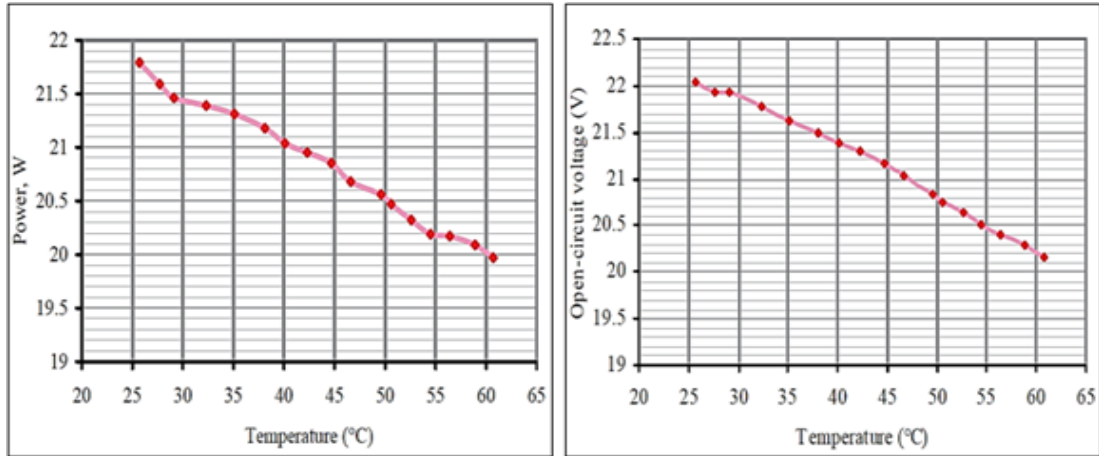
Figure 2.1. Effect of PV module temperature on P_{max} and Voc [20].

Thong et al. (2016), conducted a pilot investigation into the influence of a high photovoltaic module temperature on its performance, assuming radiation and ambient temperature stability. When the temperature reached 64 °C, the output voltage behaved linearly downward 16 V, but it was actually 21 V when the temperature was 34 °C. The same is true for the power and current, which both decrease as the temperature of the photovoltaic module rises. Based on the previously mentioned findings, efficiency was harmed as well, with losses ranging from 0.27% to 0.77% when the temperature was raised by 1°C. Unfortunately, the panel's efficiency degrades under direct insolation, as well as with linked loads or while it is in a charging position for the storage cells, thus the efficiency drops by 23.69%. Figure 2.2 depicts the influence of the heat factor on current and efficiency in absence of load [21].
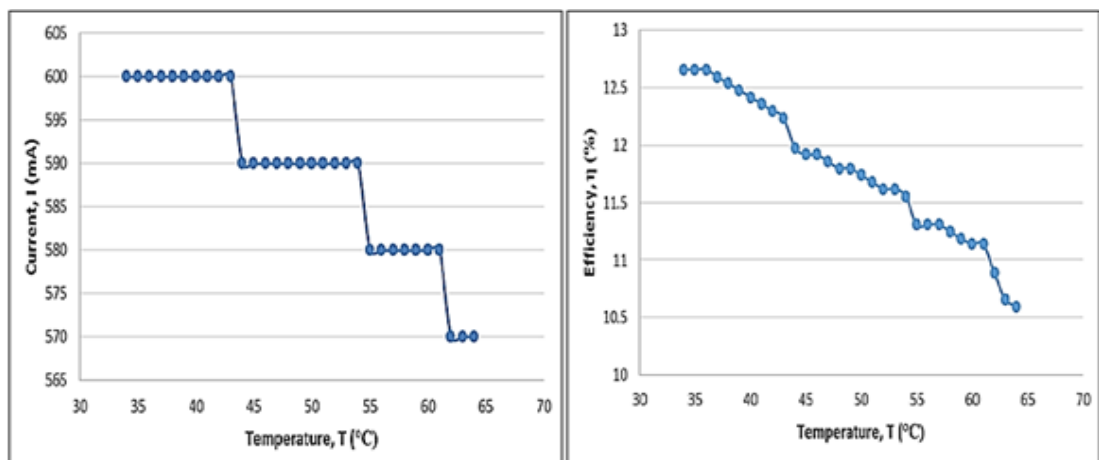
Figure 2.2. Effect of TPV surface on current and efficiency [21].

Gedik (2016), in the Turkish city of Karabük, an experimental inquiry was carried out on a solar panel put within a closed silo of an active system. The system is equipped with two sources of cooling and heating, and ambient air supplied by compressors, heaters, and cooling fans. Throughout the testing time, the room air temperature ambient to the sample stayed consistent according to four estimations 10 to 40 °C. The researcher pointed out that the ambient temperature, along with continuous irradiation, may raise the solar panel's surface temperature. After the ambient air temperature was increased to 40 °C as shown in the Figure 2.3, the back panel surface temperature increased to about 51.5 °C, noting that it was previously at approximately 25 °C within the coordination of ambient temperature at 10 °C. The researcher explained the growth of the panel's surface temperature throughout the course of the working time, as in Figure 2.4 which led to a constant decline in efficiency unless the problem is addressed with alternative cooling methods [22].
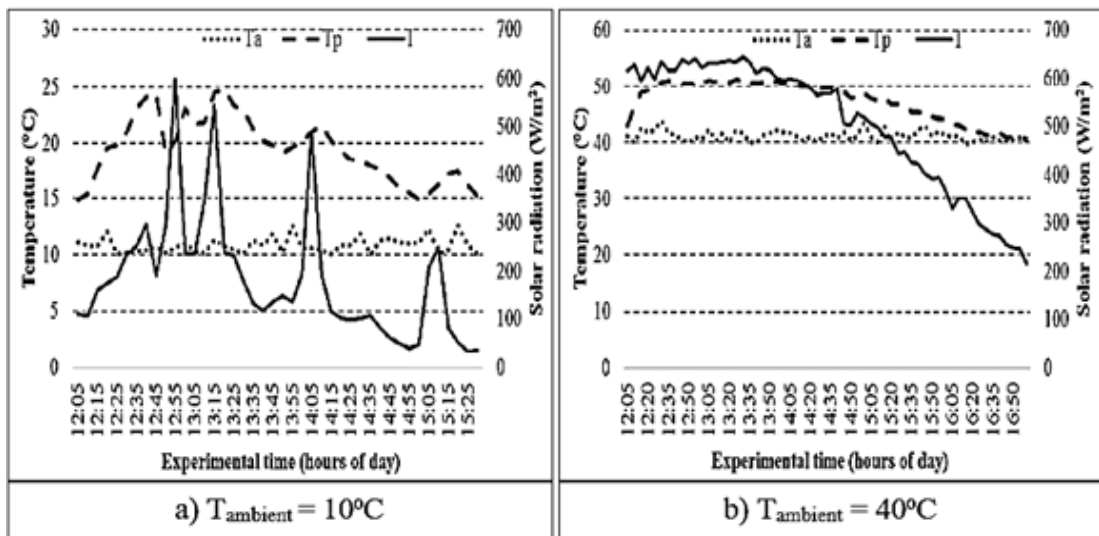
Figure 2.3. Effect of T_{amb} on TPV surface and radiation variations [22].
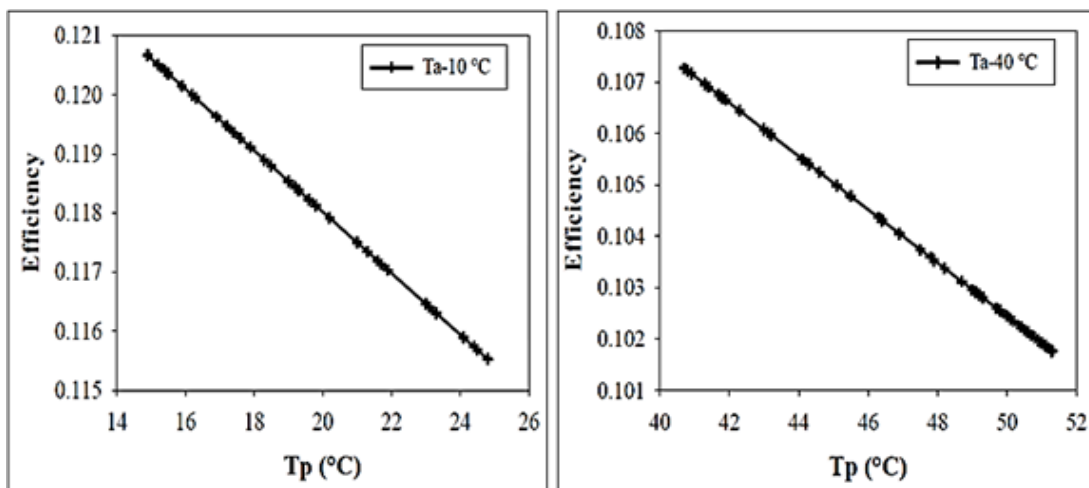
Figure 2.4. Effect of T_{PV} surface on efficiency [22].

Pradhan et al. (2017), also proved in his study on a solar panel with a nominal power 37 W the influence of 10 main external factors on the panel, including the increasingly high temperature and, as a result, a decline in the photovoltaic panel's performance. Explain the observed decline in performance by a drop in the cell voltage and maximum power parameter, as well as a decrease in the filling factor, caused by the arrival of the cell temperature at noon, notably at 1:00 PM, roughly 52 ⁰C. In the same context, the researcher noticed that the temperature of the panel's upper surface was somewhat higher than that of the bottom surface. Figure 2.5 depicts the phenomena of the three parameters decreasing when the temperature factor is increased [23].
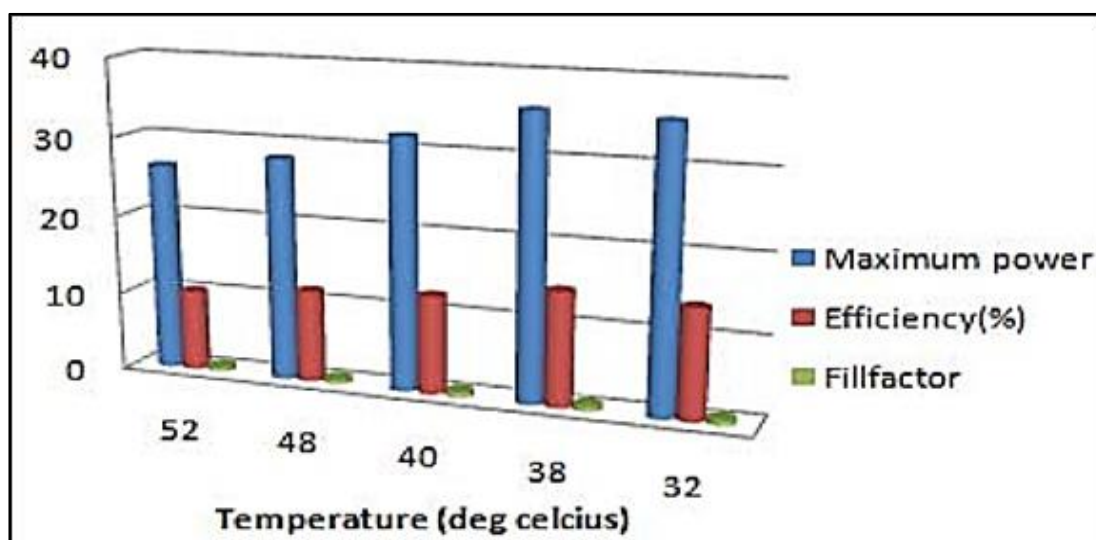
Figure 2.5. Effect of variable temperature on values of maximum power, fill factor and efficiency [23].

Kumar at el. (2018), an Indian researcher utilized his colleagues to study a photovoltaic panel's performance within a closed room (indoor test) while raising the surface temperature of the operational cell and beaming a constant intensity light irradiation source 1182 W/m. The experiment was conducted using the idea of constant radiation intensity, but with a different temperature, each time based on the thermal gradations 35 ºC, 45 ºC, 55 ºC and 65 ºC. The researchers observed the negative effects of high temperatures on the panel's performance, which they described as a (0.4%/ºC) regression in cell voltage followed by a (0.6%/ ºC) decline in maximum power (MPP) output from 2.47 W at 35 ºC to 2.02 W at 65 ºC as given in Figure 2.6. It is worth noting that there is a (0.09%/C) slight loss ratio in current, implying poor overall performance until the heat problem is solved using developed cooling approaches [24].
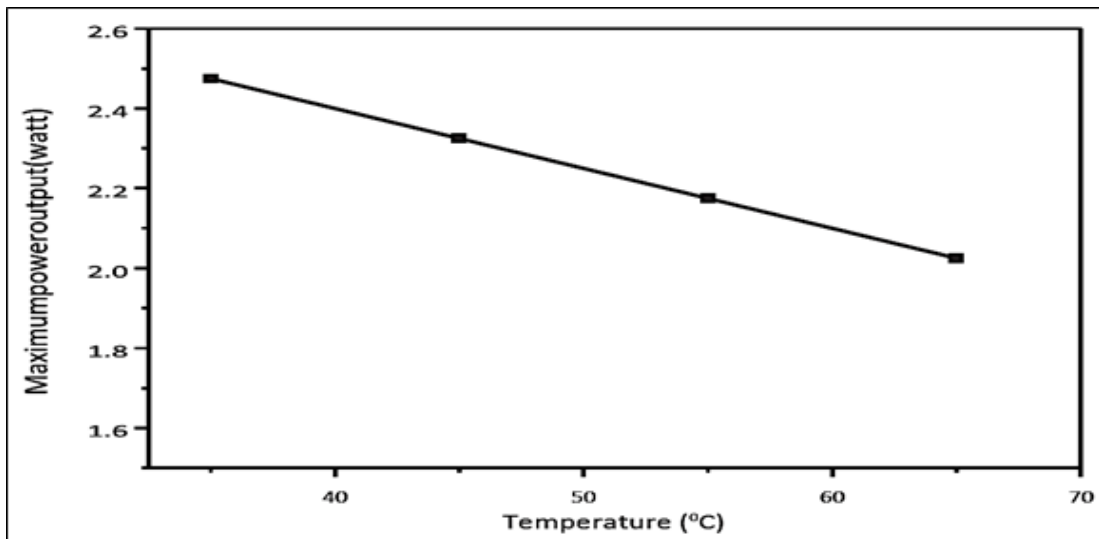
Figure 2.6. Effect of T_{PV} surface on maximum power [24].

Khelfaoui et al. (2019), proved with his group the phenomena of turning a considerable portion of the irradiance into heat within the photovoltaic module, causing the cell temperature to exceed the ambient temperature during operation. He also realized that if the temperature is not too high, increasing the radiation enhances the efficiency of the power created, because it is the only route to increase the efficiency of it. The power output is also known to be the consequence of multiplying the current and the module voltage. As a result of the investigation, it was discovered that as these two basic parameters decrease, the output power decreases, and thus the module's efficiency decreases at a rate of (0.18%/ºC), the reason being that the temperature of

the photovoltaic module rose from 18 to around 30 ⁰C. Figure 2.7 expresses the effect of module temperature on maximum power and efficiency characteristics [25].
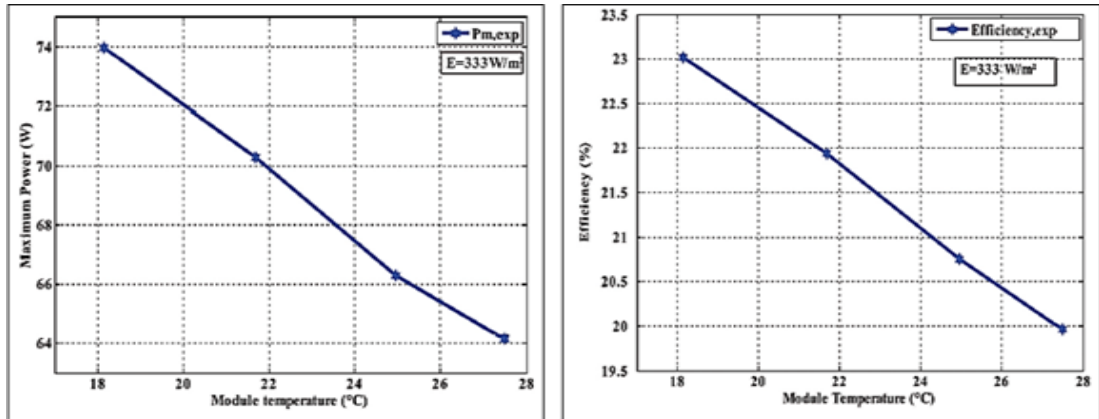
Figure 2.7. Impact of T_{PV} surface on maximum power and efficiency [25].

Ogbulezie et al. (2020), a solar energy researcher in conjunction with other researchers and using a conventional 130 W crystalline silicon panel. They conducted two tests, both (indoor and outdoor), to compare direct radiation and heat, as well as the light from Tungsten lights as a simulation of irradiation and its influence on the solar module. The module was put within an inner room into a closed box at a constant irradiation ratio, although the temperature changed. The experiment was repeated using sensors and measuring equipment and it was discovered that increasing the temperature to 70 °C negatively reversed the output voltage, lowering it from 18 V to 15 V, as well as the fluctuation of the irregular current drop. Figure 2.8 illustrates this.
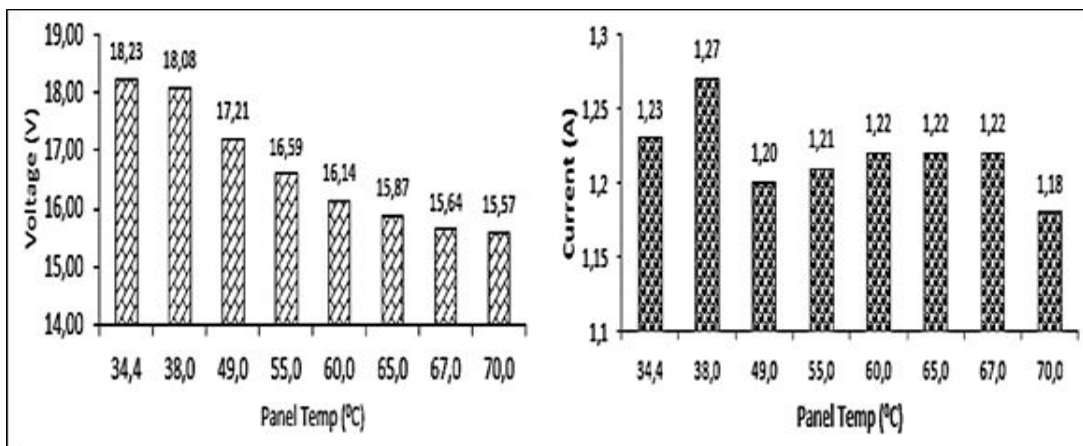
Figure 2.8. The effect of T_{PV} surface on current and voltage [26].

The module's temperature had a detrimental influence included efficiency as well as performance. Figure 2.9 gives an impression of the degradation of efficiency from 17 to 14% at the temperature climbed to 70 °C, as well as the percentage of performance that continues to deteriorate as long as the surface temperature is constantly increasing. After completing the indoor test, the researcher turned to the direct sun. He concluded that the cell voltage harmonized and responded better to Tungsten filament light sources than it did to direct sun irradiation. However, in terms of current and efficiency, the result was exactly the opposite [26].
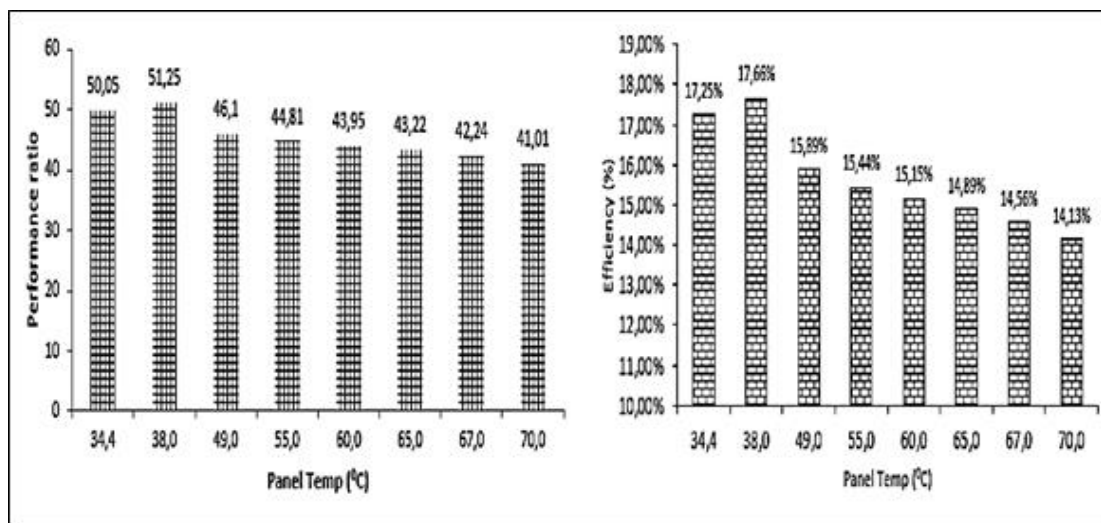
Figure 2.9. Effect of T_{PV} surface on efficiency and performance ratio [26].

Amar et al. (2021), succeeds in describing the experiment through a simulation of the monocrystalline PV module. On the other hand, realizing of the disadvantages that arise in the module characteristics owing to the cell's absorption of some radiation heat, which raises the photovoltaics' surface temperature. Temperature conditions change on a regular basis within the range 25 to 60 °C, while radiation remains constant within the range 200 to 500 W/m^2. Maximum power is one of the fundamentals of solar modules. In addition, its efficiency is determined by it. Obviously, energy is closely related to output voltage. From the modeling, it was concluded that the energy and efficiency of the module decrease linearly in line with the rise in the photovoltaic module's temperature throughout the work time. The phenomena is depicted in detail in the Figure 2.10 [27].
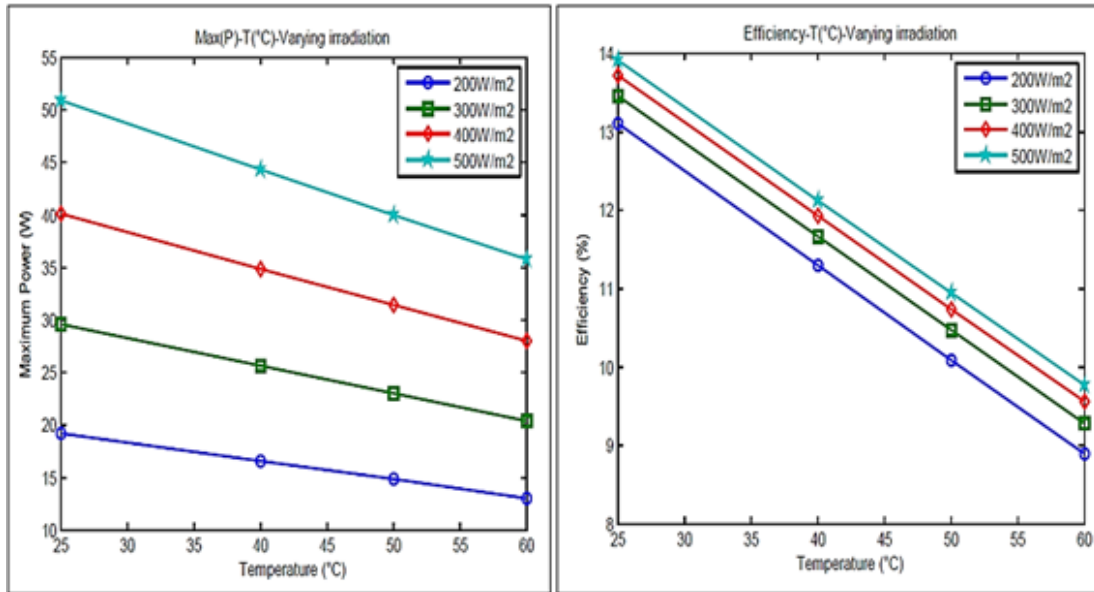
Figure 2.10. Variation of P_{max} and efficiency at constant irradiations [27].

2.3. COOLING TECHNIQUE FOR THE PV MODULE

The problem with the photovoltaic module's performance decline is obviously the high temperature of its surfaces. It has become essential to diminish that heat with various strategies of cooling to attain the best performance and efficiency, and protect the default panel's life from harsh weather. As a result, it is necessary to construct a system that functions independently in order to remove the maximum amount of heat feasible. Cooling techniques include two systems that may be distinguished by the use of natural methods and thermal loads, or more accurately, by natural conduction without the use of energy-saving devices (passive system), and if there are any (air fans, pumps, etc.), forced to agitate the cooling fluids, in this case it is referred to as (active system). Modern cooling strategies are depicted in Figure 2.11, which may be used to illuminate a study of prior and contemporary literature, highlighting the most relevant ones. In addition to those whose investigations are in agreement with our current study, it has an influence on enhancing solar module performance and attributes.
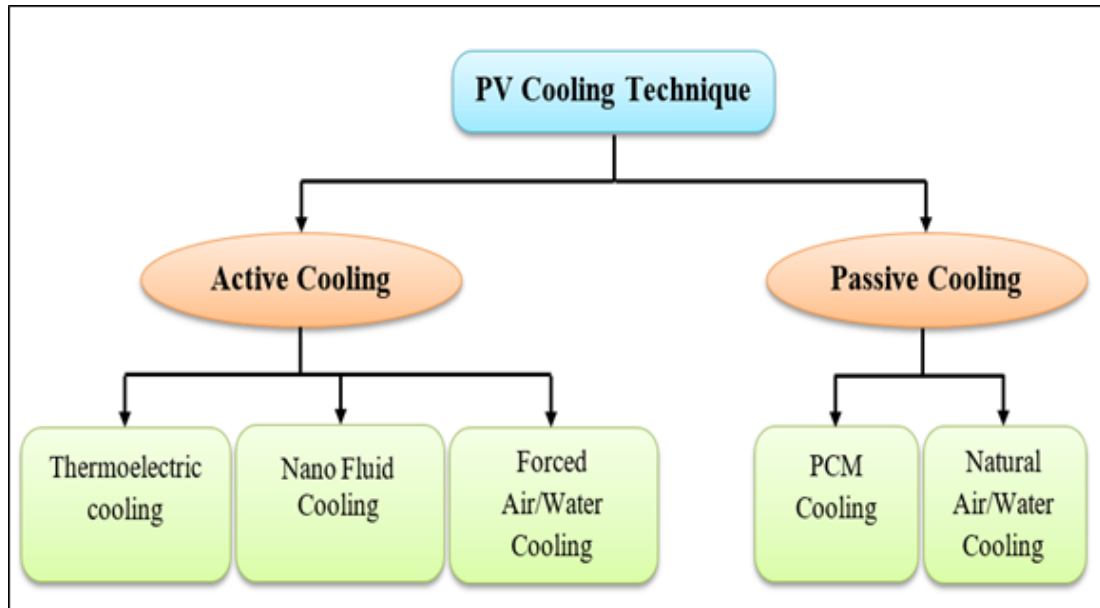
Figure 2.11. Categorization of PV modules cooling techniques.

2.3.1. Active Cooling Techniques

Active cooling technology is a term for energy-intensive technologies. This necessitates the use of equipment and accessories linked with the solar panel's cooling system in order for fluid and refrigerant movement to be continuous and outstanding throughout the working duration. Employs this technique in its work on electrical and mechanical systems such as air fans, water coolers, liquid pumping pumps, and so on. In this situation, the activity is referred to as "forced cooling." This technique is categorized according to the kind of fluid utilized. Forced air active cooling is described using small or large fans depending on the nature, type, and size of the panels in the work. For cooling water, pumps and motors or the like can be used, both of which are coercive in nature and all of which have a primary objective of dissipating the surface heat of the photovoltaic module. Active cooling technology, particularly the utilization of water-cooling, is one of the most suited solutions for the hard-dry environment [28,29].

Teo et al. (2012), devised (PV/T), a hybrid cooling system to disperse the heat created by the quantity of irradiation received. Under the solar panels, air ducts are placed in the shape of horizontal trenches, applying the active position. The pumping mechanism is carried out with the assistance of a blower device that operates to ensure

the interchange of airflow from the inlet and outlet, which are tightly built for the system. The sensors at the bottom of the panel recorded the high surface temperature before the cooling technique was used, and it was feasible to determine the efficiency, which was about 9%. In the same context, the temperature was lowered using the cooling mechanism until the efficiency improved significantly, reaching about 14%. This investigation was included in the experimental framework. The researcher compared (CFD) conclusions with empirical data to ensure they were consistent [9].

Kaiser et al. (2014), designed his forced-air cooling system on a solar module installed at the building's top. He included a pneumatic system consisting of an open channel running the length of the module's bottom side, measuring 0.11 m, which matches the panel's width to length ratio. During their research, the researcher and his colleagues came up with several strategies for increasing ventilation, including increasing the speed of the air stream from its source (fans) or controlling the size of the fans themselves, expanding the scope of the air duct, or simulating a temporary air conditioning system, to boost efficiency by lowering temperatures. The researcher also indicated that while comparing the natural inert air velocity to the forced airflow, a speed of 6 m/s is sufficient to boost the efficiency to more than (19%) when compared to relying on natural ventilation of the air, which reached 0.5 m/s when tested [30].

Habiballahi et al. (2015), use a pump that pumps cooling water with different flows and different heights to tubes installed in parallel behind the proposed photovoltaic module in order to achieve the concept of heat exchange, as dissipate the possible amount of surface heat gained from the remnants of the incident radiation. The results proved an increase Voc and Isc had been decreased somewhat when rear cooling was used, resulting in a gain in output power of 20% to 29% depending on the quantity of flow, which is a significant improvement compared to the case without flow water. The panel's nominal efficiency has climbed by around 2%, while its operating efficiency has increased by 1%, resulting in a total collective efficiency of 4.05% at the height designed for it [31].

Nižetic et al. (2016), water was directed by spray nozzles on either the interface and rear surface of the monocrystalline panel as part of the cooling system. The experiment

was carried out in Croatian weather circumstances that were mild. Twenty Spray nozzles were distributed on both surfaces; Figure 2.12 more is closely approximating the notion. The nozzles were arranged in close and efficient proportions to guarantee that the biggest area of the panel was sprayed with water, as well as to contribute to the self-cleaning process, which was regarded one of the improvement goals. The performance has increased as a result of the applied approach, with the output power of the front and rear sides increasing by 16.3% and 7.7% respectively, effective without losses. Furthermore, as the researcher pointed, out heat dispersion from 52°C to 24°C was influential factor in enhancing efficiency by 5.9% [32].
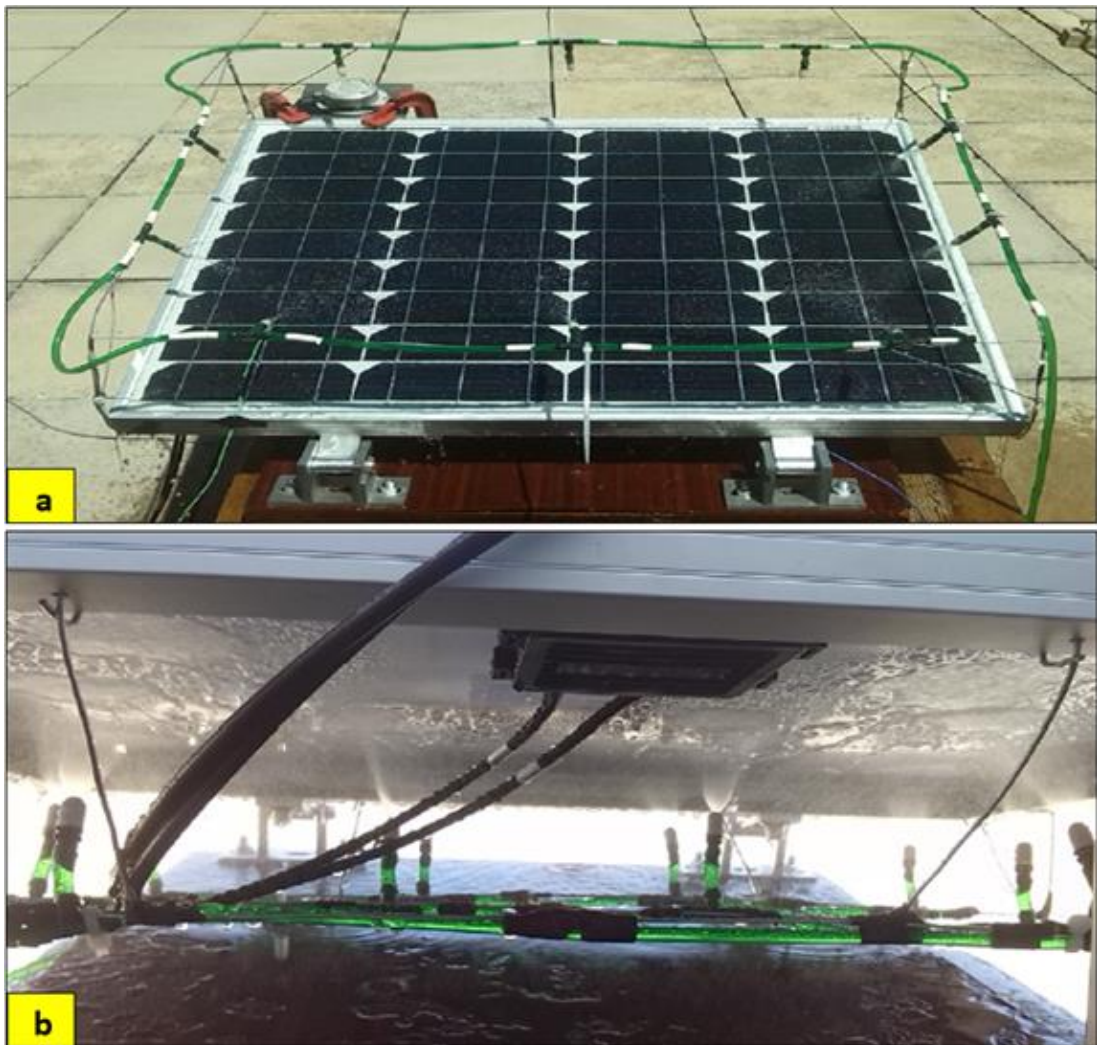
Figure 2.12. Water sprinkler, a) interface surface, b) back surface [32].

Keron et al. (2018), also studied a hybrid system (PV/T) could achieve the same objective of eliminating as much heat as possible to boost efficiency through efficient

cooling water. With the aid of a pump floating above a pre-packaged water supply, he and his colleagues devised a system that enabled water to pass through while spraying the top of the solar panel with a rated power of 5 W. Although the radiation may be a cause to boost the panel's output power, they described it as negative in terms of surface temperature, as it appears from the Figure 2.13. When compared to the absence of cooling to enable the heat to increase gradually, logically, it appears that the power increased in the cooling mode. Axiomatically, the efficiency increases as the output power increases. The total efficiency was 7% while connecting a rated load of 1000 ohms. The efficiency after using the improvement technique is 1.66%, compared to the rate 1.55% before the improvement. Finally, he emphasized that the idea may evolve in the future. When it is used in combination with a bigger system that can handle a variety of panels, it increases production power and efficiency [33].
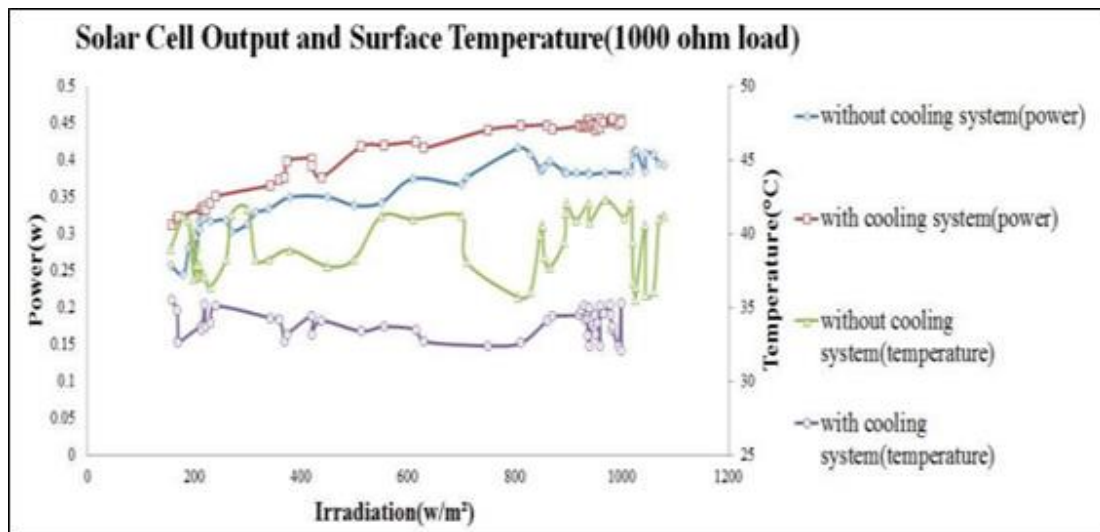
Figure 2.13. Variation of temperature and irradiation on output power [33].

Hussein et al. (2017), an Iraqi researcher who developed an effective cooling system with his colleagues studying Iraq's harsh weather in summer and its impact on the characteristics of a mono-crystalline photovoltaic module 100 W, as well as treatment by heat dissipation and further increasing the module's performance. The system was created by mixing water with zinc Nano fluid (Zn-H2O) at five distinct concentrations and according to varying flows in a ring exchanger below the panel. When using only water, the device had multiple successes in heat dissipation, reducing the heat from 76ºC to 70 ºC. In the same context, mixing water with a mass 0.3% of the Nano-fluid

at a flow of 2 L/min, also made progress in dissipating heat, but it was greater than the previous one because the heat it declined to 58 °C. Undoubtedly, the decrease in heat values enhances the output power and increases the performance efficiency by 6.5% and 7.8% when cooling with water or combining water with Nano-zinc, respectively. This is evident in the Figures 2.14 and 2.15 [34].
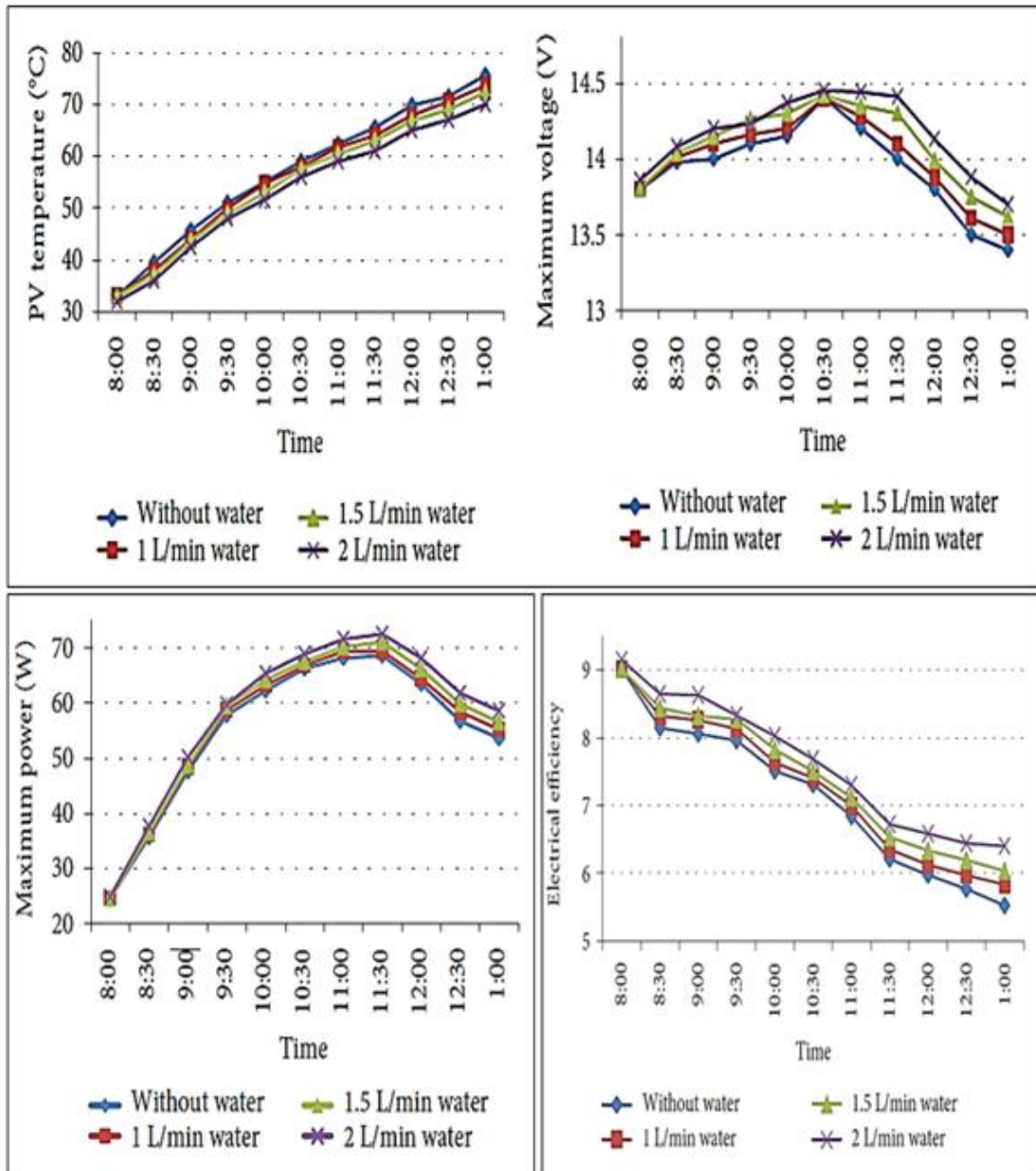
Figure 2.14. Effect of water-cooling on parameters PV module [34].
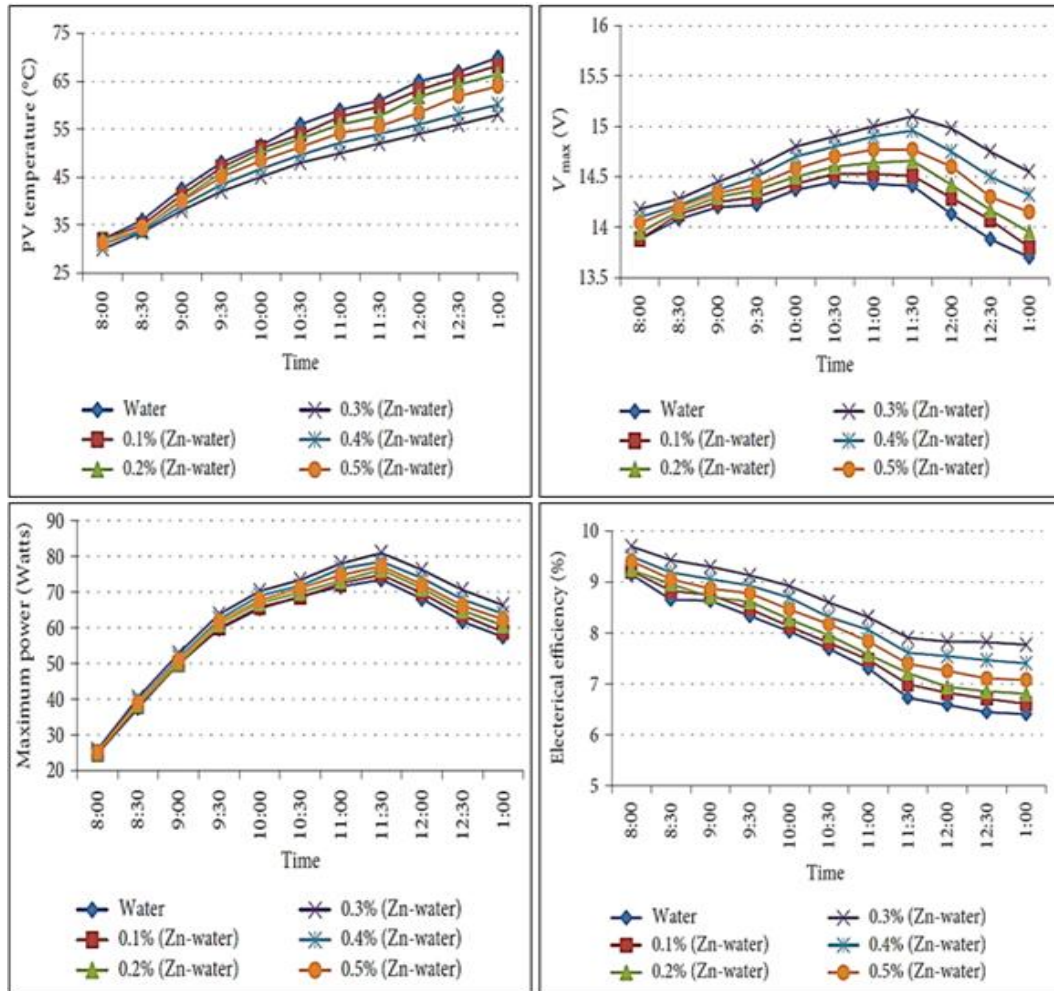
Figure 2.15. Effect of Nano fluid concentrations on parameters PV module [34].

Ömeroğlu (2018), he was able to design a hybrid solar panel (PV/T) that harvests both thermal and electrical energy simultaneously. Putting two fin models behind the PV module, according to an experimental test conducted indoors with a simulation of solar irradiation with Halogen lamps, without a doubt, efficiency must fulfill certain standards, which is why his current study to increase it from 7% to 12.5% has become necessary. Several aspects were present in enhancing efficiency, including the design, number, kind, and position of the fins, and, most crucially, the turbulent internal airflow velocity, as a result, the researcher sought to analyze three distinct types of fins, each with a different number of them. Among the necessary priorities is to demonstrate increased efficiency with more fins using simulation (ANSYS) software. The study demonstrated enhanced efficiency with additional fins. To further support the idea, 108 fins produced the best results in dispersing as much surface heat as possible and were truly satisfying, resulting in an improvement in efficiency of roughly

by 11.8%. It is comparable with 54 fins, which were very effective in terms of dissipation and efficiency despite the small number of fins designed but achieved an improved efficiency of 11.55%, which is a result not much different from the previous one thanks to the area and rates of heat transfer. For the purpose of closely examining the results, the distribution of varied and gradual flow velocities in (CFD) with values 3.3, 3.9, and 4.5 m/s as well as the heat contours that were present throughout the experiment period, which varied according to the turbulent flow velocity, were also identified from Figures 2.16 and 2.17 [35].
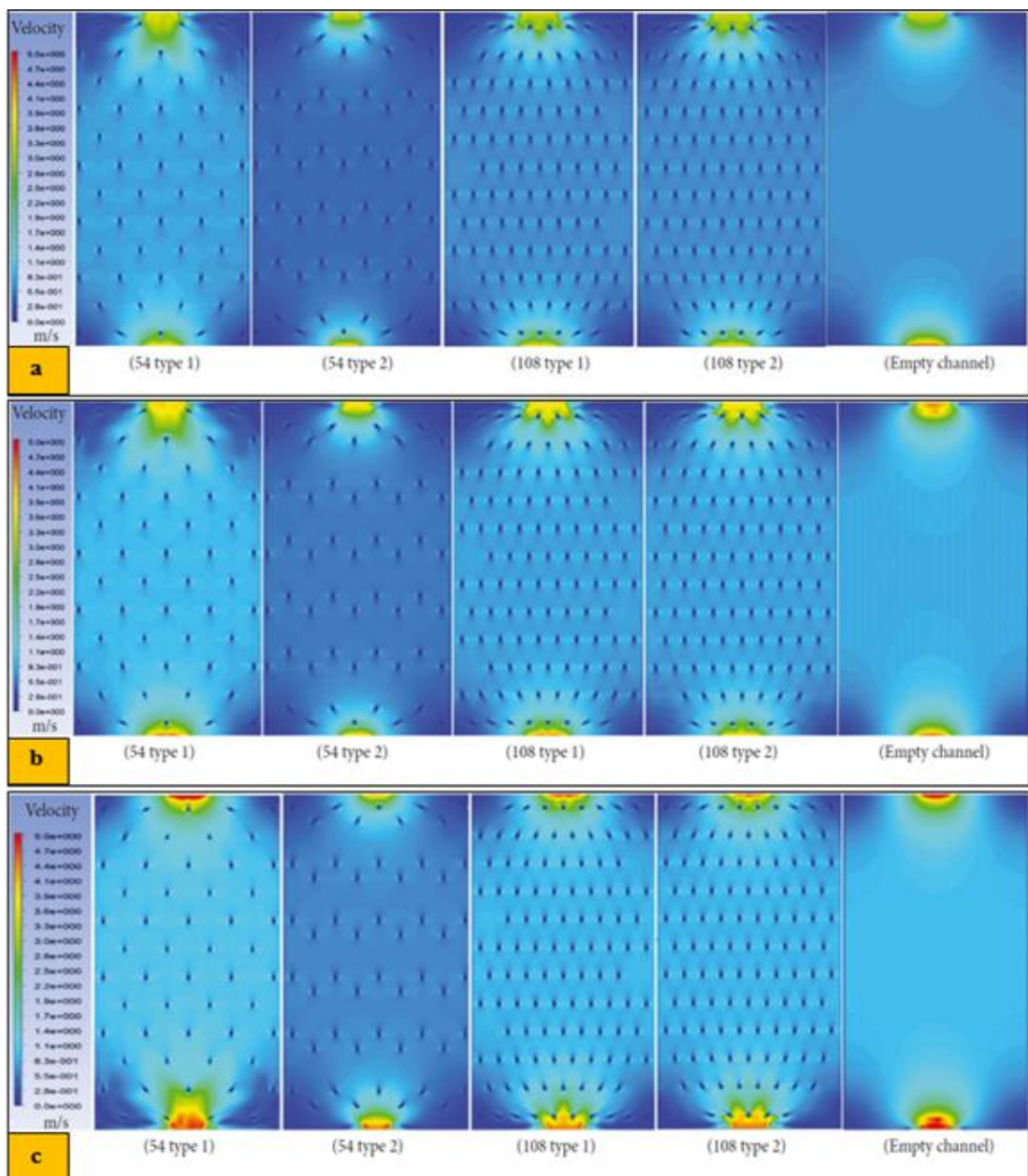
Figure 2.16. Velocity contours: a) at 3.3 m/s, b) at 3.9 m/s and c) at 4.5 m/s [35].
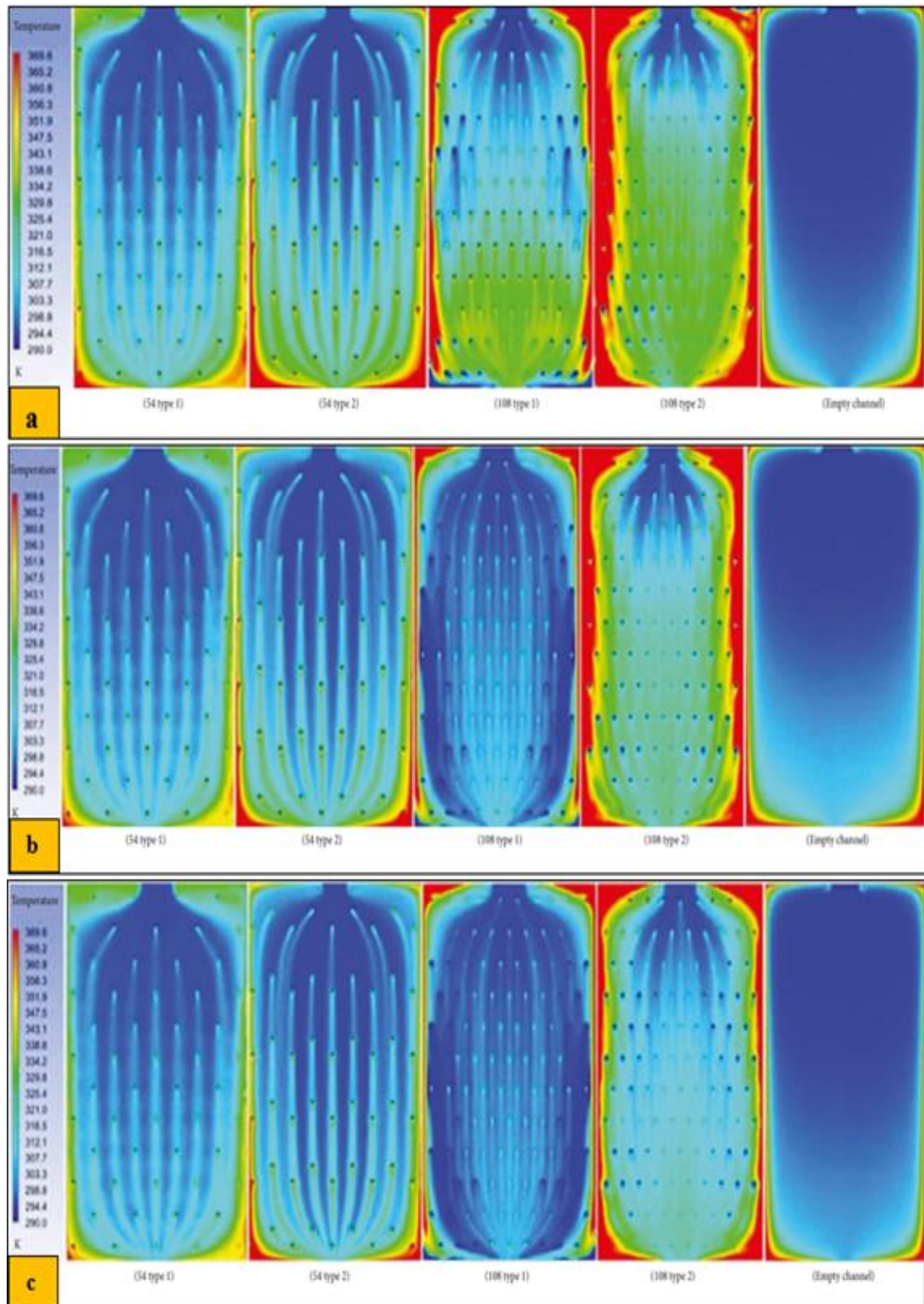
Figure 2.17. Temperature contours: a) at 3.3 m/s, b) at 3.9 m/s and c) at 4.5 m/s [35].

Ahmad et al. (2018), in the city of Qatar, and his colleagues conducted a practical test on a mono-crystalline module in which the solar panel's power was increased by dispersing heat with a water spray approach on the front surface. The system can

disperse 10 degrees of heat in around three-quarters of an hour thanks to the utilization of a water pump for the upper pipes. Consequently, compared to the reference panel, the temperature of the front and back surfaces decreased by 32 °C. In addition to boosting the efficiency of performance 10.35%. In the same context, they added a second tank to collect the hot water that was drained as a result of the heat and utilize it for home purposes. Furthermore, for his part, he stressed the need for dust removal from the rear side in order to improve efficiency [36].

Osma-Pinto et al. (2019), discuss using the forced watering principle and applying it to solar panels. Water flows ranging from 1.75, 3.75, 4.75 and 9.5 L/min fluctuating at different times on the panel's surfaces are detailed using three panels and two distinct cooling techniques. The first is direct (continuous) irrigation, which is defined as the continual pouring of water directly onto the panel's front surface. The second type of irrigation is indirect (intermittent), in which the cell is exposed to a distinct reality in which it cools and heats in response to the presence of the influencer. Cooling by intermittent irrigation at a spraying rate of 3.75 L/min will dissipate 70% of the heat, and further flows were studied in the same context, namely 3.75 and 2.34 L/min. It was with the same effectiveness in accomplishing dissipation as its predecessor [37].

Muslim et al. (2020), and her colleagues employed a novel cooling method in Baghdad, which involves forcing water in reverse on the front and rear surfaces of the PV/T system. In order to incorporate upper and lower cooling at the same time and prepare it for comparison with the performance of the uncooled reference panel, special cold rooms are designed with installed tunnels at angles 60º, 30º, and 0º to direct water to the photovoltaic module. Obviously, after each cooling approach, there must be an improvement in performance, including capacity and efficiency. The thermal efficiency of the first module climbed to 80% when the flow was (4 L/m), whereas the other flows only attained 54% efficiency. In comparison to the uncooled panel, the maximum flow applied to the system resulted in efficiency improvements of 17%, 15.3%, and 13.6% for modules (I, II, and III) respectively. When the flow rate increases, electrical power grows intuitively as a collection of voltage and current for all panels [38].

Arifin et al. (2020), they collaborated on a mathematical study with their colleagues to model a solar panel, deal with surface temperature, and evaluate its influence on all module attributes. A practical design was carried out in an Indonesian city with mild weather, with a surrounding temperature of 35 ⁰C compared to the modeling findings. Figure 2.18 a, b depicts a made-of-aluminum heat sink system with fins that are each 0.03 m high and mounted vertically on the back surface. The fins were perforated to promote air exchange and remove as much heat as possible, and the system's air source is a fan with an inlet flow of 1.5 m/s. After enforcing the logical assumptions of the system design indicators and placing the experimental cooling panel's inputs in the outdoors and submitting them to simulation programming (CFD), impressive results in temperature reduction and performance improvement were seen, with the temperature dropping by 13.6 ⁰C. In the same context, he claimed that the increase in radiation is responsible for the increase in the temperature of the solar module, which is in accordance with the evidence of all researchers. Finally, depending on the technique, the electrical module's properties (Voc, Isc and MPP) have been enhanced, attaining, in order, 10%, 1.18%, and 18.67% [39].
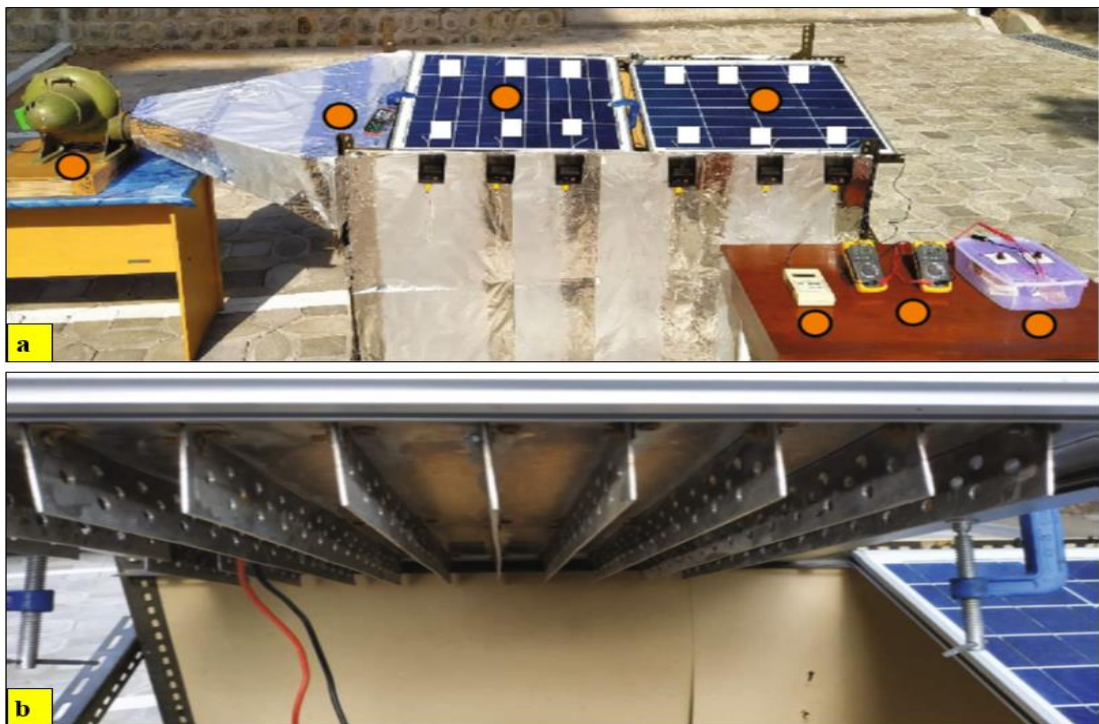
Figure 2.18. a) Experimental procedure of PV panel b) Installation of the fins on the back of a PV panel [39].

Kadhim et al. (2020), an Iraqi researcher recently conducted a study on a photovoltaic module employing the principle of evaporation through groundwater in the city of Baghdad to evaluate the effectiveness of the Earth's thermal energy and the practical benefit of its water in heat dissipation and dust removal. The system was built using four suggestions; the first was to use cellulose as a pillow to cool the back surface of the PV module. The second was to place the spray nozzles on the upper side of the panel, as well as cool the two sides together with a constant flow, and the last is to use the Arduino controller to pump the forced water on both sides together to apply the flow change. The heat value of the two surfaces of the cooled panels decreased as compared to the uncooled one, with the pillow test achieving a drop of 4 °C, the spray nozzle achieving a decrease of 8 °C. Likewise, the combined test achieved a decrease 12.2 °C. Logically, the dissipation increases when the flow is increased, so the last test reached roughly 12.6 ºC. Based on the empirical description of the test provided, it can be considered analogous to our current work [40].

Benato et al. (2020), set up an experimental effort with them that featured studying the most important cooling system equipment (nozzles). The author completes what the designers have determined regarding the angles of the nozzle intake and their connection to the flow pressure. It is irrational to marginalize a certain part of the panel (edges) by not getting them wet with water, and this research was prepared for this purpose. Water nozzles in three distinct forms 90º, 180º, and 360º were employed, and in varied numbers, as seen in Figure 2.19. The design 90º was chosen from among the best-suggested angles, and because of its location, it allowed for full wetting of the panel's edges as well as continuous cleaning, resulting in the highest heat dissipation 24 ºC, corresponded to the highest improvement efficiency by approximately 13% [41].

Figure 2.19. Diversity of number and design of the angles PV panel nozzles [41].

Jafari (2021), a Turkish researcher, recently finished a one of a kind investigation analysis in which he specialized in studying the enhancement and analysis of photovoltaic panels' energy in conditions that combine the use of underground energy and its role in cooling on the one hand, and the installation of a heat exchanger behind the panels on the other. Two heat exchangers, one in the shape of a heat sink made of (polycarbonate) positioned behind the panels, and the other (geothermal) sunk at a distance of 3m in the subsurface, were constructed to take advantage of the subterranean cooling of water, as indicated in the experimental schemata Figure 2.20. The researcher listed both his numerical and experimental results, which were similar. The experimentally enhanced efficiency of the panels was 9.8% compared to the uncooled panel's 6.2%, whereas the efficiency attained according to the simulation applied to the system was 11.6%. The researcher was interested in thermal imaging because he utilized a thermal camera to demonstrate the temperature gradient of the surface of the panels that had been chilled and those that were uncooled, as illustrated in Figure 2.21. Finally, the researcher mentioned the idea of using hot water output for additional home needs in the future [42].
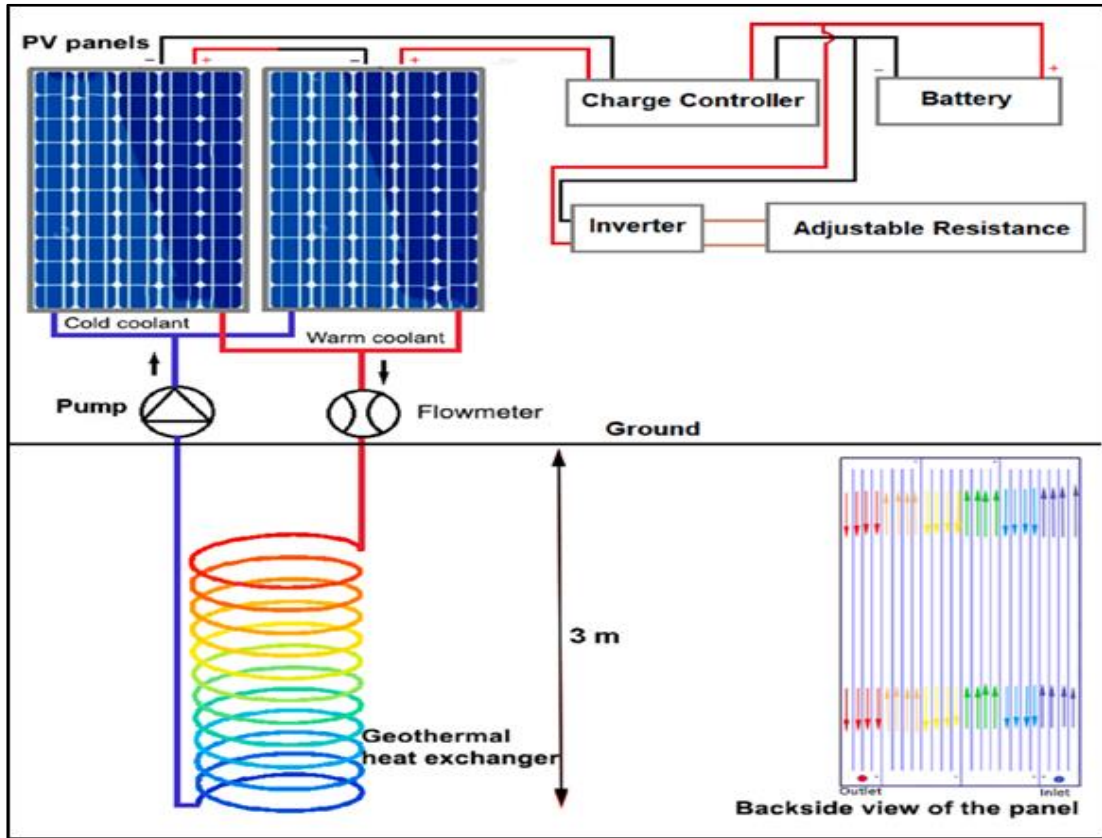
Figure 2.20. The experimental schema of cooling [42].
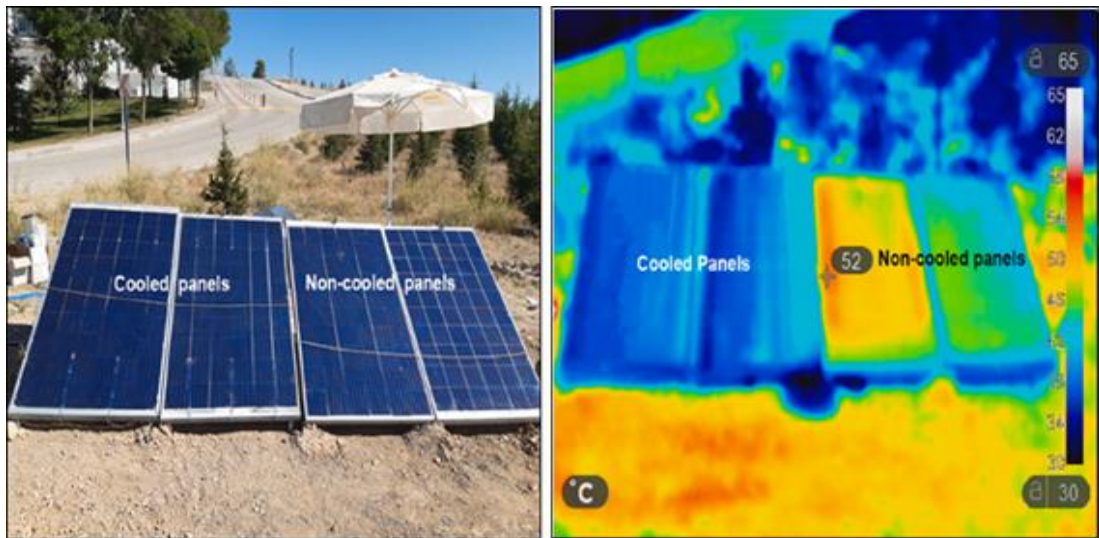
Figure 2.21. Realization of infrared thermal camera images of PV panels [42].

Laseinde et al. (2021), is concerned about increasing the output power of solar panels and improving their efficiency by referring to the significant economic feasibility benefit of being satisfied with a set number of chilled panels using cooling techniques

rather than multiple panels. The experimental investigation included the design of a system consisting of spray nozzles installed on the upper panel's surface that draws water forcibly from a controlled pump using the feedback principle of controlling a programmed sensor (Arduino) over the excess water flowing according to the panel's surface temperature so that it does not exceed the minimum permissible standard. After a thorough investigation, it was discovered that the system's efficiency had increased by 16.65% [43].

Gomaaa et al. (2022), developed the (PV/T) system methodology to assess the optimal design of box ducts (fin ducts) conveying coolant in terms of thickness and flow quantity, as well as their influence on the photovoltaic panel's overall characteristics efficiency. To assess the properties numerically using the simulation program (ANSYS), the diameters of the cooling fins attached to the panel were built with diameters (3 and 15 mm), as well as different flow rates 0.5- 4 L/m and varied radiance. Despite the fact that the panel's surface temperature in the extreme hot environment exceeds 70 °C, the results revealed that at the maximum flow 4 L/m, it achieved The highest drop in the exit water temperature was achieved from the designed exchangers 3 and 15 mm, reaching 37 °C and 34 °C for the thin and thick designs, respectively. In the same context, and according to the results, the optimal flow rate for both designs was 3 L/m in line with our current study, and concluding by saying that the radiation, flow rate, and kind of design all had a significant impact on enhancing the Photovoltaic panel's features [44].

2.3.2. Passive Cooling Technique

One of the methods of photovoltaic panel cooling is characterized by its passive work without consuming energy, since there is no moving equipment in general, whether mechanical or electrical, as in forced (active) cooling. As there are passive air and water systems, passive cooling techniques are described according to the design of the system. The passive air cooling system is distinguished by the use of natural ambient air that circulates naturally without the use of fans, blowers, or the like in metal fins installed at the back of the panel to dissipate heat, thereby achieving the cooling function that is often referred to as "natural cooling" (convection). The studies

discovered that using an air heatsink resulted in a 13% increase in efficiency when modeling radiation with lighting in the 200 to 800 W/m^2 range [45]. Gravity is the fundamental working principle in passive water cooling technology, since it rotates and rises without the use of any electric pumps. Despite the passive system's simplicity and low cost, we would like to point out that active cooling was more efficient. In the same context, other passive cooling strategies, such as diversion, natural conduction, the panel's surface coating, reflecting mirrors, evaporative cooling, and the water immersion method, are also used in conjunction with phase change materials (PCM) [46]. We have compiled a collection of research that studied a variety of passive cooling approaches and that was accomplished without the usage of any energy.

Mittelman et al.(2009), carried out a numerical analysis of the operational photovoltaic module, simulating the geometry of the installation of heat dissipation ducts (fin exchangers) behind the module for cooling by radiation and convection in a quiet negative manner, using natural air as the operating material passing through the heat dissipating ducts. The study focused on cooling channel design because of its relevance in increasing efficiency, concluding that the spacing of scattering fins and their short length provide better performance than lengthy paved ones. He also stated that the small height of the channels increases the possibility of losses in the rate of irradiation, resulting in more opportunities for heat dissipation, especially when the channels are spaced from 5 to 20 cm, as the temperature drops from 10 to 20 °C, resulting in a 2% in efficiency [47].

Cuce et al. (2011) the other looked at the effect of open passive cooling by testing the performance of a photovoltaic cell with a heat sink installed behind it to simulate sunshine indoor the test room. The irradiation was carried out at various rates ranging from 200 to 800 W/m^2, with the findings demonstrating that the highest amount of cooling was attained when the irradiation intensity was reached 600 W/m^2, with the passive cooling efficacy decreasing at 200 W/m^2. Intuitively, an increase in power factor is directly connected to an improvement in efficiency; hence, 20% is the amount of improvement achieved by the cell compared to its non-finned counterpart [48].

Chandrasekar et al. (2013), thermal degradation of the photovoltaic module must be eliminated. He and his colleagues shed light on a uniquely very efficient passive cooling technique consisting of cotton wicks put behind the panel on one end and immersed in beaker-like water containers on the other, as shown, Figure 2.22 a, b. Water was employed as the panel's working medium, along with nanomaterials that were combined in particular proportions. The temperature of the panel reached 65 °C without any noticeable cooling, but when water wicks were put below the panel, the temperature dropped by 30% thanks to the moisture factor, which allowed the wicks to be moistened during the period of test. The heat lowering percentage was 11% and 17% when (CaO) and (Al_2O_3) nanoparticles were mixed with water, respectively. The heat reduction ratio decreased when the efficacy of the capillary cotton fibers to absorb water deteriorated due to nanoparticles suspended in the pores of the wicks. Before cooling, the PV panel's output power was 41 W, but once the heat was dissipated by water, it increased to 47 W. When the Nano fluids entered the wick structures, the output power decreased 44.6 W. The panel's efficiency was 9% before the wicks were installed, but it climbed to 9.7% and 9.5% with the addition of (AL_2O_3/water, CaO/water) nanoparticles, respectively [49].
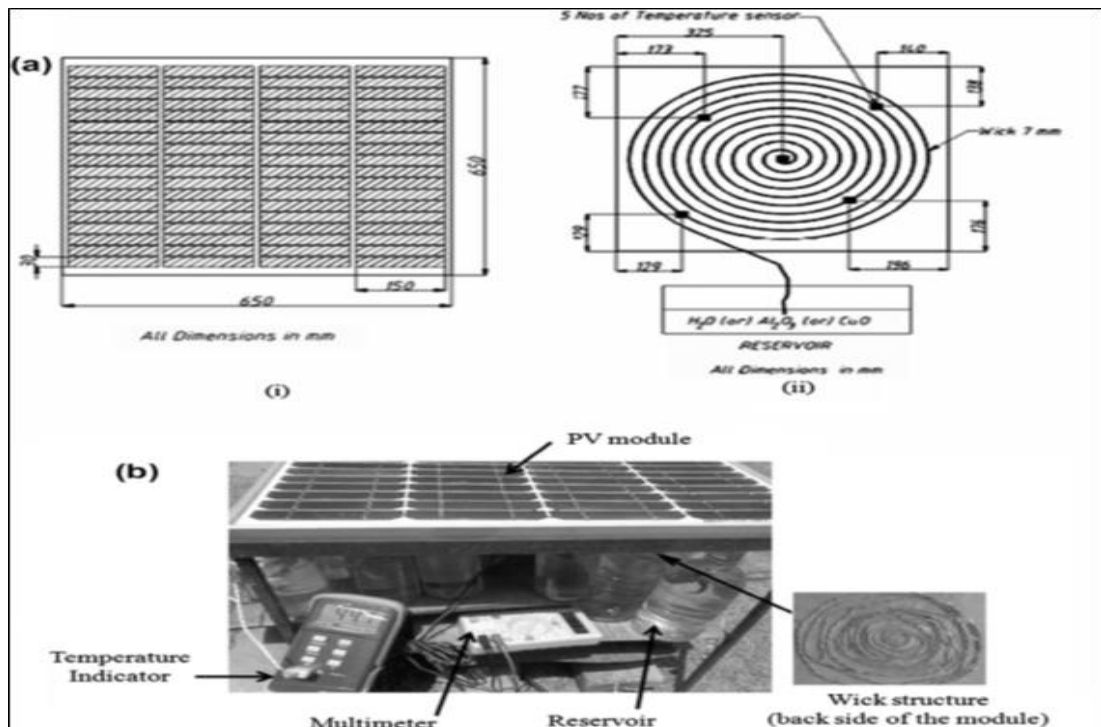
Figure 2.22. a) Front and back sides of the PV module with the wick coil diagram b) Passive cooling of the PV module [49].

38

Abdulgafar et al. (2007), innovation in Iraq, notably in the city of Dohuk, was achieved by overcoming the harshness of the solar panel's high temperature by submerging the panel in water at a set level to enhance efficiency. The photovoltaic panel was immersed at different depths, ranging from 1 to 7 cm. The results showed that the depth 6 cm was the most effective in increasing electrical characteristics, as it achieved the highest level of efficiency improvement by 11%. In the same vein, the researcher discovered that when the depth is greater than 6 cm, the efficiency decreases. Perhaps the reason is due to the electrolyte's contact and interaction with the main connections of the electrical panels. He added that his findings were consistent with many prior studies and references [50].

Mehrotra et al. (2014), also went on about the application of the water immersion approach, which he found to be effective in terms of increasing efficiency and economic feasibility for photovoltaic panels. The experiment was conducted in the open air, with the panel being dipped in a basin of water at various depths, as shown in Figure 2.23. The results show that the heat of the panel lowers with depth of immersion; the deeper the immersion, the lower the temperature, and thus all properties improve, including electrical efficiency, which rose by around 18% over its uncooled predecessor at the depth 1cm. This study lent support to the idea by determining that the technique might be used on a bigger scale by inserting the panels or array at the bottom of oceans, bays, and other bodies of water and the like [51].
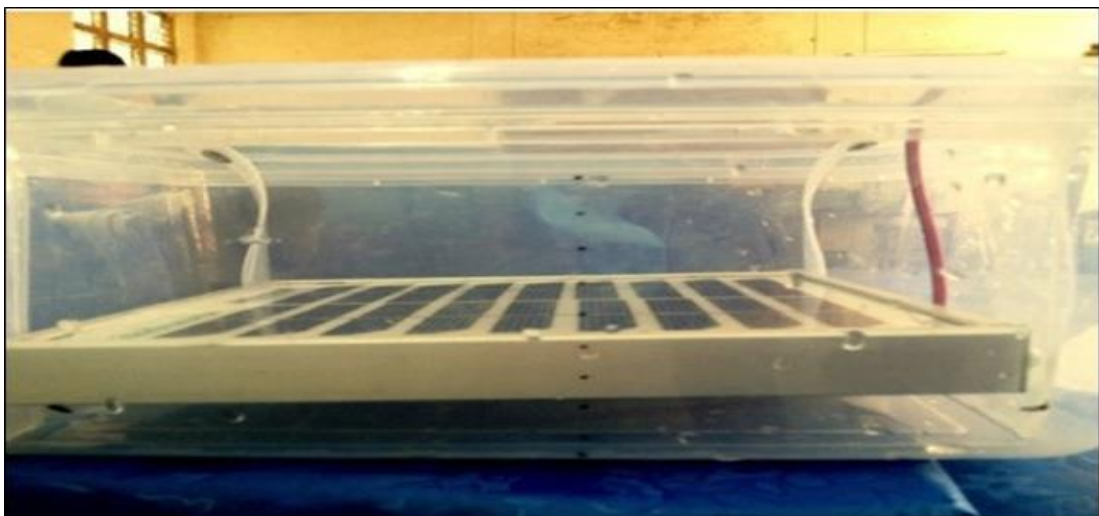
Figure 2.23. PV panel dipped in water [51].

Chandrasekar et al. (2015), the heat sink and cotton wicks were linked to form a dual system. They collaborated on its design and application of the technique in the hot weather of the metropolis of India, targeting the heat of the PV panel, dissipating it, and dispersing it until it had fulfilled the improvement phenomenon. Due to the effect of evaporation cooling upon natural air contact with the surface of the wet wick, red water was utilized to infer about soaking the cotton wicks visually, which achieved a temperature decrease of 12% compared to the reference panel. When the two systems are applied together, the wicks' water evaporation joins with the heat-dispersing aluminum fins, resulting in a heat reduction rate of 20% based on the concept of convection. Heat reduction was achieved by photovoltaic passive cooling, resulting in a profitable return of 14% in power output [52].

Elnozahya et al. (2015), was able to investigate the cause of the decline in efficiency in the tough hot climate and compare it to the reference panel using the experiment with the two passive systems applied to the PV module. It allowed them to come up with the solutions they needed. Because no effective pump was utilized, the experiment was characterized by inactivity (passive cooling). Instead, it depended on gravity evaporative cooling descending from water tanks to spray nozzles, as explained in the Figure 2.24. Aside from that, alternating manual self-cleaning has been implemented. According to the data, the heat of both sides of the plate was lowered by 39.9% and 45.5%, respectively. The thermal degradation of the panel surfaces was also demonstrated by infrared thermal imaging. The output power of the uncooled panel was 69.4 W, and its improvement, as is known, is dependent on the heat dissipation ratio, so it increased when the two systems were applied and recorded an improvement 89.4W. According to the same approach, the panel's efficiency increased by 11.7% after it was 9% before initiation of applying cooling techniques [53].
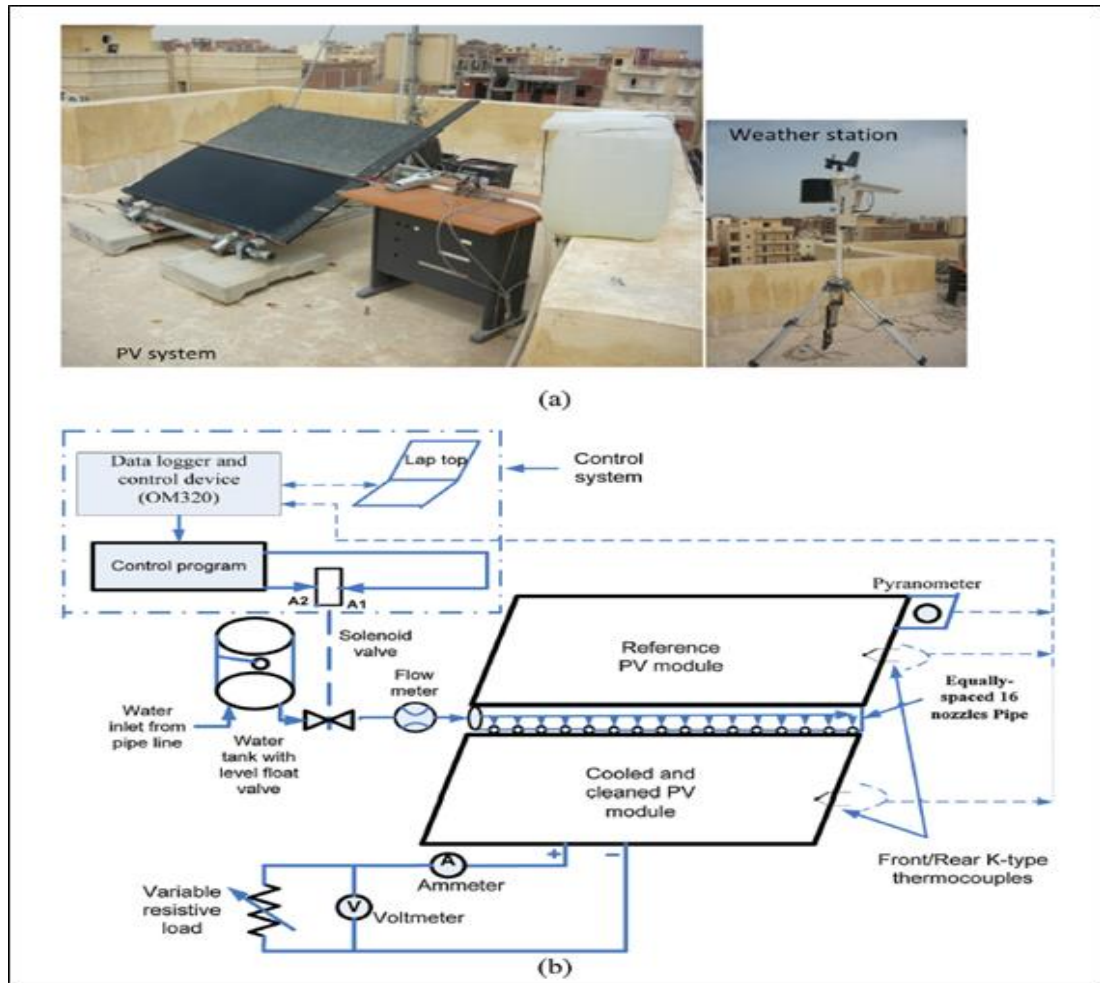
Figure 2.24. Integrated cooling and cleaning system for both the schematic and photographic design of the PV module [53].

Čabo et al. (2018), the heat exchanger fins are constructed differently this time, and the dissipation system is set up in two ways. In order to offer excellent passive heat dissipation. The panel's back was affixed with an L-shaped metal heat sink, parallel to the water-glue in the initial design. In the second design, the fins were randomly positioned on the rear of the panel, and they were likewise perforated with parallel holes. The two prototypes are intended to test the impact of wind gusts on passive cooling. The results revealed that the second system with perforated fins responded faster and had a greater efficiency improvement by 2% than the first during periods of wind gusts as well as a variable irradiation rate [54].

Fakouriyan et al. (2018), they devised a (PV/T) system that combines photoelectrical and thermal systems and is based on monocrystalline panels. It was well known for its

efficiency and simplicity. Its purpose is to save energy by collecting water and returning it to the solar collector to satisfy hot water demands. Shower nozzles with coordinated spacing were positioned behind the panel to accomplish liquefied water-cooling and cover most of the surfaces. Simultaneously, the water is returned to the tank in a heated condition, completing a full cycle that produces both electric and thermal energy. Under the suggested cooling and convection circumstances, all efficiencies evolved and improved at various rates, with the electrical efficiency reaching about 12.3% and the thermal efficiency increasing by roughly 49.4%, resulting in a total efficiency of 61.7% [55].

Luboń et al. (2020), in their paper, he attempted to explain an experimental concept of two passive cooling techniques for solar panels. One technique is characterized as taking water from a faucet and pouring dumping it like a river runoff over the panel's front surface, simulating a water membrane, as for the other spraying mechanism spraying can be depicted by splattering rain scattered over the panels, as seen in Figure 2.25.

The former is undoubtedly one of the most well-known approaches, while the latter is regarded fairly uncommon in addition to the scarcity of working it owing to its simplicity and side effects. When compared to the uncooled module, the cooling efficiency with the continuous flow of the nozzle achieved a thermal drop of 25 ℃ vs 45 ℃ for the reference. Similarly, energy has generated about 20%. The finest utilized strategy for dissipation is the continuous water thin film from the nozzle, which obtained a twofold reduction value and reached 20 °C, while the rain representation cooling achieved a half-value reduction. The reason for the failure is obvious: the latter leaves stains on the surface, as well as disperses its drops owing to collisions with the panel's surface, and therefore wide regions of water were deprived due to the failure to deliver it sufficiently covered to the all parts of panel [56].

Figure 2.25. Cooling of PV array by atomization of rain [56].

Wongwuttanasatiana et al. (2020), a passive system is designed and implemented that uses a low-cost, energy consuming method to cool the photovoltaic panel and increase its efficiency. The system was described using three boxes on which the photovoltaic panel was installed, which were in order (the surface is engraved with grooves, the other is hollow with tubes, and the third is finned), as shown in Figure 2.26. Starting with the concept of heat absorption. All three worked as a central heat sink behind the panel, whose three gaps were filled with palm wax, which is a photovoltaic phase changer material (PCM). The system was able to dissipate heat more than 6% through the results, giving the impression of a 5.3% rise in efficiency, and so the panel's performance percentage improved to around 4.8%. According to the obtained experimental results, the fin box filled with (PCM) provided the best thermal and electrical performance properties among the other boxes, and the researcher indicated that the material (PCM) might not work as an enhancer when the intensity of irradiation drops to below 500 W/m^2 [57].
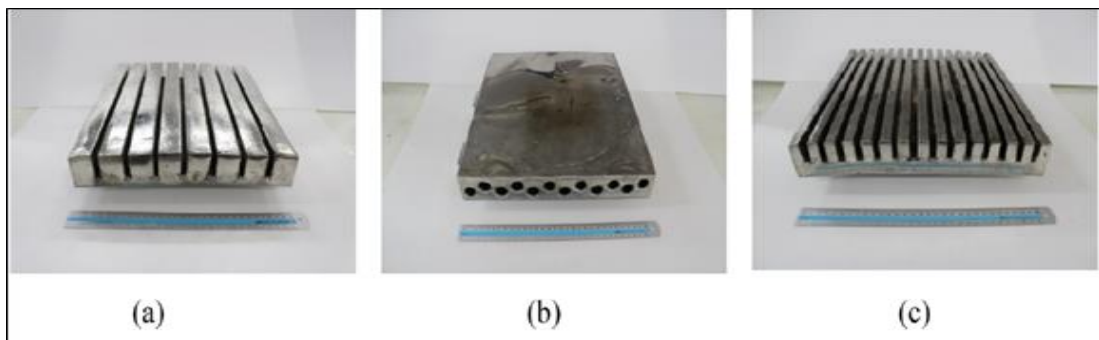
Figure 2.26. PCM Cooling Tanique: a) gullies, b) pipes, and c) fins [57].

2.4. THE CURRENT EXPERIMENT'S SCOPE

The previously investigated in-depth analysis of the studies and literature all points to the danger of overheating the photovoltaic module's surfaces. For obvious reasons, researchers are still engrossed in the problems of efficiency decreasing during operation, necessitating the use of various cooling techniques. Water, in particular, is one of the greatest operational cooling solutions due to its high conductivity and quick absorption, and it has everyone's support. Many studies have focused their attention on effective cooling, and a few have designed a passive water cooling system despite its low cost and low energy consumption. However, despite the panel's continuous improvement during its application, little attention is paid to the flow rate and its direct impact on performance efficiency. As a result, our present focus has been on passively cooling the panel by spraying water on the front and rear nozzles, as well as opening various flow rates and comparing them to the reference panel. One of the most essential features of this experimental assessment and a basic difference from earlier literature is to describe the problem of Iraq's harsh weather in summer, which causes electrical and thermal damage to the PV module. It is worth noting that enhancing performance is not limited to cooling alone, but also includes cleaning, and removing dirt in all favorable climatic circumstances to extend the life of the panels. As a result, various flow rates were used to investigate the changes in the monocrystalline PV panel's thermal and electrical attributes. Finally, the extra cooling water was utilized to irrigate the damaged crops, which are now suffering from drought, particularly during the summer, and this is one of the economic feasibility considerations.

PART 3

EXPERIMENTAL WORK AND INSTRUMENTS

3.1. INTRODUCTION

This chapter describes the instruments, testing equipment, and data collection methods used in this experiment to suggest a photovoltaic panel cooling technique. The outer testing took place in August 2021 on flat terrain in the open air at the Technical Institute located in the Baqubah city of Diyala governorate, which it's have in climatic conditions within the region (latitude 33.74437º North, longitude 44.65735º East) According to the topographical in Figure 3.1. As it is hot and dry in the summer, while frigid in the winter. The average temperature in Iraq ranges from above 48ºC in July and August to below zero ºC in January. The subtropical weather in the Arabian Desert and the subtropical humidity in the Persian Gulf have a direct impact on Iraq weather.
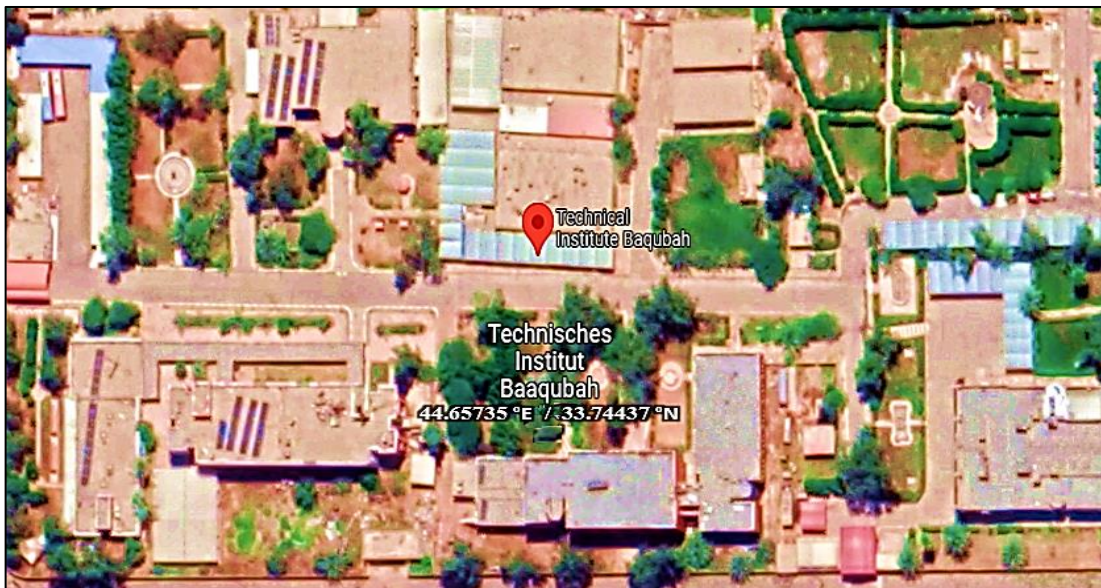
Figure 3.1. The Technical Institute in Baqubah city of Diyala governorate/Iraq.

The goal of this research is to develop two liquefied water-cooling technologies for photovoltaic panels and to analyze the efficiency gains in electricity conversion from light fall when the photovoltaic panels are subject to different water flow rates on both sides of the panels and different pumping times. Spraying water on the front and rear surfaces of the solar panel to remove as much heat as possible. The experimental portion of our present study comprises the use of three mono-crystalline PV module panels mounted on an iron bracket coated with anti-rust paint, with the first panel serving as a reference panel for comparison. Both are attempting to improve solar cell efficiency. Below is a description of the design three panels:

1. The first test was examining the reference panel without any cooling equipment in order to determine the impact of the panel's temperature on its electrical attributes, performance, and efficiency.
2. The second test involved a study of the PV/T upper cooling system in response to changing weather conditions, employing water as a working fluid sprayed of variable flow rates over the front surface of the panel.
3. The third experiment focused on the lower cooling approach, which involved spraying working water on the rear surface of the solar panel with varied flows throughout multiple periods and variable weather conditions.

On the day of the test, the panels for these tests were not all adjacent to one other; but instead, each case its day, and its own panel.

3.2. DESCRIPTION OF EXPERIMENT

3.2.1. The Panel without Cooling System

Utilized (mono-crystalline silicon diode) photovoltaic panels in this study were; Table 3.1 displays the parameters of the PV panels under standard test settings:
 (T = 25 $^{\circ}$C, R = 1000 W/m^2, and AM = 1.5) for comparison as a standard case (STC).

Table 3.1. The Photovoltaic PV Panel Specifications

Parameter	Value
Photovoltaic Panel Type (PV)	IS-100P (Mono-crystalline)
Dimension of the Module (L*W*H)	$1200 \times 540 \times 40$ mm [±2mm]
Arear of PV panel	$\approx 0.63 m^2$
Number of cells	(4×9) = 36 cells
Dimension of the Cell (L*W*H)	125 x 125 mm
Maximum Power (Pmax)	100W
Power Tolerance	[±3%]
Voltage in Maximum Power (Vmp)	17.8 Volts
Current in Maximum Power (Imp)	5.62 amps
Voltage open circuit (Voc)	22 Volts
Short circuit current (Isc)	6.15 amps
Maximum System Voltage	1000 Volts

The installation angle of the PV panels (with an angle of inclination of 33 ⁰C) was adequate for the circumstances of Diyala / Baquba based on the geographical position to receive the greatest radiation fluxes, according to the specifications of the photovoltaic panel presented are given in Table 3.1. On the reference panel, the effect of intense direct heat was studied. Figures 3.2 and 3.3 provide a realistic representation of the experiment as well as an experimental plot.
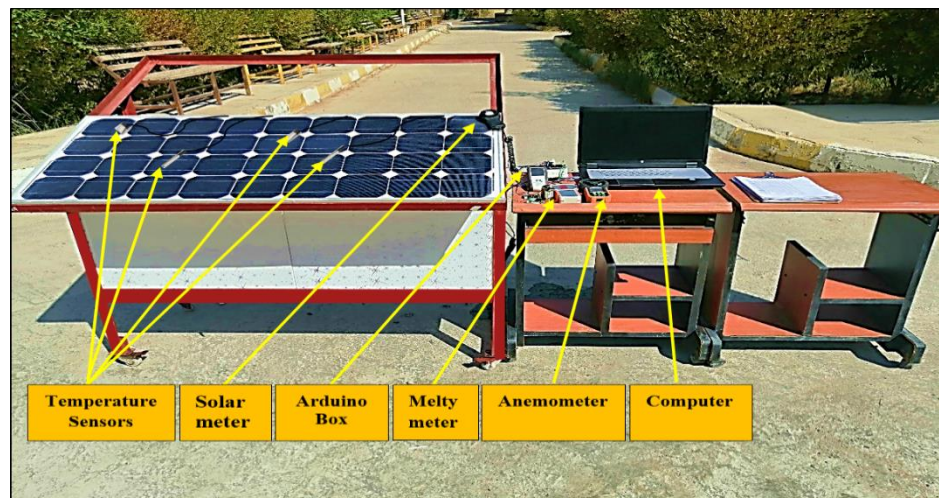
Figure 3.2. Outdoor experimental setup (uncooling panel).
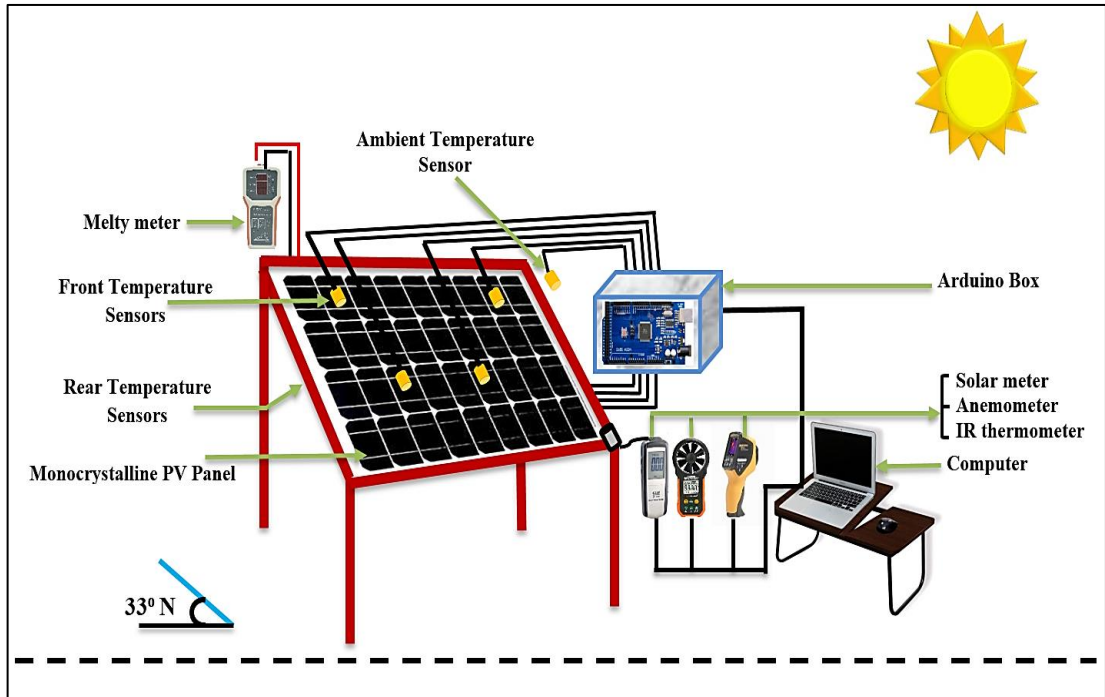
Figure 3.3. Schematic diagram of the experimental setup (uncooling panel).

3.2.2. Design of the Proposed Cooling System

Two cooling systems we used to dissipate high temperature and enhance the panel's efficiency. In both techniques, we used the panel with the specification shown in Table 3.1. According to the experimental schemes, we describe the technical aspects and equipment for each of them.

3.2.2.1. Upper Cooling Technique

The purpose of the upper cooling system, according to the experiment is to dissipate as much heat as possible. This has a direct impact on power productivity as well as efficiency. The solar panel is fixed on an iron frame base supported by a (PVC) tube fixed on top of the photovoltaic panel and water spray nozzles are placed on it, see Figure 3.4. Based on the set of fluxes that occur during the work and through the measuring devices used, we learn about the maximum output power as well as the efficiency of the solar panels. Figures 3.5 and 3.6 show the upper cooling case, which included in situ imaging as well as the experimental plot.

| Anemometer | Melty meter | Solar meter | Temperature Sensors Front &rear | Water drain | Spray Nozzle | Arduino Box | Flowmeter | Water Source |
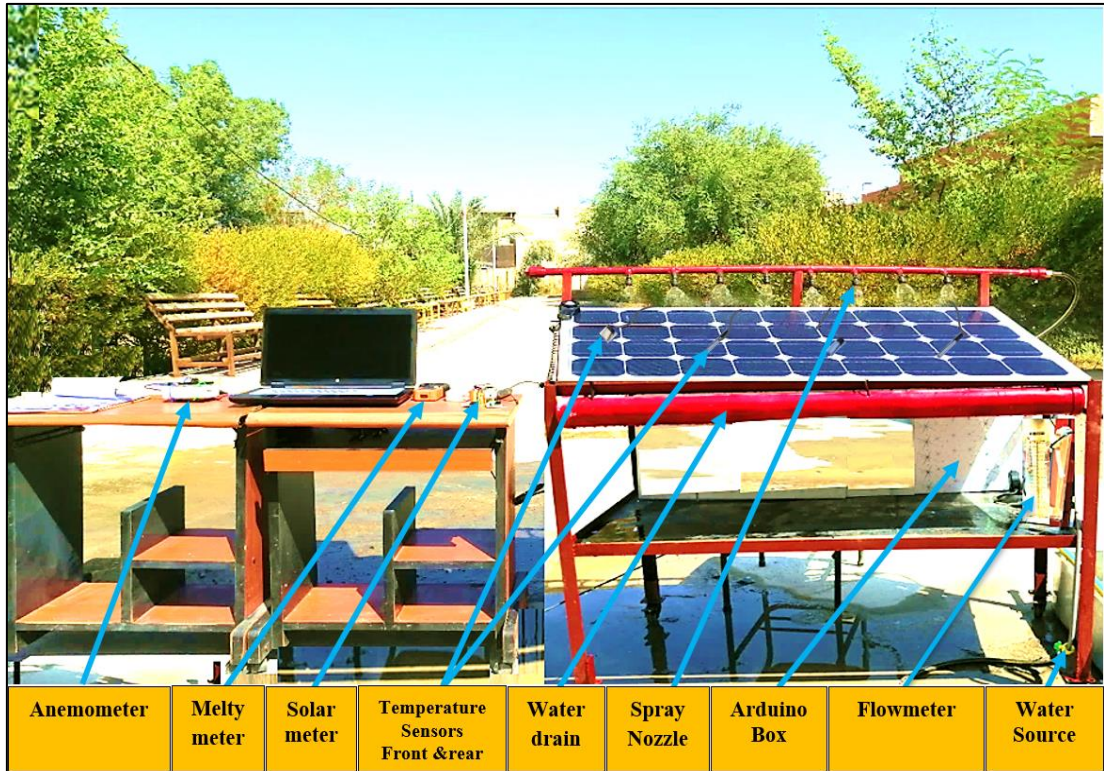
Figure 3.4. Outdoor Experimental Setup (Upper Cooling).

Figure 3.5 Upper water nozzle spraying.
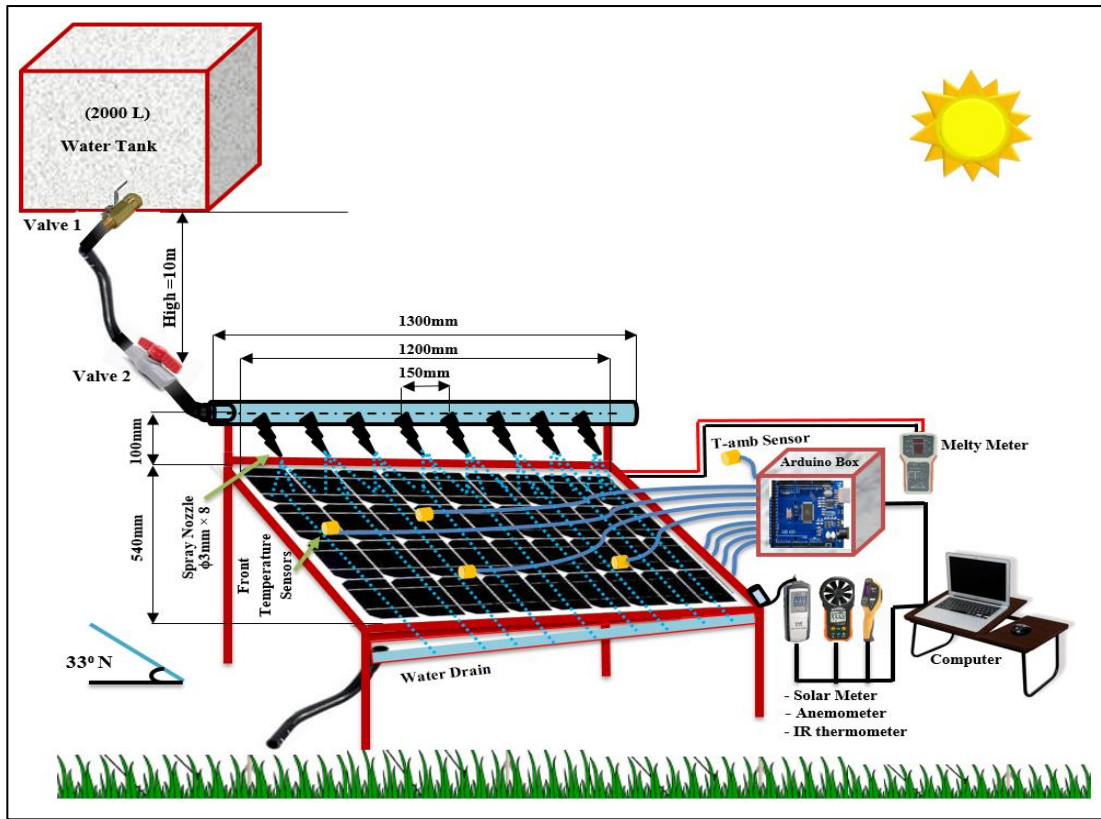
Figure 3.6. Schematic diagram of the experimental setup (Upper Cooling).

3.2.2.2. Lower Cooling Technique

Lower nozzle cooling is a second cooling technique, which allows to remove a significant part of the thermal energy from the surface of the PV panel using a panel with the same parameters as Table 3.1. It is characterized by the repetition of the cooling system shown in paregraph (3.2.2.1) except that the nozzle is now located at the rear of the panel, with measurements and dimensions available in the indicative diagram, depending on the number and shape of the nozzle used and its location see Figure 3.7. Nozzles at maximum flow rate 3 L/m as shown in Figure 3.8, the total orifices are symmetrically dispersed at the rear of the panel at an acceptable angle to ensure that the water coming out of the nozzle completely covers all the panel area, and as shown in the pilot diagram 3.9. The measuring equipment shown can be used In the pictures to see how much energy and efficiency can be enhancement.

Figure 3.7. Outdoor Experimental Setup (lower cooling).

Figure 3.8. Lower water nozzle spraying.

51
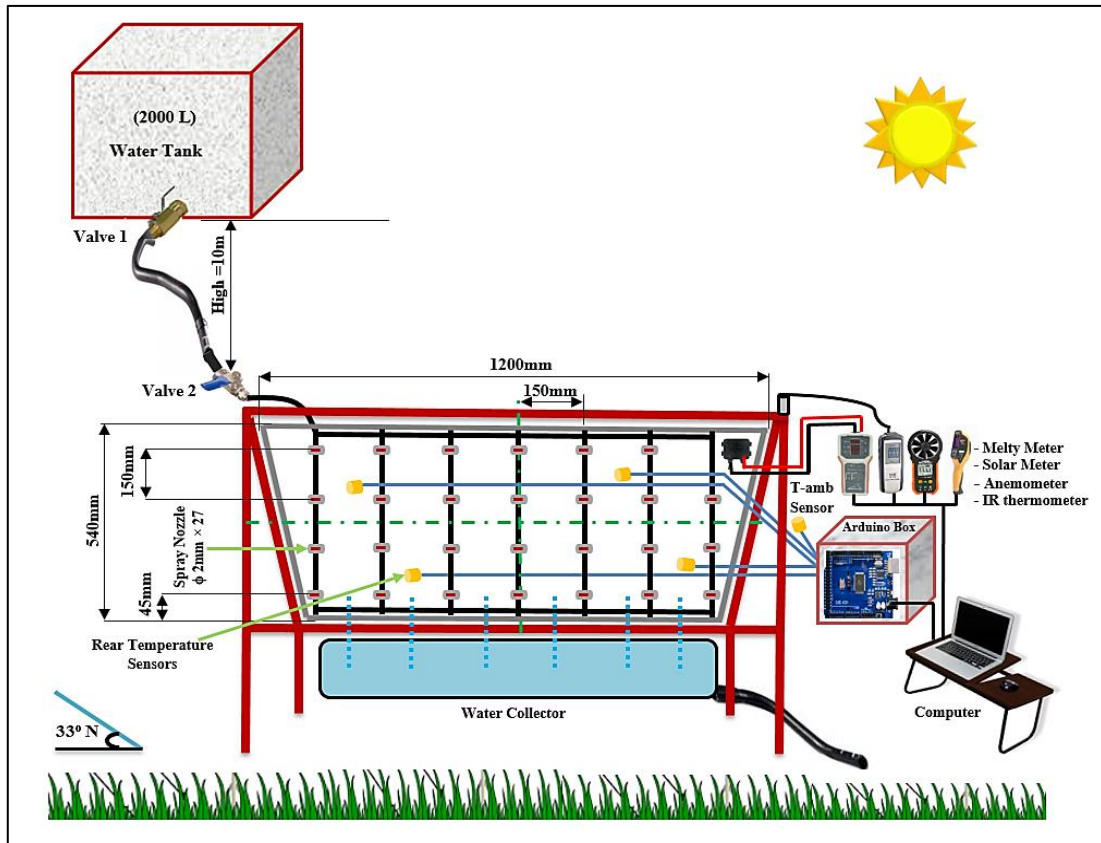
Figure 3.9. Schematic diagram of the experimental setup (lower cooling).

3.3. EXPERIMENTAL COMPONENTS

3.3.1. Uncooled System Design

3.3.1.1. Photovoltaic Panel

In these experiments, three photovoltaic panels were used; each test had its panel. The solar panels used were of a certain type (IS-100P). It is monocrystalline, and consists of 36 cells, as shown in Figure 3.10. Under (STC) standard test conditions, the solar panel can generate a maximum of 100 W of power. When exposed to maximum solar energy, it can usually generate current about 5.62A. As mentioned earlier, the technical features of this solar panel were enumerated in Table 3.1. It should be noted that its dimensions are PV (1200 mm × 540 mm), which makes it ideal for study.
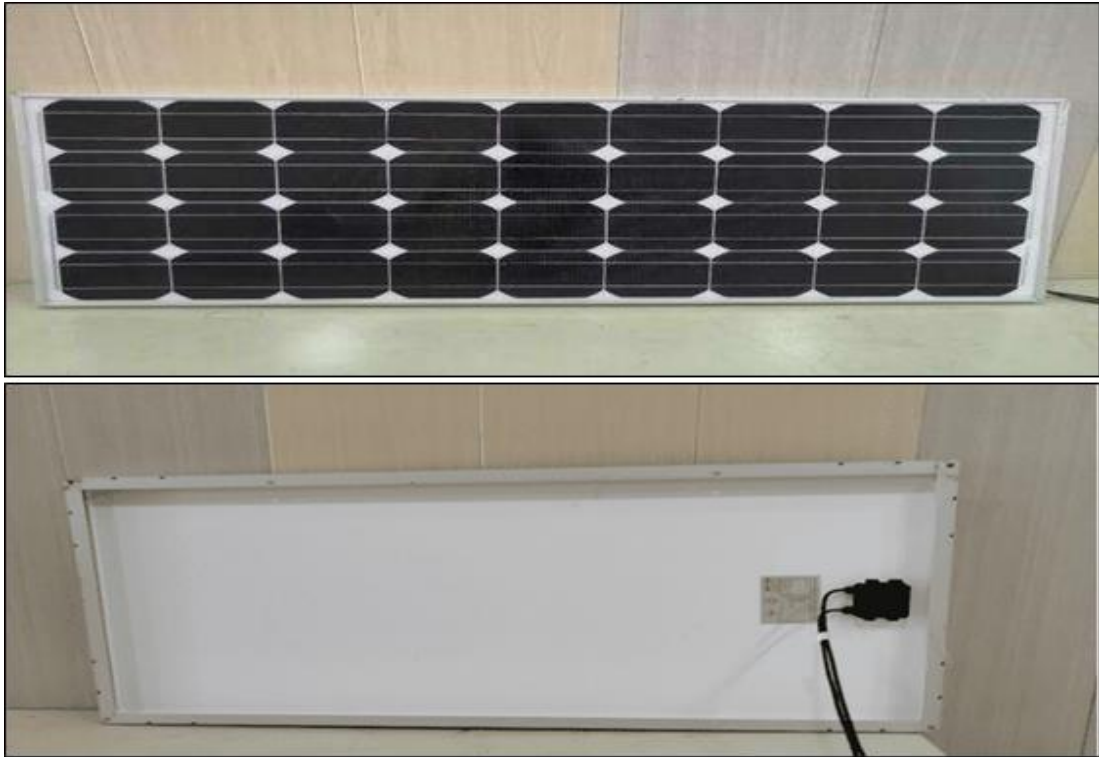
Figure 3.10. The front and rear surface of the photovoltaic panel in this study.

As shown in Figure 3.11, the key component of a photovoltaic panel is depicted. The panel employed in this investigation consisted of (9×4) gives us (36) from monocrystalline solar cells, whose parameters are listed in Table 3.1. In the specification table, the maximum power point voltage (Vmp) and current point (Imp) are also stated, along with the maximum power output at 1000 W/m^2 and 25 °C.
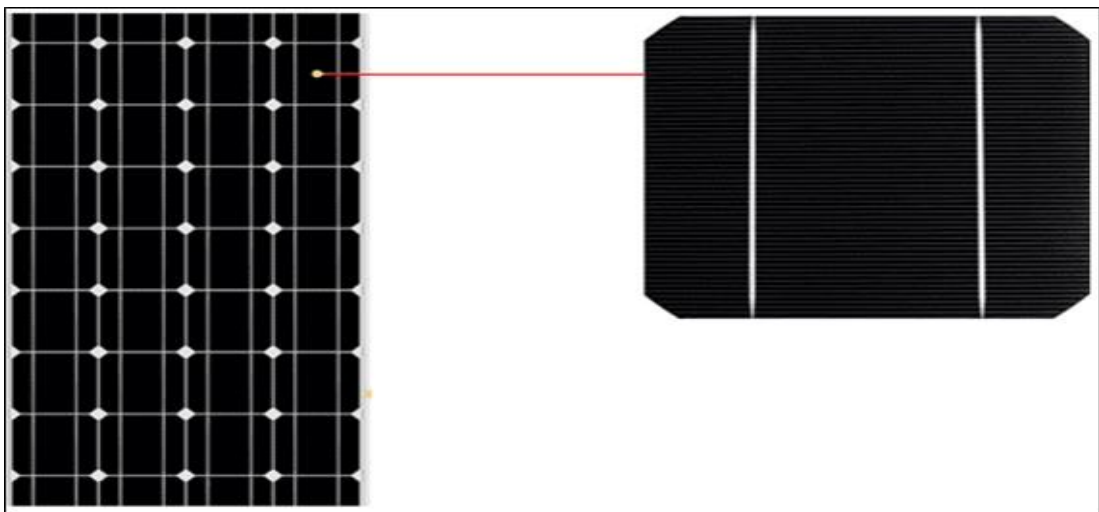
Figure 3.11. Mono-crystalline silicon photovoltaic cell.

3.3.1.2. Steel Stand

In our current study, an iron stand supported the solar system. It measures (1400 mm x 550 mm). The stand is made of a base on which the panel rests, as well as legs at the end supported by movable rollers. As well as directing it to the south at an angle of inclination of 33º. For durability and lightness, the stand consists of steel angles and rulers 1.5 mm thick and coated with anti-rust paint.

3.3.2. Cooling System Design

The cooling system requires additional elements to provide everything required to achieve actual cooling, as the photovoltaic panel is the most important and basic element in all the tests, and as a result it was used in accordance with the parameters mentioned in paragraph (3.3.1.1), but by applying cooling technique to it. Material and components as below:

3.3.2.1. Water Tank

The galvanized steel tank utilized in both cooling systems has a zinc coating on its surface. The zinc coating protects the metal against corrosion, and the walls of the tank are painted to prevent corrosion. Because it is insulated with a galvanized layer, galvanized iron has a stronger rust resistance than plain iron, in addition to having a canopy that protects it from the hard summer heat and averrable weather. Water tank with a capacity of up to 2000 L made with 1.5 mm thick sheets. Two throttle valves are located in the tank, which control the flow of non-potable water to the experiment site at the bottom of the building. Because the tank is in the upper portion of the building, 20 m from the test site, a throttle valve is installed at both the top and bottom to control the amount of water and flow rate entering the cooling system pipe. This creates a strong and effective pressure.

3.3.2.2. Valves

The flow of water from the tank is controlled by two major throttle valves, one at the tank's outlet and the other at the entrance of the upper or lower feed pipe. The first valve, located at the tank opening, is same in both technologies; while the second valve, which feeds the cooling water tube, is different depending on the diameter of the cooling nozzles' feeding, tube. The completely open valve permits a maximum flow rate of 1-3 L/m. The two types of valves are seen in Figure 3.12.

Figure 3.12. Upper and lower cooling technique valves.

3.3.2.3. Pipes

Different sizes of plastic tubes and rubber couplings were employed. The feeding tube for the upper cooling nozzles was made of (PVC) with a nominal diameter of 1/2 inch and was perforated using an appropriate perforating machine to allow the water nozzles to be installed. The lower cooling nozzles' feeding tube is constructed of a flexible rubber material with a diameter of 5 mm that is firmly closed on the nozzle by pouring glue on it to ensure no leakage, as well as plastic and iron accessories that were employed as connectors between the cooling system's components. These tubes are closely attached to one another, ensuring that the flow procedure is completed without any leakage. Pipes, accessories and connections in Figure 3.13.
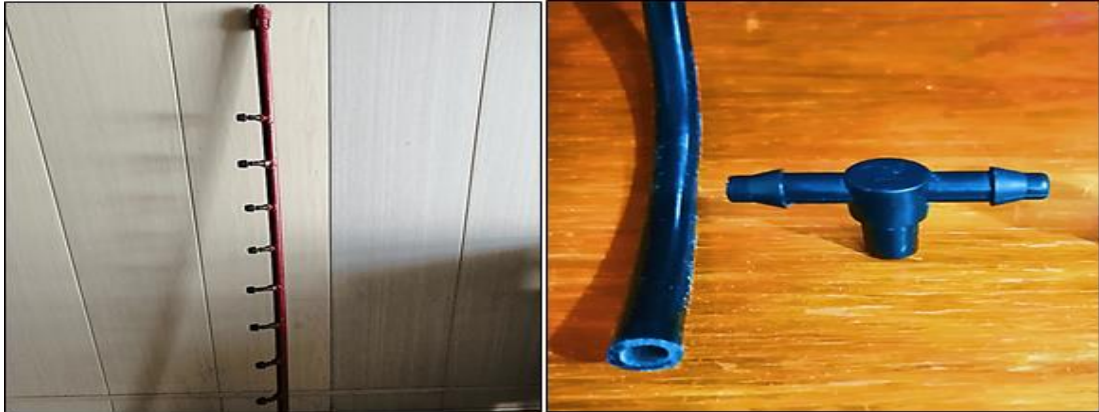
Figure 3.13. Upper and lower cooling technique pipes.

3.3.2.4. Water Spray Nozzles

Cooling technique on the upper and lower types, the water spray nozzles must be installed according to the required measurements and designs in order to achieve cooling. Because each system had its own nozzles, the water spraying nozzles differed between the two techniques. We inserted eight plastic nozzles with a 3 mm flowing hole, twisted on the tube at an angle of 60º from the axis during the upper cooling in the hopes that the flowing water would create a hierarchical flow to cover the biggest surface of the panel. The suggested method called for the employment of 27 nozzles with a water flow hole of 3 mm mounted on rulers spread horizontally on the rear surface of the solar panel according to consistent measurements, the shape of the upper and lower nozzles illustrated in Figure 3.14.
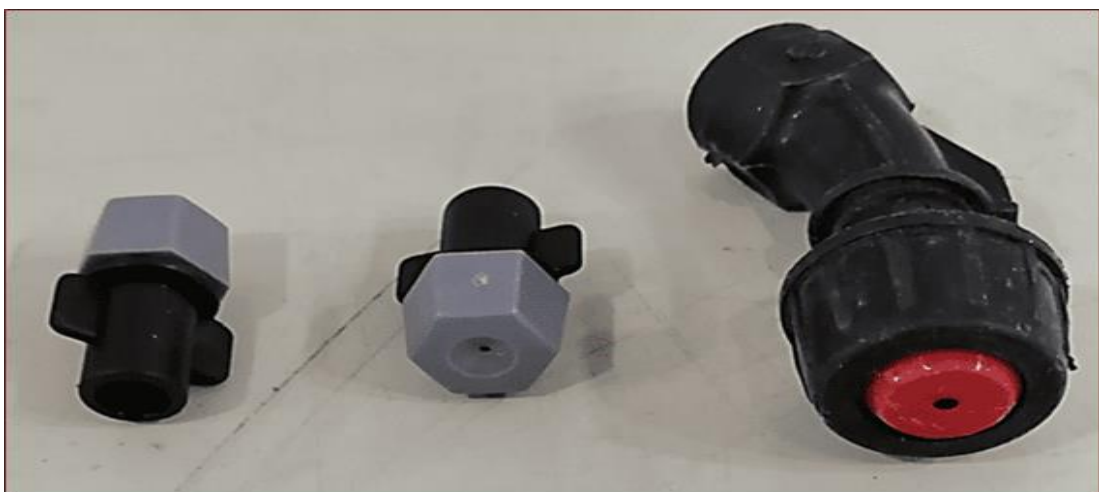
Figure 3.14. Upper and lower cooling technique nozzles.

Because the nozzle is roughly 30 mm away from the panel's surface, installing the nozzles with this number and at a 90º from the axis enable a direct and focused spray flow perpendicular to the panel and covering the biggest feasible area. Finally, nozzles with both technologies can get water through the plastic tubing and rubber connections installed above and below the panel, as indicated in the Figures 3.15 and 3.16.

Figure 3.15. Experimental setup module upper cooling technique nozzles.

Figure 3.16. Experimental setup module lower cooling technique nozzles.

3.4. MEASURING INSTRUMENTATION AND EQUIPMENT

In order to achieve the present study's goal and learn the results. Measuring tools and equipment shall be available as detailed below:

3.4.1. Digital Solar Power Meter

A solar radiation meter (CEM DT-1307) (sunlight power) is a device that measures solar energy by aiming its lens at the sun and setting it parallel to the solar panel. This instrument calculates the amount of direct solar radiation based on its intensity resolution of clarity: $1BTU/ (ft^2*h)$. The unit of measure is W/m^2. Figure 3.17 depicts the instrument.

3.4.2. Digital Anemometer

A Digital Anemometer Model (PM 6252A) used into this study to measure wind velocity, which ranges from zero to 30 m/s with a 5% accuracy. Figure 3.18 displays the equipment.

3.4.3. Solar Panel Multi Meter

The current study's cooling system is meant to improve the solar panel's electrical characteristics, thus the (elejoy WS400A) meter indicated in Figure 3.19 should be employed. The power rating range is 0.1~ 400 W and more information may be found in the appendix. During the test, its functioning principle is demonstrated by connecting its poles to the power outlet placed behind the solar panel, allowing us to determine the voltage, current, and generated electricity.

3.4.4. Mechanical Flowmeter

The use of a gauge to control the flow of the mass of water exiting the tank is required for several flows. In our present experiment, we are using a (Z-3001) type flowmeter listed in the Figure 3.20. Its specifications are indicated in the appendix with a flow rate of 0.5 – 8 L/m and a restricted operating temperature of 4 – 80 °C.

To manage the flow rate of water entering the pipes in both cooling systems, the pressure must be set at a minimum of 6 bar. There are two approaches to guarantee that the flow rate corresponds to the planned mass: either by repeating the pumping experiment in volume until the desired flow is attained, or by using a graduated volumetric flask.

Figure 3.17. Digital solar power meter

Figure 3.18. Digital anemometer

Figure 3.19. Solar panel multi meter

Figure 3.20. Flowmeter

3.4.5. Temperature Measurements

The surface temperatures of a solar panel may be measured using three distinct instruments, each of which has its own set of benefits, which we will listed through below:

3.4.5.1. Data logger and accessories (Arduino)

The Arduino type (MEGA 2560) is a device that uses sensor wires to read data from the surface of a solar panel. Arduino is a free and open source electrical platform that can turn incoming input into a digital file. The tools and accessories attached to it, as well as its construction as we utilized it in our current investigation are depicted in Figure 3.21.

Mega Card for Arduino Digital input/output with 54 pins, a 16 MHz crystal wave checkered, USB for digital data transfer, electrical outlet, ICSP header, reset and power on button are available on the microcontroller board, in addition to 16 analog inputs and 4 UARTs (hardware serial ports). For that, all of these outlets are available. As soon as you start inspecting and testing, simply use a USB cord to connect it to a computer or turn it on using an AC to DC converter or battery, providing the proper period to switch between automated test intervals. The Vero board is also a basis for the Arduino board, since it connects all of the components, including sensors, cables, and pins. It receives DC power from the source and distributes it to all components, on one side, it connects to the Arduino board, while on the other, it connects to the. The data receiver to take the signal from the board's sensors and relays it to the Arduino. As a result, the reference becomes something that is assured to work it is saved on a computer or similar device. Table 3.2 shows the properties of the sensor (DS18B20), which is an important component of the Arduino and is more typically utilized in cooling strategies by functioning as a thermometer in our current investigation of its water-resistant feature. Its temperature accuracy is ($\pm$ 0.5°C) from the range -55°C to 125°C. Its sheath was utilized to monitor the surface temperature of the board on one side and the ambient temperature on the other during the test days.

Table 3.2. Specifications of waterproof temperature sensor.

Power Supply	3 V – 5.5 V
Size of sheath	6 × 50 mm
Size of sheath	"RJ11/RJ12, 3P-2510, USB"
Connector	"Red: VCC, Yellow: DATA, Black: GND"
Pin definition	1meter, 2m, 3m, 4m are available upon request
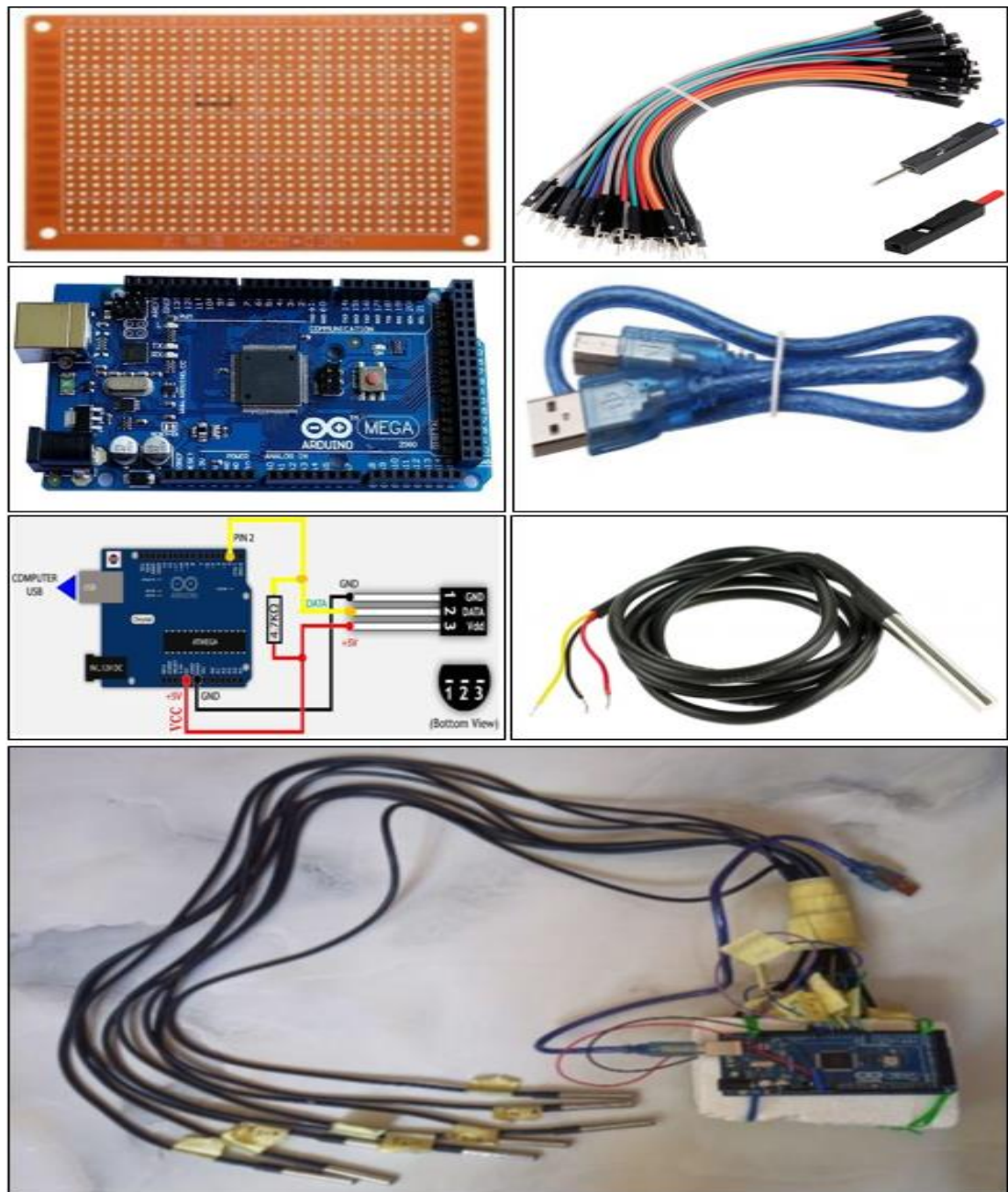
Figure 3.21. Assembly accessories Arduino of data acquisition.

3.4.5.2. Sensors

Two types of digital thermometers were used to test the acceptability and accuracy of the sensors, the first (TPM-10) used to measure the ambient temperature working with a supply voltage of (1.5VDC) and the other temperature controller module SONGLE (W1209) that worked as a digital sensor to display the temperature with an input and an output voltage of (12VDC). Keep in mind that these two sensors are provided to support the sensors used in the Arduino system and to evaluate their accuracy when testing with and without the daily cooling system by taking the rate of each individually or jointly to enhance the accuracy of the data. Figure 3.22 shows the two types respectively.

Figure 3.22. Digital temperature sensors.

3.4.5.3. Infrared (IR) Camera

One of the helpful measurement techniques for measuring the surface temperature of the PV module is IR thermography. Thermography is defined as the measuring of thermal energy released from an object using an infrared and measurement camera. Infrared or thermal radiation has a wavelength range that is longer than visible light,

which is why infrared is not visible. Every material that has a temperature greater than zero emits heat. As a result, the hotter the material, the more IR radiation it emits. Infrared cameras view visuals that are distinct from what human eyes perceive. These cameras can detect and display infrared radiation without coming into physical touch with the target. A thermal camera module (Fluke VT04) was employed in this study. To calculate the average temperature on the photoelectric surfaces, the camera is infrared (IR) worked. May be seen Figure 3.23 shows an image of the camera (IR) with the marking the main components.
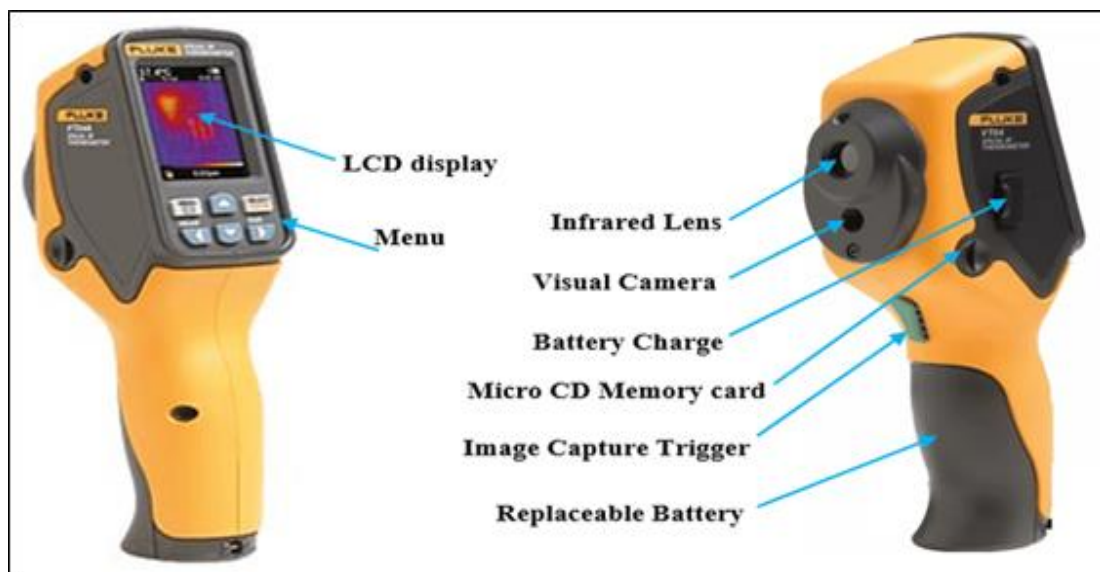
Figure 3.23. Photograph of an infrared camera.

The photos recorded by the infrared camera are saved on the device's SD memory card. The SD memory card is removed and inserted into a USB card reader before being transferred to the computer for image storage. The photos collected on the SD card are analyzed using the Smart View Computer. Image analysis is done using digital numbers that represent the surface temperature as well as the precise capture time, as seen in the schematic Figure 3.24. Near and far guiding can also be used to manage distance and approximation. It also offers a number of different clarity settings for displaying the temperature and its gradations. The emissivity utilized in this experiment ($\epsilon = 0.95$), as well as the exact distance for the object and the temperature of the atmospheric, should all be considered when sending object characteristics to the camera.
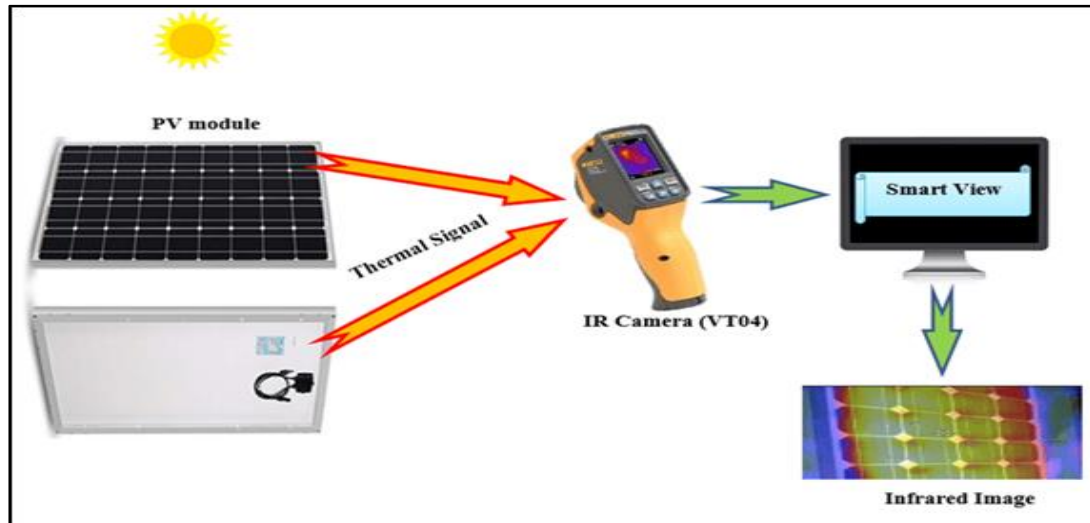
Figure 3.24. Setup for thermography outdoor.

3.5. EXPERIMENTAL PROCEDURE FOR PV

During August 2021, three south-oriented and tilted 33 °C photovoltaic panels were prepared for experimental application. This month is sunny, bright, dry and hot, with temperatures reaching 60 °C. Data were collected over the course of a month for results. However, before every test, there are a few fundamental steps that must be followed in order for the findings to be useful, which we will detail below:

1. Clean the front and rear surfaces of the photovoltaic modules of any dust or dirt carefully before placing and installing the panel on its holder.
2. Ensure that the temperature sensors are mounted by contacting the front and rear surfaces, and we are keen to cover them from the top with an opaque tape. In addition to attaching the thermocouples to the data logger (Arduino) and ensuring the USB connection through computer.
3. During all testing periods, we provide an electrical supply to the computer so that so that it may continue to work without interruption.
4. Startup computer and the data recorder (Arduino), as shall be prepared equipment and sensors and operate all electrical measurement tools before start any step of experiment.

5. Before beginning any stage of the experiment, make sure that the computer and data logger (Arduino) are synchronized, and that the batteries in all electrical gauges as well as the equipment and sensors are fully charged.

6. The water level in the feeding tank must be monitored to ensure that it is entirely filled in order to obtain a high water pressure.

Following the installation of the panels and provision of the necessary supplies and equipment, the trial setup was required. During the month of August, several tests were conducted to evaluate the performance of solar panels with and without cooling, following the procedures below.

3.5.1. Uncooled System

The uncooled system includes the following components:

1. The first test of the photovoltaic panel was done in the first ten days of August 2021, meaning from 1 to 10th august, however days 8, 9 and 10th were chosen from it as a relative rate without any cooling technique by attaching all of the measuring equipment as well as the sensors as shown in the previous photographs. According to weather data in these days, the effect of rising temperatures on its effectiveness of panel has been investigated.

2. Devices and equipment allowed us to collect experimental data from 7:00 AM to 3:00 PM, which included capturing data every 10 minutes until the time to halt the test was reached, following which the findings were evaluated using the permitted programs.

3.5.2. Upper Cooling System

The upper cooling system includes the following components:

1. The second test entailed testing according upper cooling technique utilizing that have been described spray nozzles previously. The tests were carried out from August 11 to 18th, with three specific days 11, 12 and 13th chosen to collect the

data by programming the Arduino every ten minutes to record the temperature of the solar panel.

2. To guarantee that the biggest area of the panel is covered with water, the spray nozzles are developed based on two primary factors: the diameter of the nozzle aperture and its number. The eight nozzles were attached to a plastic tube (PVC) that was blocked on one end and connected to a source originating from a 2000L upper tank filled with water located at the top of the building, 10 m away from the experiment location.

3. Two valves were Installation, one in the front of the top tank and the other at the intake of the pipe carrying the nozzles. Controlling the valves as well as constructing and placing the nozzles at a 60° from the horizontal pipe plane allowed the needed flow to be accomplished. The flows were tested according to varied percentages, as they were 1, 2 and 3 L/m for each of the three test consecutive days, and so the data collection technique was based on each ratio. We also find all dimensions, distances and design measurements through the pilot scheme 3.6.

4. Depending on the measuring devices and sensors deployed on the front and rear panels, the experimental procedure was monitored from start to finish in the allotted period, it is worth noting that the radiation intensity was measured by positioning the scale above the photovoltaic panel surface to ensure the tilt angle. The wind speed was determined at a distance of 30 cm from the panel.

5. Over the course of eight days, the test was repeated, with three days chosen as a relative average of the findings. The data was gathered and sent to a computer, where it was then analyzed using the necessary analytical programs to compare the efficiency of the panels with and without the use of cooling technology. This cooling system's substantial goal is to get dissipate of as much heat as feasible while keeping the panel cold for as long as feasible, also cleaning it of any dirt that might obstruct radiation and diminish effectiveness.

3.5.3. Lower Cooling System

The lower cooling system includes the following components:

1. The lower cooling system was the subject of the third experimental setup, which was carried out in the final ten days of August, with three days 19, 20 and 21th chosen as a relative average for preparing the data. Every ten minutes, the test was repeated in the data recording.

2. The mesh of the spray nozzles in the lower cooling is built in a completely different way than its predecessor. It required Installed 27smaller nozzles with an opening of 2 mm or less, straight and not twisted, affixed to horizontal rulers with a strong adhesive, and connected to a network of plastic tubes, open on one end and tightly closed on the other to prevent water from leaking through, according to the measurements and dimensions given in the Figure 3.9. This system gets its water from the same tank that as mentioned previously at the top of the building.

3. The existence of two valves, one at the front of the top tank and the other at the entry to the mesh tubes of the nozzles, as well as the flowmeter, were two important instruments that tried to manage the rate of various flows in the current study. The flows were carried out on certain days in which ranged from 1-3 L/m. They were then distributed among the ten days in test August, with varying flow rates, and chose 19, 20 and 21th from the same month as relative rate and deemed actual test days, respectively, with a different flow rate on each day.

4. The instruments and equipment were ready for the whole ten-day testing period. The Final data was collected by using sensors to monitor the procedure during the experiment's days and register weather conditions. Sending data to a computer and evaluating the findings allowed us to compare the three techniques used in our present study and determine which one increases the PV panel's efficiency and performance.

It is worth mentioning, the harshness of Iraq's hot weather and its dryness in summer, especially in August, led to a scarcity of irrigation water. Therefore, there was a need to take advantage of the falling and excess cooling water in the lower basin attached to the design of the system due to the implementation of the two systems (upper and lower cooling) in irrigating crops and gardens as an economic benefit from the principle of no waste in the water level.

PART 4

RESULTS AND DISCUSSIONS

4.1. INTRODUCTION

The performance of photovoltaic panels without cooling, as well as strategies to improve it using different types of upper and lower cooling nozzles, is the focus of this chapter's results. External testing was carried out in (State of Iraq/ Diyala Governorate) in a tropical climate. The month of August of the year 2021 was chosen with three days for each case of examination and the average was taken on the grounds of the Technical Institute building at coordinates (33.3ºC north and 44.36ºC east) south with a variable inclination, usually on a sunny and clear summer day. The readings were recorded every ten minutes, and an average of half an hour was taken from 7:00 AM to 3:00 PM.

In this chapter, we review the experimental results of the three cases, as follows:
Case 1: uncooling test; Case 2: cooling of the panel by an upper nozzle at a flow rate of 1, 2 and 3 L/m. Case 3: is similar to Case 2, except that the panel is cooled by a nozzle from lower at flow rates of 1, 2, and 3 L/m, and their efficiencies were compared.

4.2. WEATHER DATA

Atmospheric conditions can be regarded as a vital element in the amazing performance of the cells because the photovoltaics are installed outside and subjected to external climatic variables that differ from one place to another. As a result, the PV cell's efficiency and productivity differ from one site to the next. Experts and solar producers have pinpointed the parameters at which PV modules work at their best. The sun's intensity is 1000 W/m^2, the temperature is 25 ºC and the amount of air is 1.5 AM.

These air needs are restricted; it may be challenging to deal with both of them at the same time, for each region and their exceptional circumstances, which may differ from these requirements. Below is a summary to cover the main environmental component of Iraq's conditions in the following paragraphs [58].

4.2.1. Solar Radiation

Figures 4.1 shows the radiation cases recorded during the month of August 2021 from the hours of 6:00 AM to 6:00 PM, for the global average radiation. In general, the solar radiation range is 500-1000 W/m^2 at the highest rate of solar radiation. During this month, the maximum-recorded value of global radiation was 888 W/m^2 at 12:00 PM, while the Figure 4.2 summarized the condition only for the test at 7:00 AM to 3:00 PM for every half hour of the day. The photovoltaic modules convert most of the incident radiation into energy, while the remainder is stored as heat within the panel due to the high temperature of the PV module when it is operating.
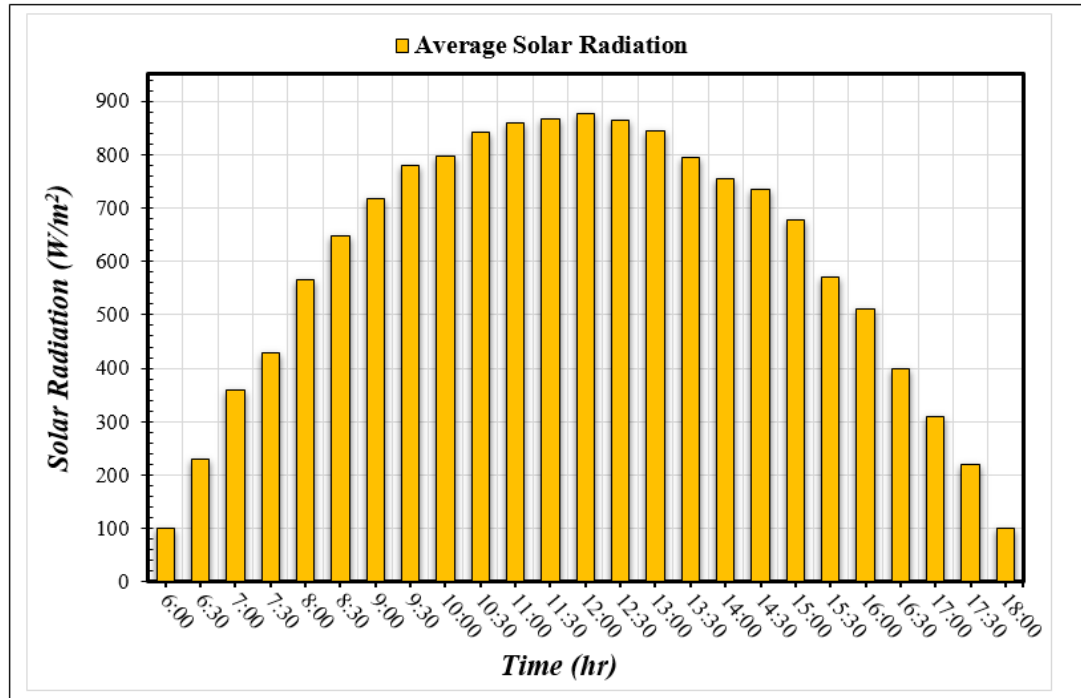
Figure 4.1. Variation of radiation from sunrise to sunset in August 2021.
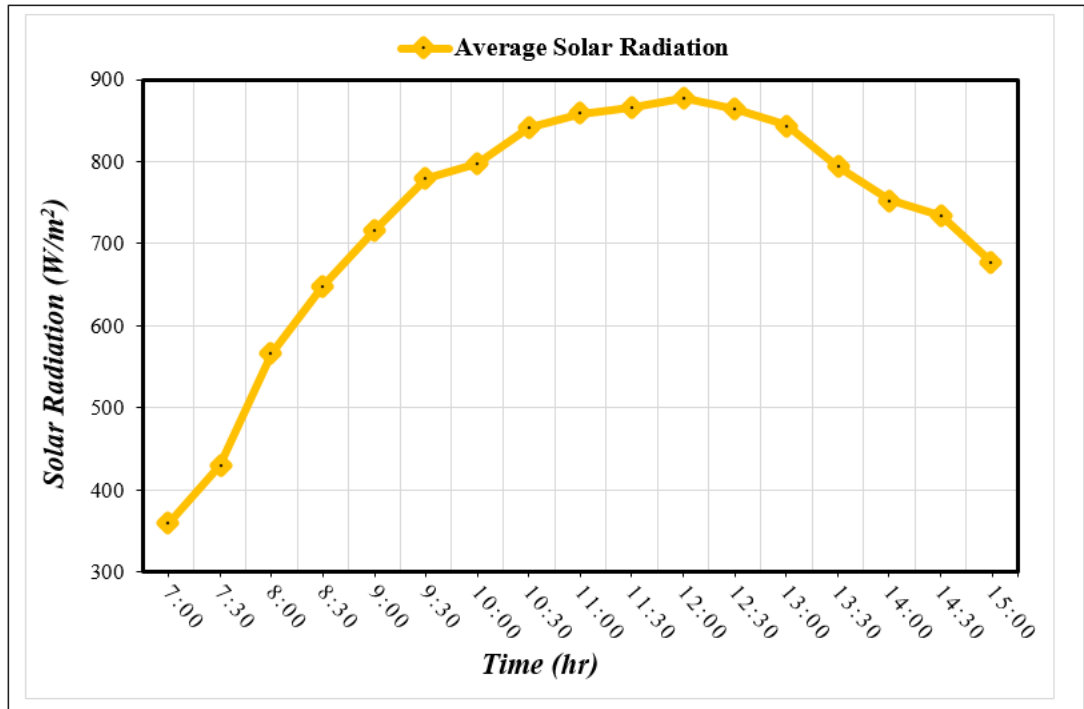
Figure 4.2. Variation of Solar Radiation during the Testing days in August 2021.

4.2.2. Ambient Temperature

Figure 4.3 depicts the average ambient air temperature in August 2021, as well as the actual photovoltaic panel testing days during that month. Despite the fact that the greatest temperature occurs at 52 °C, the Arduino recorded the highest average temperature at 1:00 PM. The reason for this is the absorption of radiant heat during the day. Figure 4.4 depicts the average ambient temperature during the actual testing hours of days from 7:00 AM to 3:00 PM. Figure 4.5 studies the effect of changing ambient temperatures on the amount of irradiation falling during the day since the hour from 6:00 AM to 6:00 PM during August 2021.
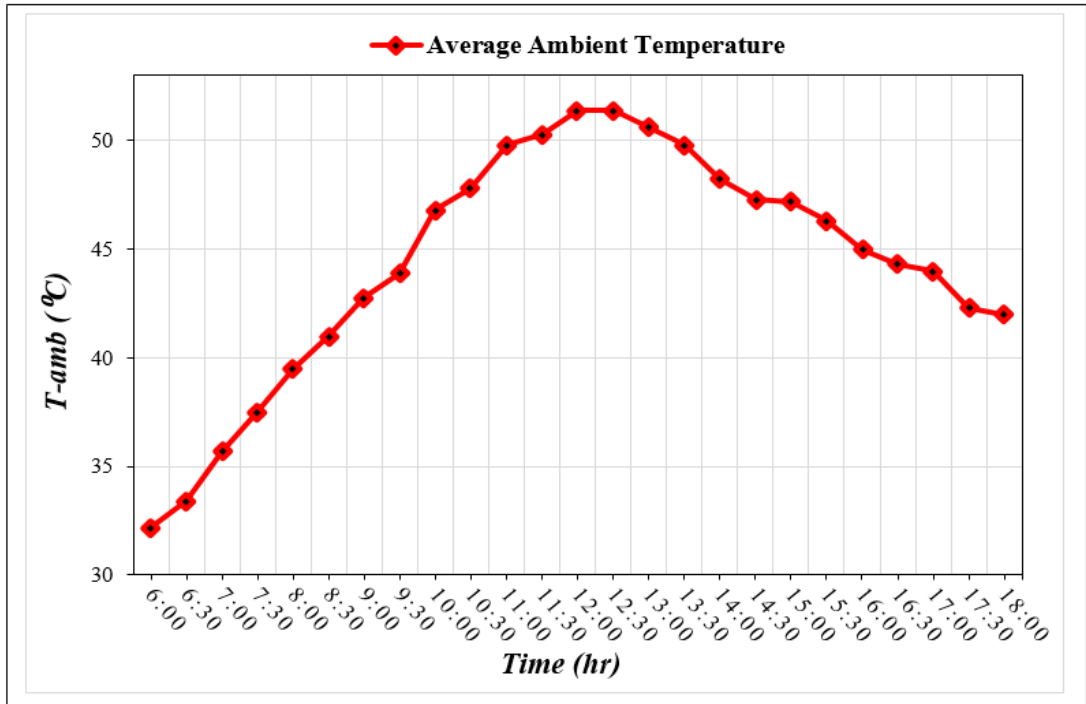
Figure 4.3. Temperature variations with time during August 2021.
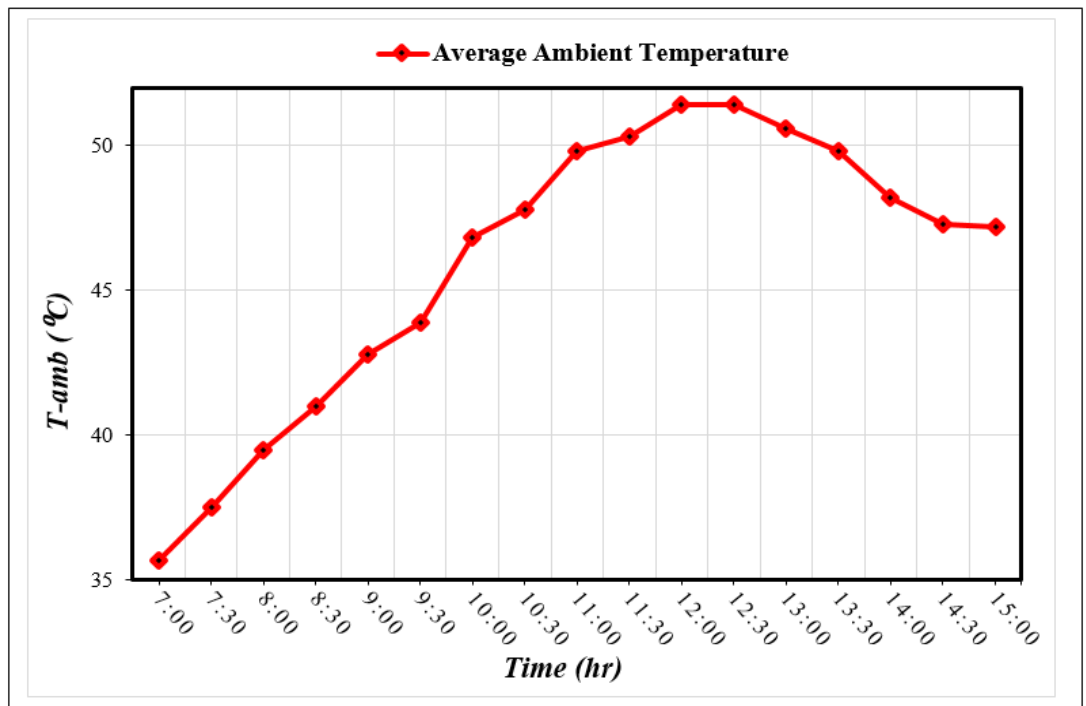
Figure 4.4. Changes in ambient temperature during testing days in August 2021.
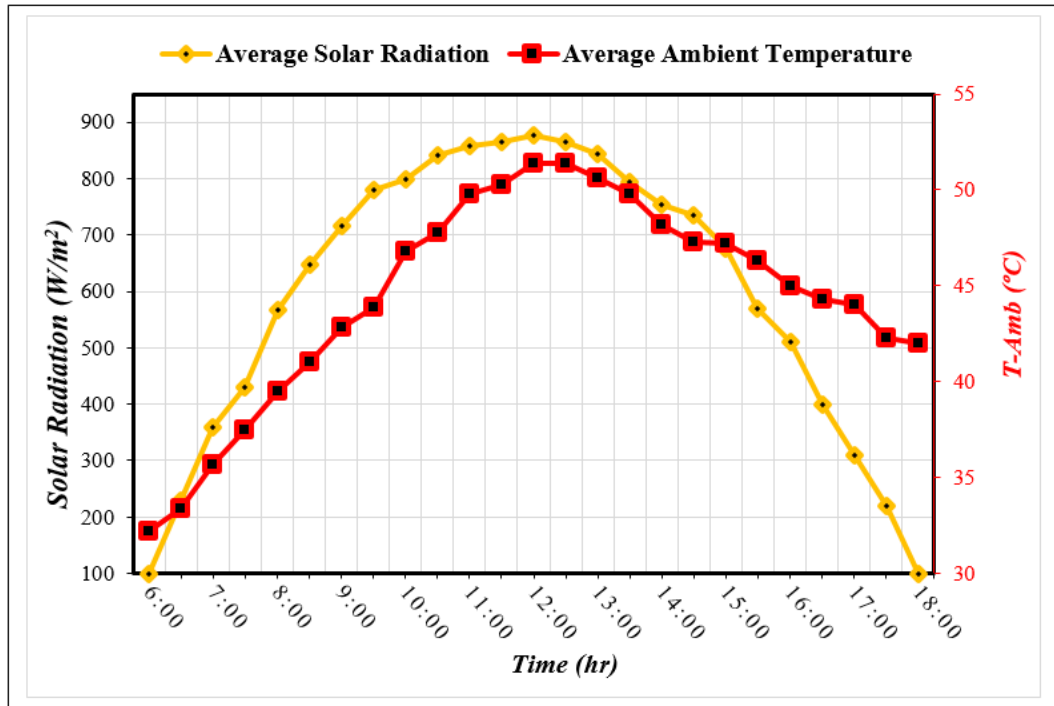
Figure 4.5. Ambient temperature fluctuations with solar radiation in August 2021.

4.2.3. Wind Velocity

The average wind velocity ranged between 0.2 m/s and 0.9 m/s and was recorded at about 0.9 m/s as a maximum value at 16:30 PM, as well as the wind velocity readings for the test days were recorded from 7:00 AM to 3:00 PM, as shown in the Figure 4.6. Figure 4.7 shows the average wind velocity as well as the effect it has on the amount of radiation received from the sun during the test.
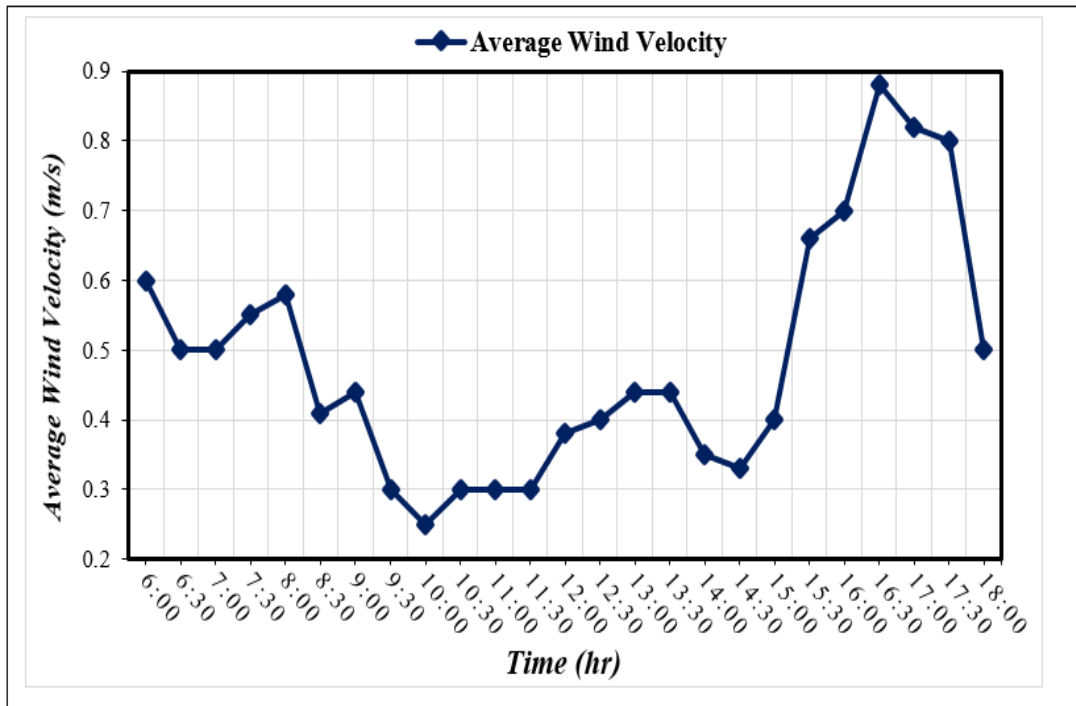
Figure 4.6. Wind velocity variation from sunrise to sunset in August 2021.
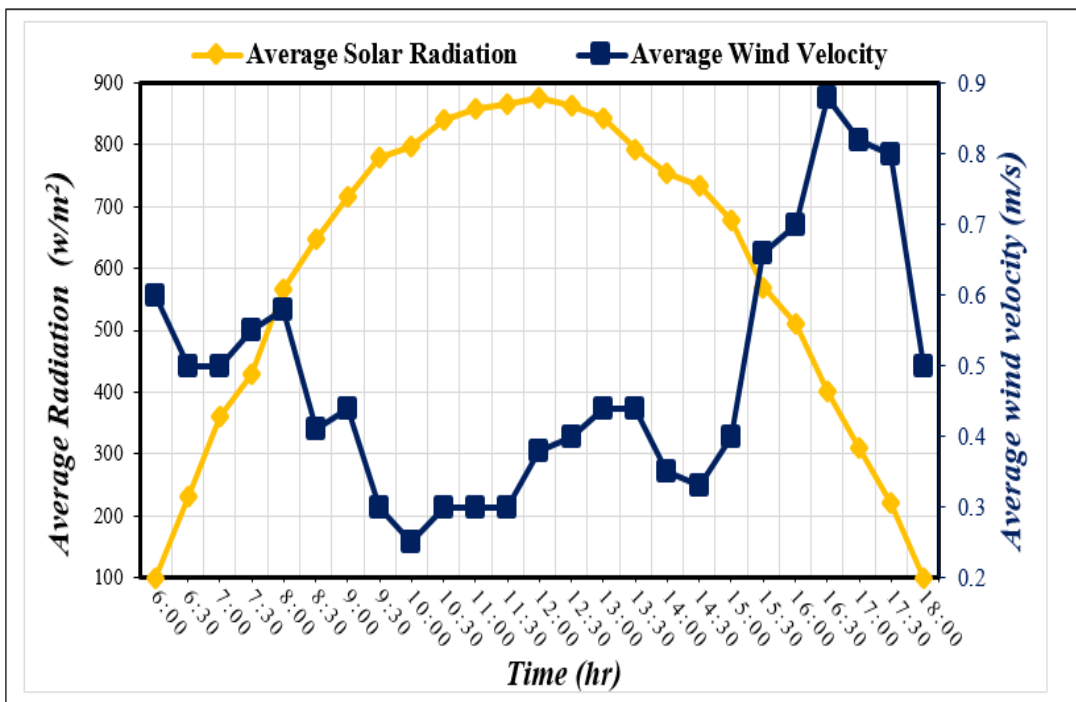
Figure 4.7. Variation in wind velocity and solar radiation with time in August 2021.

4.3. TEMPERATURE OF A PHOTOVOLTAIC PANEL (PV)

Examine the experimental findings in three cases, debate, and evaluate them as follows:

1. The first aspect is to demonstrate the effect of rising temperatures on the performance and effectiveness of PV panels. The tests were examined on an uncooled photovoltaic panel for six days, with an average of 8, 9 and 10th August 2021.

2. The second goal is to look into the impact of the cooling process on PV panel power generation and efficiency by using a water spray nozzle upper cooling technique. A different flow rate 1, 2 and 3 L/m was utilized for three days per flow, and the average was calculated on 11, 12 and 13th August 2021.

3. The third scenario includes studying the effects of the cooling process on solar panel power output and improving efficiency by employing a lower cooling technique for photovoltaic panels with water spray nozzles. The test was carried out in the same way as in paragraph (2), with a different flow rate every day ranging from 1, 2 and 3 L/m over three days for each flow rate, but with different weather conditions. Adopt the average for test days and use it to prepare the results (August 19, 20 and 21th, August 2021).

This system is known as the PV/T system because the cooling system will dissipate the heat from the PV panel and result in higher efficiency. This stored and output temperature can be used in applications (greenhouses, chemical processes, etc.). In other words, we have achieved double benefits from the PV/T system (thermal & electrical).

4.3.1. Without Cooling Techniques (Reference panel)

Produce solar panels made of semi-conductive materials or other materials. This means that a significant amount of the irradiation will result in an increase in the temperature of the PV module. The reduction in band gap of a semiconductor with rising temperature is best understood as the energy of the electrons in the panel decreasing,

requiring more energy to break the bond. Reduced bond energy decreases the gaps in the semiconductor module. As a result, raising the temperature lowers these gaps [59].

4.3.1.1. Front Surface Temperature of the Panel

According to the readings performed during August, Arduino recorded the average surface temperature for the front panel without cooling; it was 66 °C at 12:00 PM, as shown in Figure 4.8.

4.3.1.2. Rear Surface Temperature of the Panel

Obviously, the temperature of the photovoltaic panel gradually increased starting from 7:00 AM, approximately at 12:30 PM, reached its maximum temperature of 70 ⁰C on the same day as shown in Figure 4.9. For some reasons, including the operational duration of the panels, as well as the movement of electrons when generating energy, there was a difference between them and the temperature of the front surface of the panel itself by 4 ⁰C. Figures 4.10 and 4.11 depict the effects of ambient temperature. The greater the ambient temperature, the higher the temperature of the photovoltaic panel, as measured by its performance in the absence of cooling measures. Both figures show that the front panel temperature was 16 °C higher than the ambient temperature, whereas the rear panel temperature was 20 °C higher at 12:00 PM.
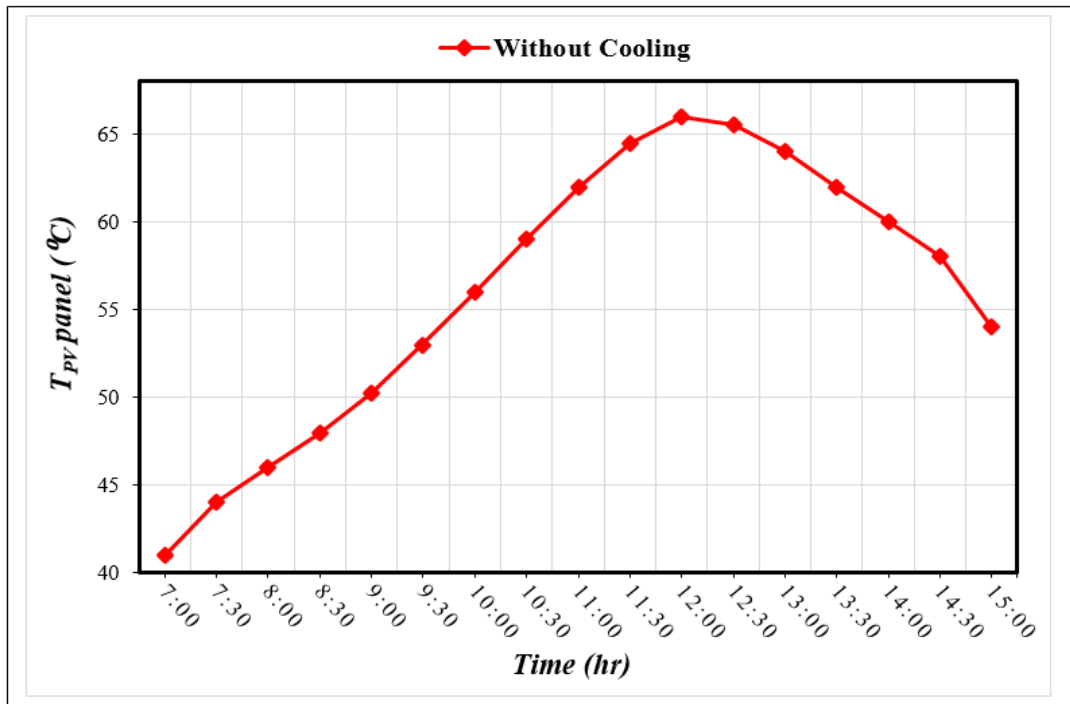
Figure 4.8. Surface temperature of the front PV panel without cooling.
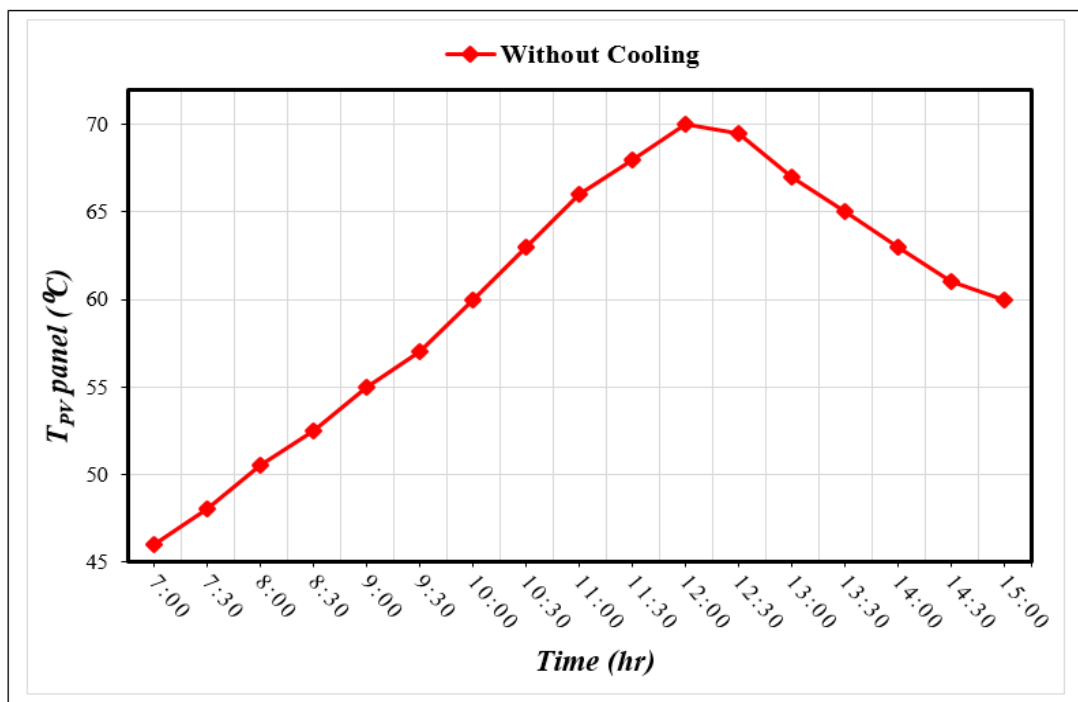

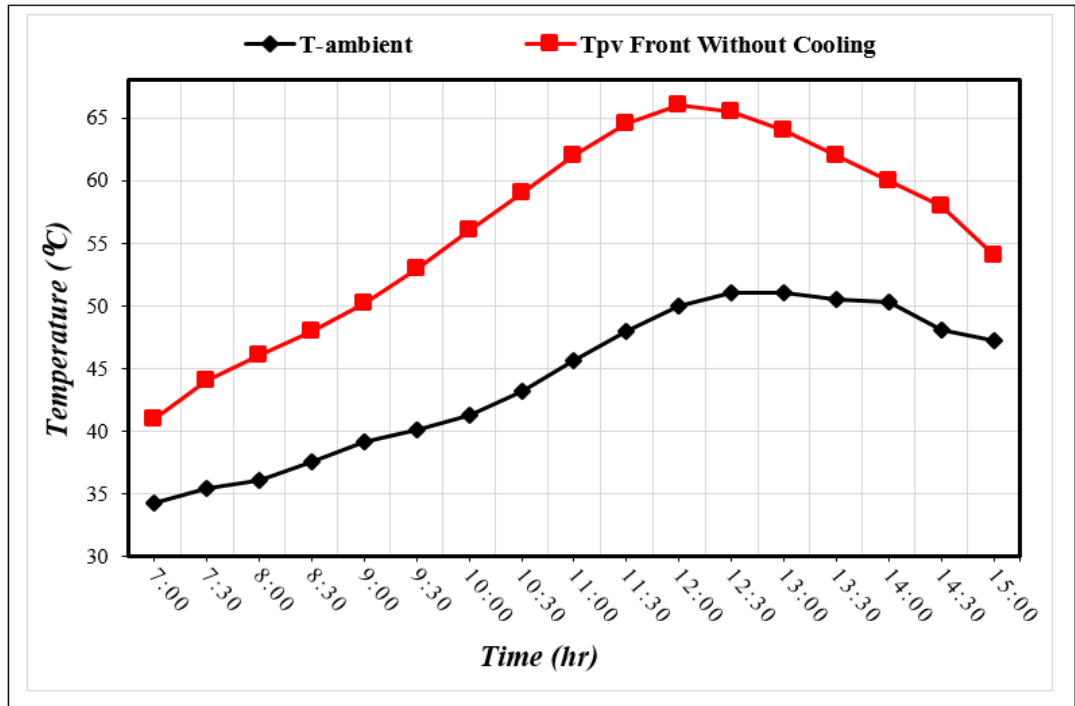Figure 4.9. Surface temperature of the rear PV panel without cooling.

Figure 4.10. Effect of average ambient temperatures on the front PV panel without cooling techniques in August 2021.
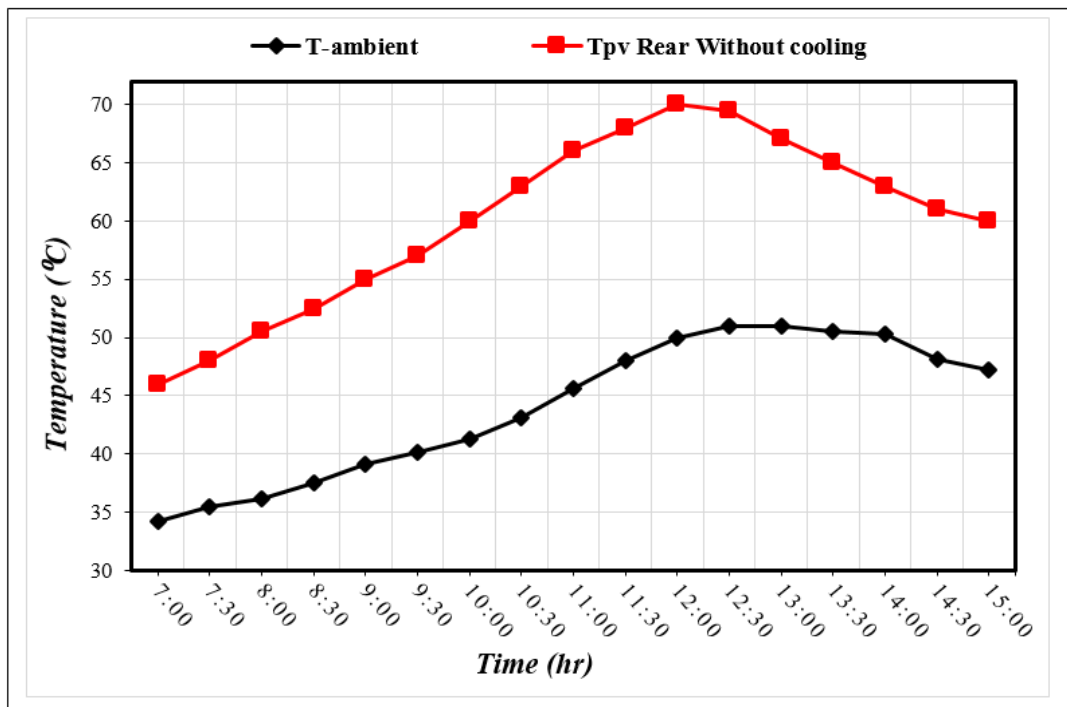
Figure 4.11. Effect of average ambient temperatures on the rear PV panel without cooling techniques in August 2021.

4.3.2. The Effect of Cooling Technique on PV/T Temperature

There are various cooling strategies for solar panels that are described by design to prevent the reflection of radiation from causing high temperatures, but most of them are useless because of their flaws, such as ineffective paints that do not last long, dusty manufactured glass surfaces that are difficult to clean, in addition to their high cost. On the other hand, water has a refractive index of 1.3, which makes it a viable communication medium, as glass and air have 1.0 and 1.5 respectively. Not only is it cooling, but it also helps keep the surface clean [60].

4.3.2.1. Effect of Using Upper Cooling on PV Temperature

The temperature of the front and rear surfaces of solar panels for upper cooling using a water spray nozzle is discussed in this part, as well as its impact on the performance of the PV module. The system's testing changed depending on the amount of flow. The applied nozzle flow rates were 1, 2 and 3 L/m. The system was tested for ten days for each applied flow, after which the 11, 12, and 13th of August were used as an average mean to analyze the upper flow results recorded in the same month.

4.3.2.1.1. Front Surface Temperature

The upper cooling system significantly decreased the temperature of the photovoltaic panel when contrasted to the uncooled panel, with a flow rate of 1 L/m lowering the panel temperature by 16 ℃ and a flow rate of 2 L/m lowering the surface temperature of the PV panel by 20.5 ℃. The third flow, 3 L/m was used. The temperature of the front surface after cooling became 36 °C, by a flow of 3 L/m compared to the temperature of the reference panel's surface, which arrived to 66 ℃ at 12:00 PM, meaning the thermal drop was by 83.33%. Figures are used to illustrate each scenario 4.12, 4.13, and 4.14 respectively. Figure 4.15 displays the study's results. To compare the three flow rates and it was evident that the effect of 3 L/m of water spraying on the cooling panel occupied the maximum proportion of dissipating the surface heat of the photovoltaic panels.

Figure 4.12. Effect of upper cooling on the temperature of the front surface at a flow of 1 L/m.

Figure 4.13. Effect of upper cooling on the temperature of the front surface at a flow of 2 L/m.

Figure 4.14. Effect of upper cooling on the temperature of the front surface at a flow of 3 L/m.

Figure 4.15. Effect of upper cooling on the temperature of the front surface at flows of 1-3 L/m.

4.3.2.1.2. Rear Surface Temperature

The temperature of the uncooled rear panel reaches 70 °C, and all flows experience a thermal reduction as a result of upper cooling. The panel temperature was reduced to 54.6 °C with a flow rate of 1 L/m, and the lowering rate was about 15 °C, but spraying water with a flow of 3 L/m produced better results until it reached 42 °C, despite the fact that it was 70 °C at 12:00 PM, meaning the thermal drop was by 66.66%, as shown in Figures 4.16, 4.17, and 4.18, respectively. By combining and comparing the results of the three rates of flow presented in Figure 4.19, we can see the reality of the thermal reduction accomplished by spraying 3 L/m and employing the upper cooling mechanism and applying it to the solar panel.

Figure 4.16. Effect of upper cooling on the temperature of the rear surface at a flow of 1 L/m.

Figure 4.17. Effect of upper cooling on the temperature of the rear surface at a flow of 2 L/m.

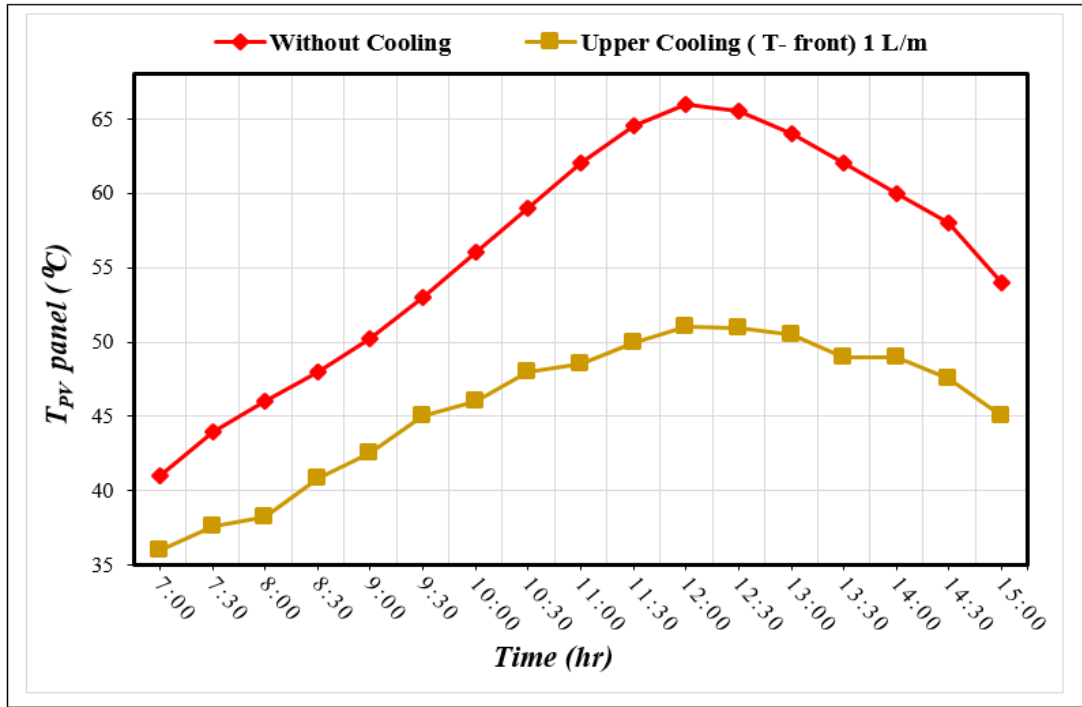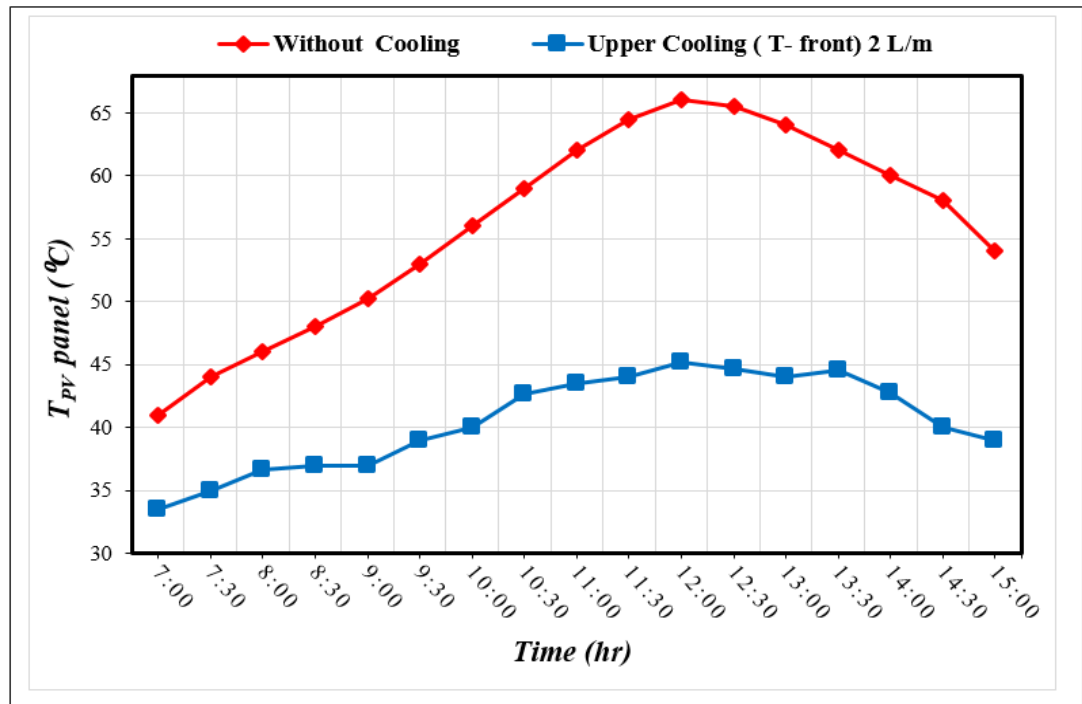

Figure 4.18. Effect of upper cooling on the temperature of the rear surface at a flow of 3 L/m.

Figure 4.19. Effect of upper cooling on the temperature of the rear surface at flows of 1-3 L/m.

4.3.2.2. Effect of Using Lower Cooling on PV Temperature

Similar to upper nozzle cooling in principle, but differs in the location; kind, size, and number of spray nozzles. It still uses the same photovoltaic panel specs and has eight temperature sensors placed randomly on the front and rear sides of the PV panel surfaces. The first experiment utilized a water flow rate of 1 L/m, the second used 2 L/m, and the third used 3 L/m. The dates 19, 20 and 21th of 2021 were set aside for a practical study of this cooling system, with two days given for each flow, in order to be able to study the effect of lower cooling on the front and rear sides of the panel, and adopt a recorded average for each.

4.3.2.2.1. Temperature of the Front Surface

To investigate how the lower cooling technique affects the front panel's surface temperatures. Due to the lower rates of heat transfer through conduction and the impact of convection on the rear surface of the PV panel, the lower cooling accomplished is less heat dissipation than the upper cooling. In spite of that, the temperature of the

panel dropped by around 10 ℃ at a flow of 1 L/m, whereas the temperature of the upper cooling dropped by 15 ℃ at the same flow. With a flow rate of 2 L/m, the temperature of the front panel dropped significantly, reaching 47 ℃ compared to 66℃ for the uncooled panel. Finally, at 12:00 PM, with a flow rate of 3 L/m, there was a considerable drop in the front panel's heat of around 22 ℃. Because of the reduction by 50%, panel efficiency and performance have increased. Figures 4.20, 4.21 and 4.22 display the lower cooling results. Figure 4.23 combines the three flows to demonstrate the benefit of lower cooling by decreasing the temperature of the front panel's surface, as well as the need to increase the nozzle's high spray rate to 3 L/m to achieve maximum heat reduction at 12.00 PM. This flow and timing produced the greatest results.

Figure 4.20. Effect of lower cooling on the temperature of the front surface at a flow of 1 L/m.

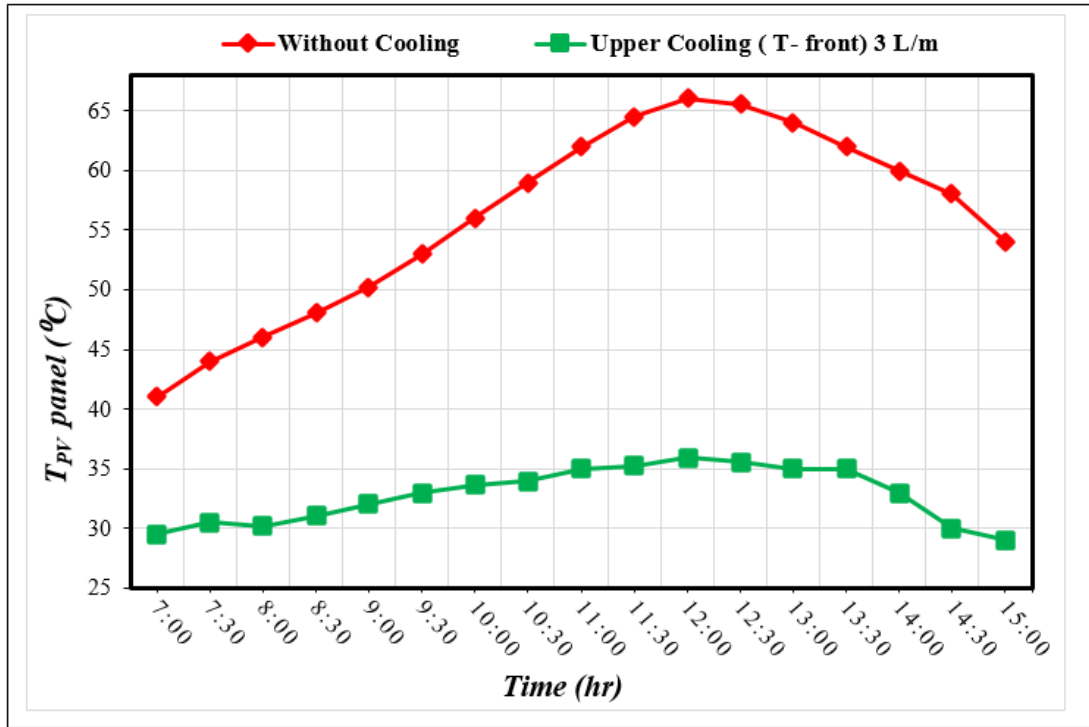Figure 4.21. Effect of lower cooling on the temperature of the front surface at a flow of 2 L/m.

Figure 4.22. Effect of lower cooling on the temperature of the front surface at a flow of 3 L/m.
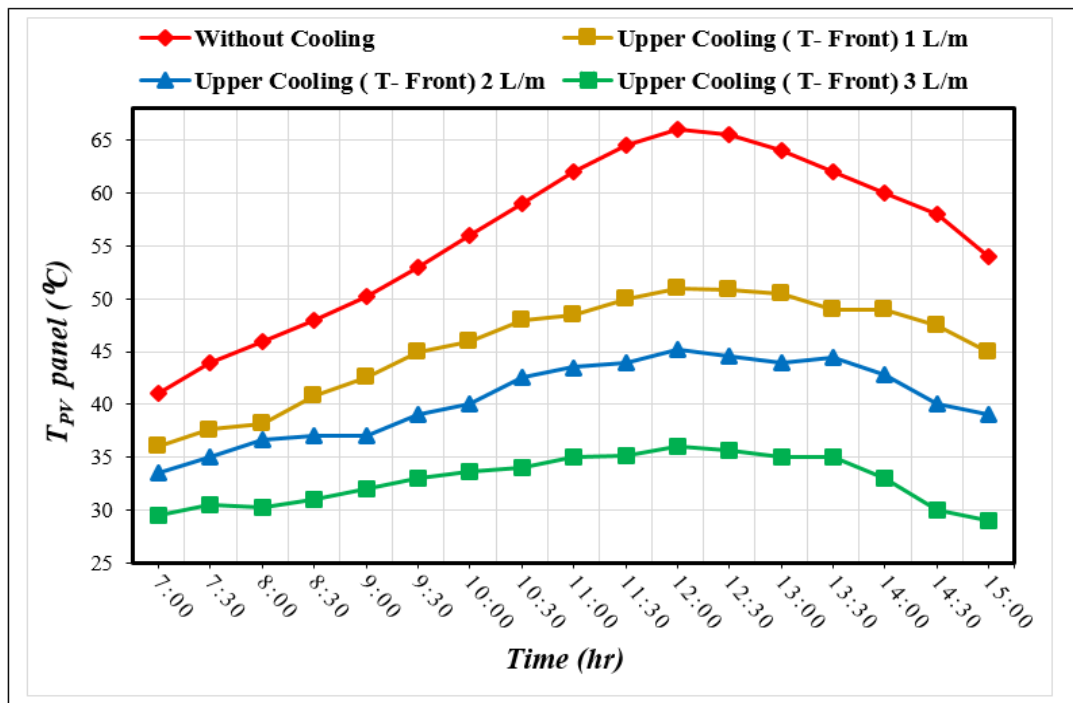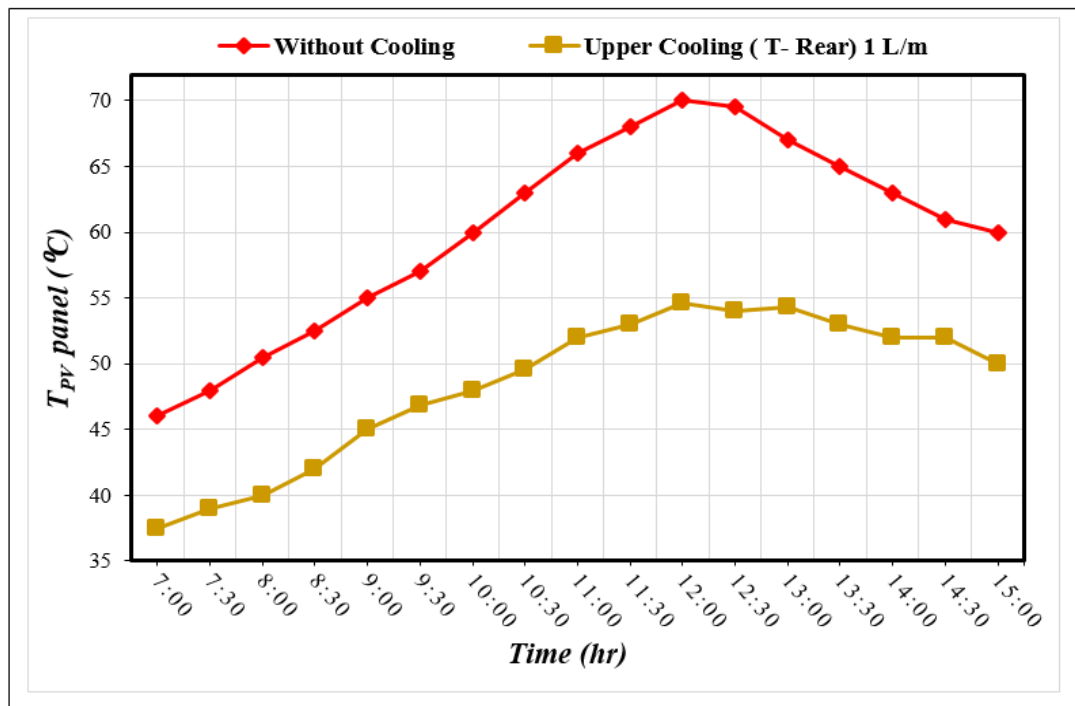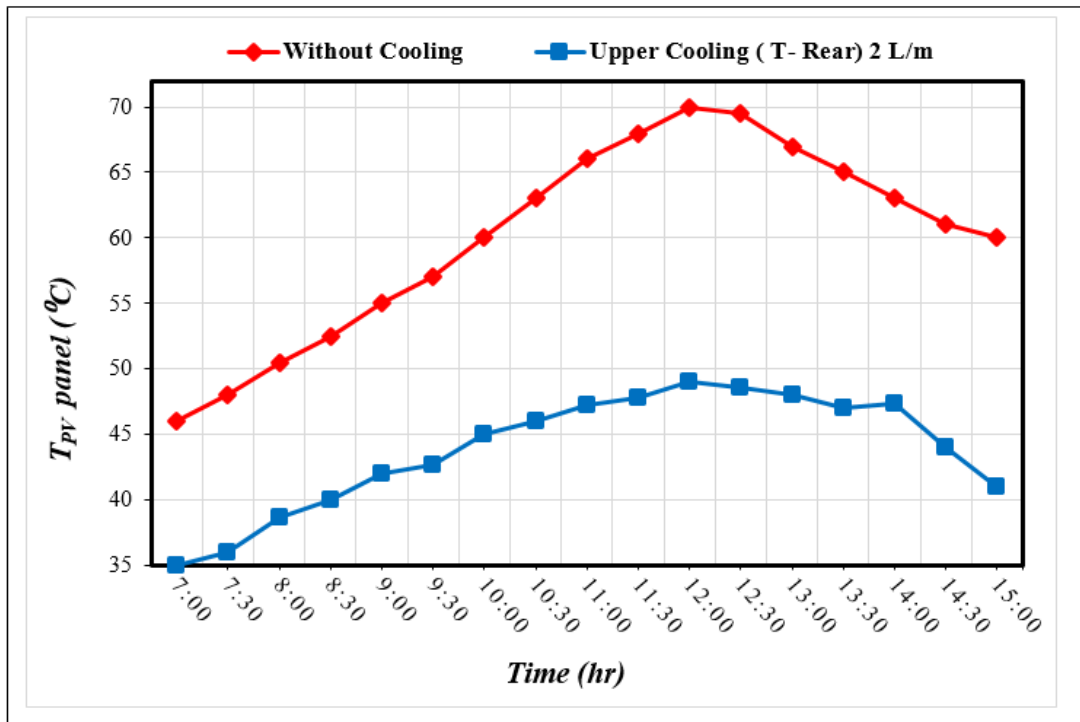
Figure 4.23. Effect of lower cooling on the temperature of the front surface at flows of 1-3 L/m.

4.3.2.2.2. Temperature of the Rear Surface

Figures 4.24, 4.25, and 4.26 demonstrate a considerable reduction in rear surface temperatures, especially when the flow rate 3 L/m is applied. The temperatures dropped by an average of 75% but were higher and those reached by the same technique on the front surface, despite the fact that the two experiments were conducted on the same day and under the same conditions. The surface temperature dropped significantly when the spray flow rate 2 L/m was increased, it reached 45.5°C. In conclusion, Figure 4.27 shows that the temperature on the b surface of the same technique is four degrees lower than the front surface, which is due to the concentration of spray nozzles and their proximity to the rear panel's surface, as well as the interaction of the surrounding air with the panel. All the temperature curves shown have been inferred by logging Arduino data with the help of sensors distributed on the panel surfaces as well as an ambient temperature sensor.
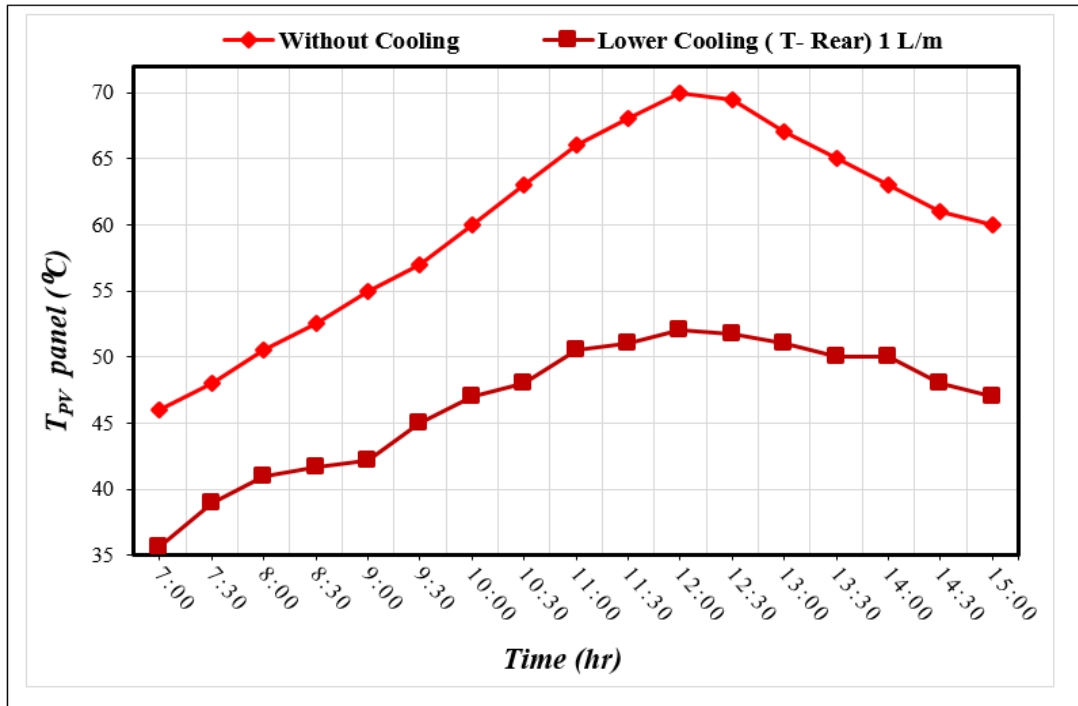
Figure 4.24. Effect of lower cooling on the temperature of the rear surface at a flow of 1 L/m.
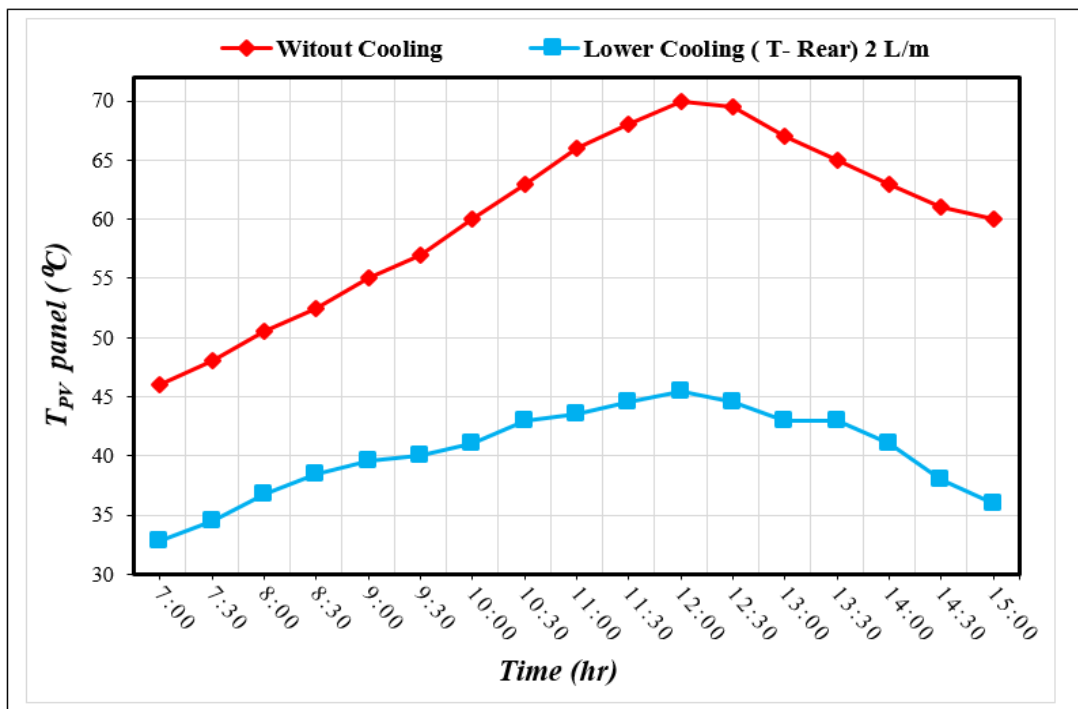
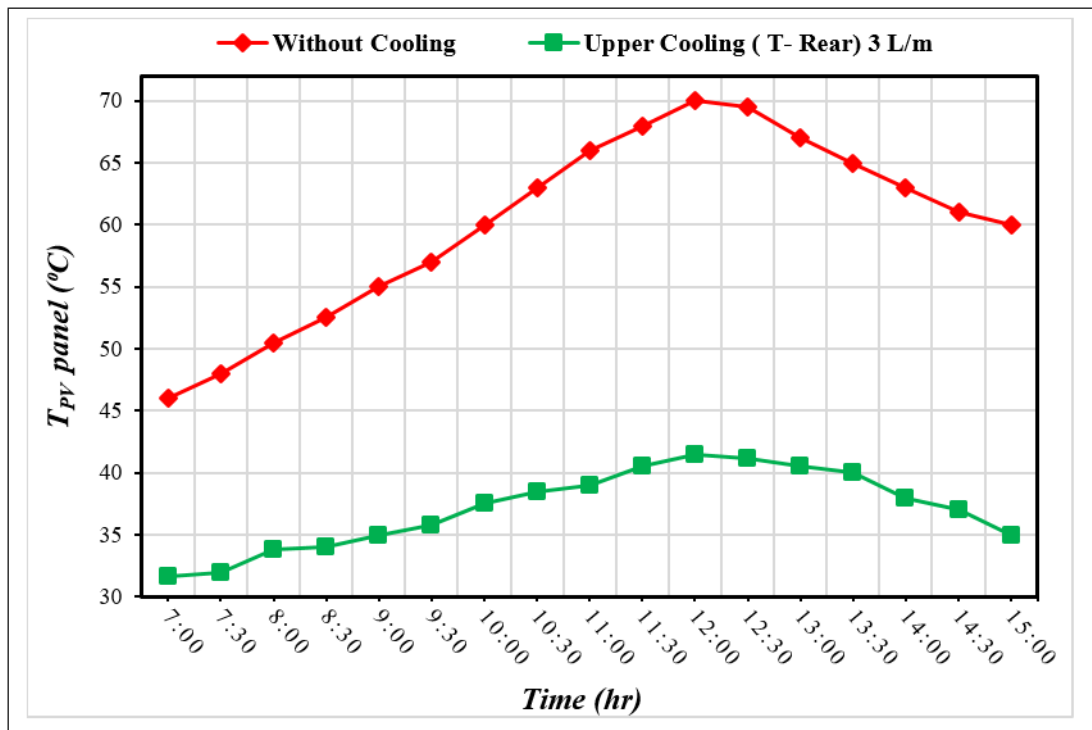Figure 4.25. Effect of lower cooling on the temperature of the rear surface at a flow of 2 L/m.
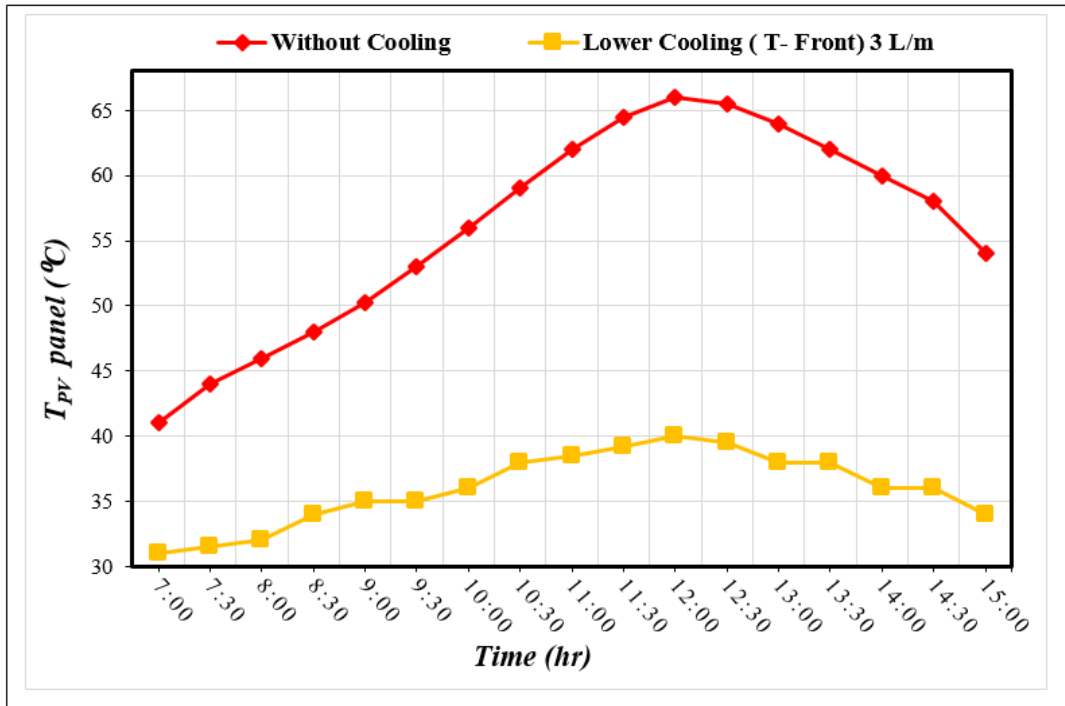
Figure 4.26. Effect of lower cooling on the temperature of the rear surface at a flow of 3 L/m.
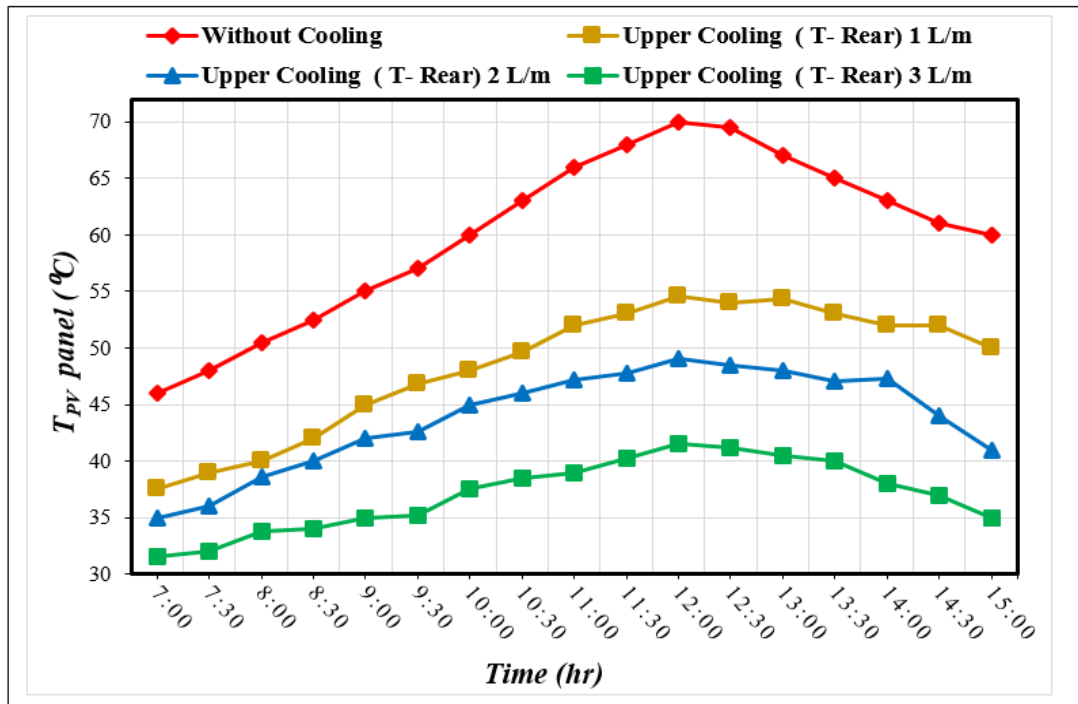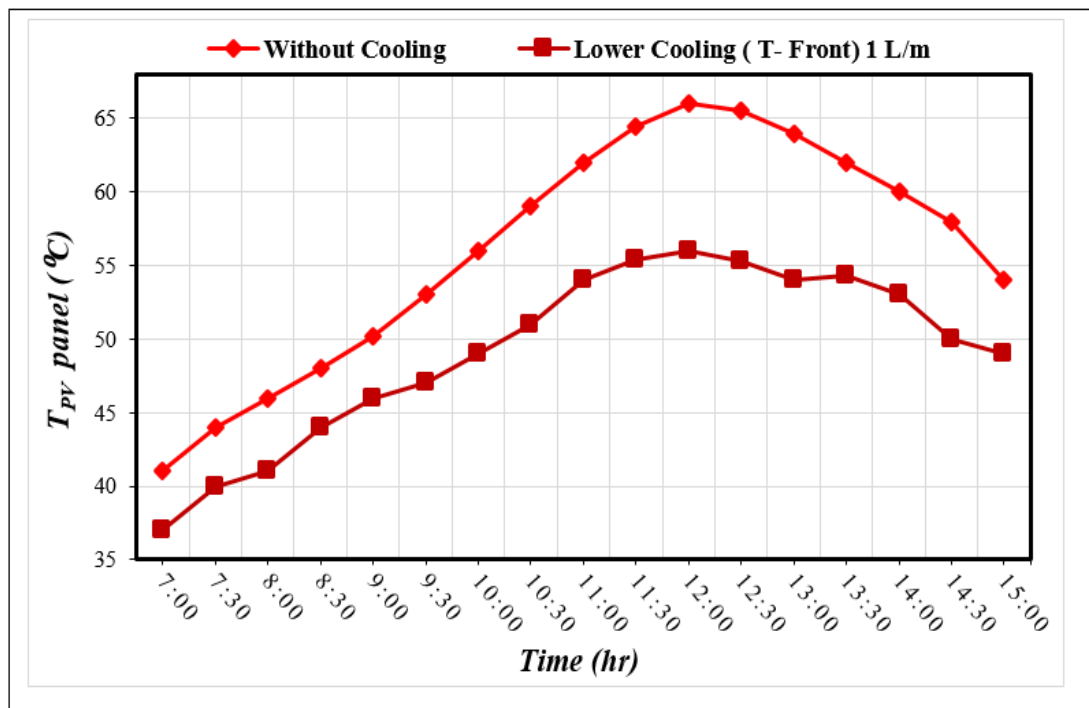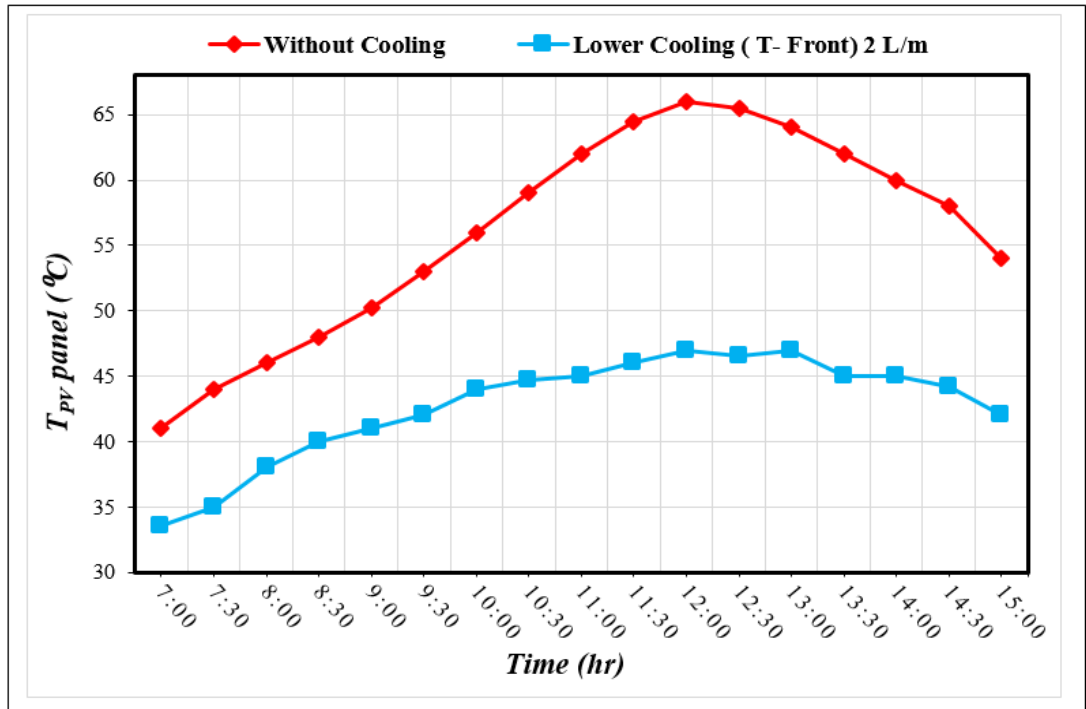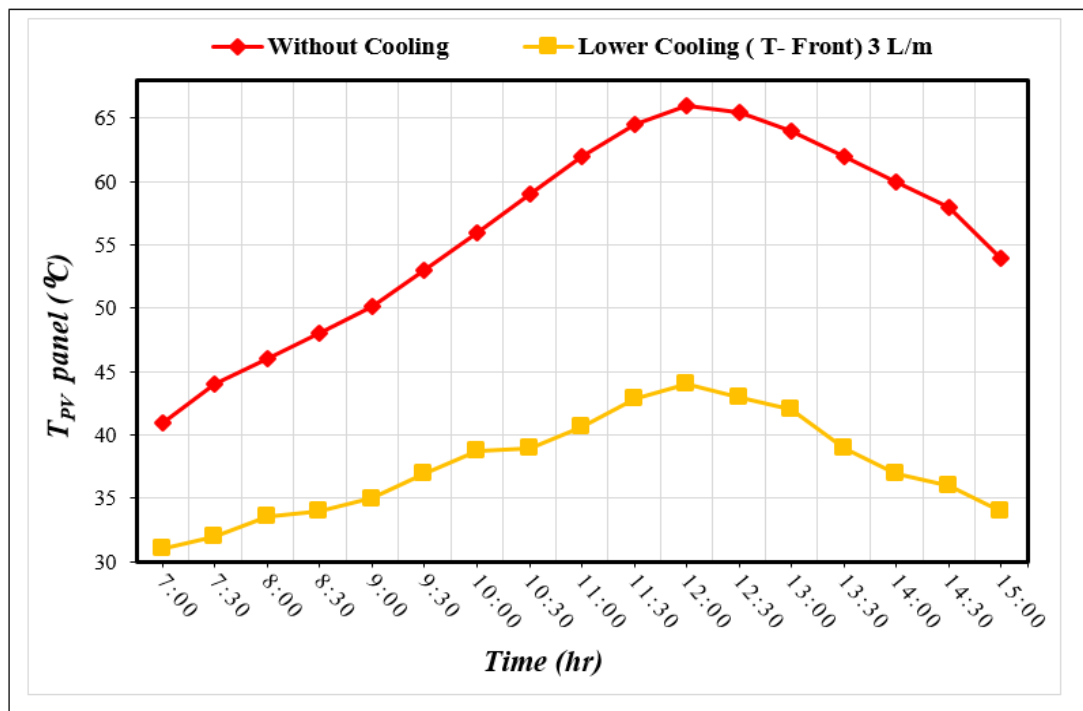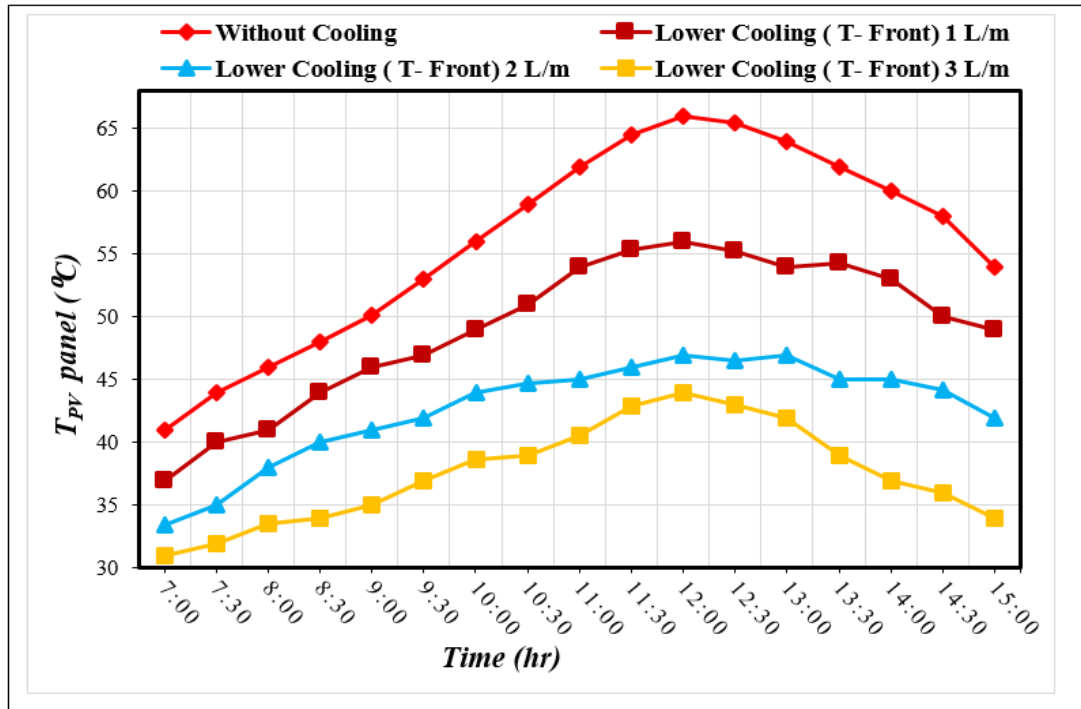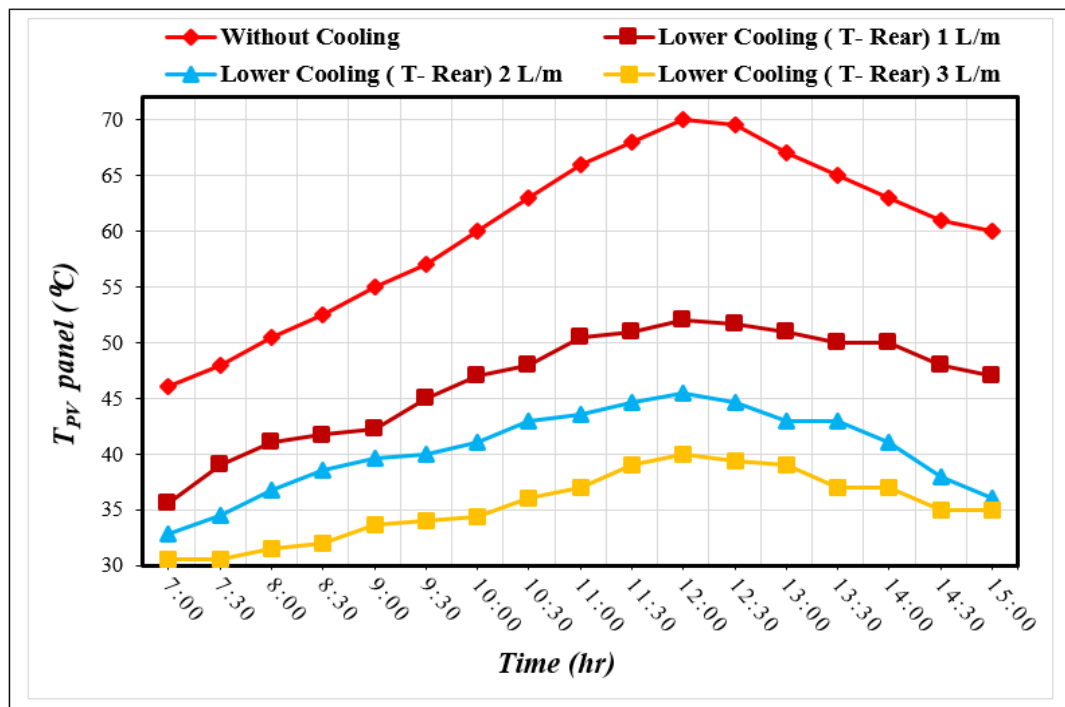

Figure 4.27. Effect of lower cooling on the temperature of the rear surface at flows of 1-3 L/m.

4.3.2.3. Summary of the comparison between the panels

After applying cooling techniques and determining the efficiency of the photovoltaic panel, comparing the temperatures of the front and rear surfaces of the solar panels with the uncooled panel is important. The results of spraying water on both surfaces of the PV panel depended on the flow amount of each approach and the weather conditions on the day of the test.

Figures 4.28 and 4.29 show that at a maximum flow rate of 3 L/m, the front surface temperature of the upper and lower cooling types both decreased significantly, by a percentage of heat reduction of about 83.33% and 50% for the upper and lower cooling techniques, respectively. At maximum flow, the heat reduction rates for the front and rear surfaces were 66.66% and 75% at lower cooling, respectively. We discussed the reasons behind this, especially in terms of the spray nozzles' placement and closeness to the rear surface, despite the fact that the uncooled panel's rear surface temperature was 70 °C. Summarizing the above, we can infer that upper cooling is the most effective solution for reducing the temperature differential between the front and rear panels. The lowering of the panel temperature increased as the rate of water flow from the nozzle gradually increased. According to the percentages, we've provided, as seen by the drop in surface temperatures to half of what they were in the uncooled panel, the flow rate 3 L/m is the most feasible for both approaches and this is a promising indicator that the efficiency of solar panels is improving.

Figure 4.30 show the influence of flow rate on PV panel temperatures in a bar chart. As the temperature of the PV panel drops, the rise in flow rate is a valuable signal for increasing the panel's power and efficiency. The results indicated that the temperature of the uncooled photovoltaic panel peaked around 12:00 noon. However, when the two cooling procedures were utilized, the panel's temperature dropped by nearly half. The quantity of radiation reflected by the solar panel with the cooling system is relatively low, which is worth noting. Water molecules may absorb molecules from the electromagnetic spectrum as radiation passes through the water layer. This absorption happens across a certain wavelength range. The absorption happens mostly in the infrared spectrum, which is fortunate [61].
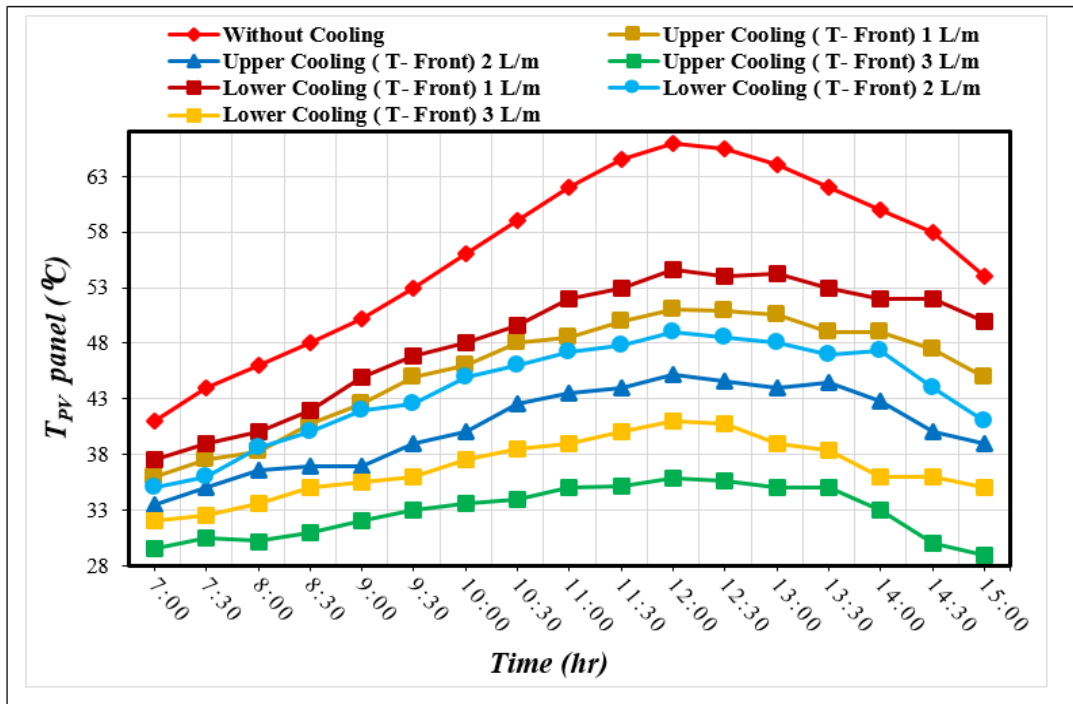
Figure 4.28. Effect of upper and lower cooling techniques on the temperature of the front panel surface.
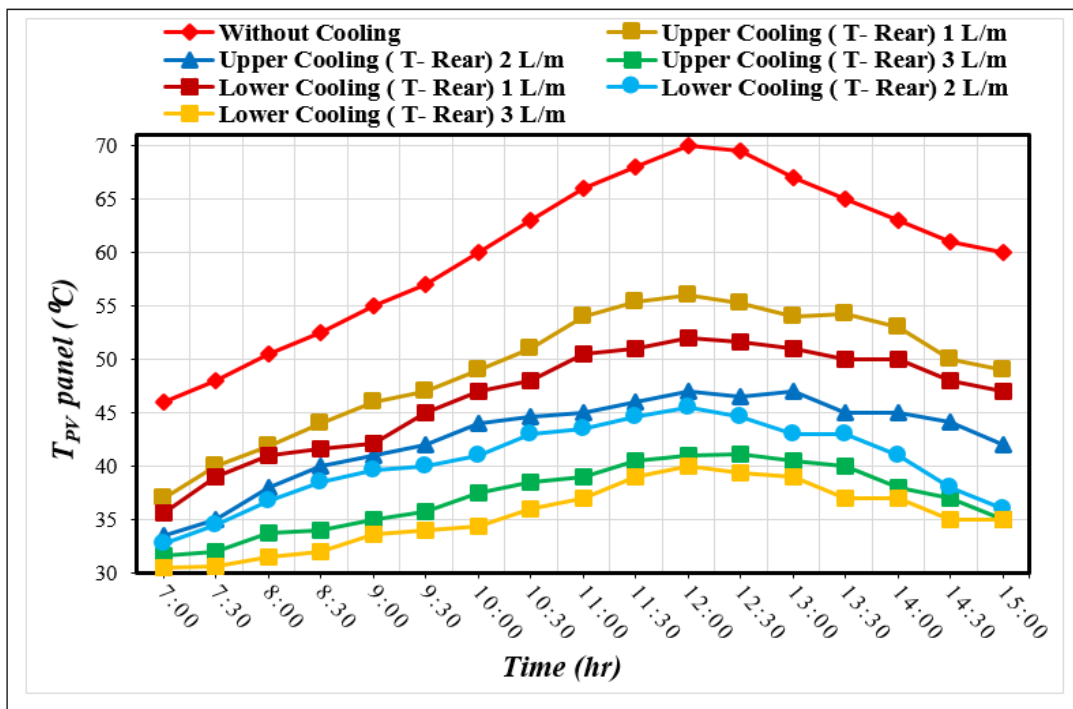
Figure 4.29. Effect of upper and lower cooling techniques on the temperature of the rear panel surface.

90
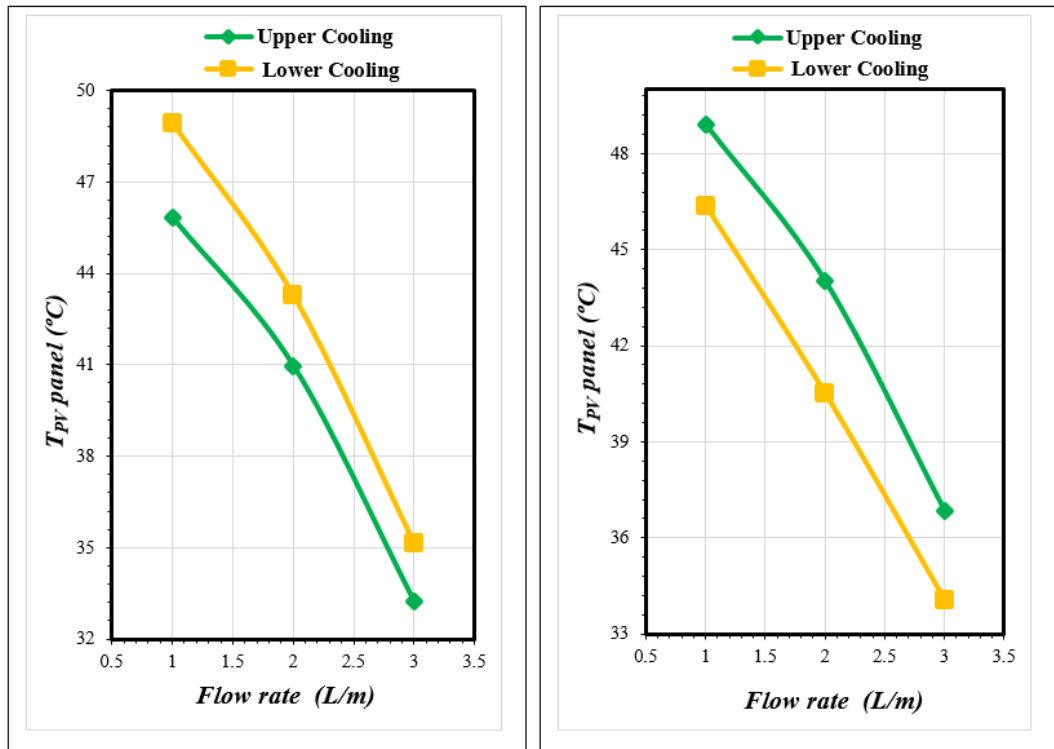
Figure 4.30. a) Flow rate's effect on the heat of the front PV panel b) Flow rate's effect on the heat of the rear PV panel.

The temperature distribution of the surfaces of the front and rear solar panels, as well as the uncooled panel, is shown in the Table 4.1 of the upper and lower cooling system throughout the day, every half hour, for the period from 7:00 AM to 3:00 PM. When compared to lower cooling, Figure 4.31 demonstrates that upper cooling is the best option for achieving the greatest percentage of panel temperature drop at the flow rate 3 L/m at precisely 12.00 noon. The two systems rank well in Figure 4.32, because the results are convergent at the same flow rate; when we apply upper cooling, heat reduction from the front surface is more effective than that from the rear surface.

Table 4.1. Temperature distribution of cooled and uncooled PV panels

Time	Without cooling		Upper cooling						Lower cooling					
			1 L/m		2 L/m		3 L/m		1 L/m		2 L/m		3 L/m	
	front	rear	front	rear	front	rear	front	rear	front	rear	front	rear	front	rear
7:00	41	46	36	37.5	33.5	35	29.5	31.6	37	35.6	33.5	32.8	31	30.5
7:30	44	48	37.6	39	35	36	30.5	32	40	38	35	34.5	32	30.6
8:00	46	50.5	38.2	40	36.6	38.6	30.2	33.8	41	39	38	36.8	33.6	31.5
8:30	48	52.5	40.8	42	37	40	31	34	44	41.7	40	38.5	34	32
9:00	50.2	55	42.5	45	37	42	32	35	46	42.2	41	39.6	35	33.6
9:30	53	57	45	46.8	39	42.6	33	35.2	47	45	42	40	37	34
10:00	56	60	46	48	40	45	33.6	37.5	49	47	44	41	38.7	34.4
10:30	59	63	48	49.6	42.6	46	34	38.5	51	48	44.7	43	39	36
11:00	62	66	48.5	52	43.5	47.2	35	39	54	50.5	45	43.5	40.6	37
11:30	64.5	68	50	53	44	47.8	35.2	40.3	55.4	51	46	44.6	42.9	39
12:00	66	70	51	55	45.2	49	36	42	56	52	47	45.5	44	40
12:30	65.5	69.5	50.9	54	44.6	48.5	35.6	41.2	55.3	51.7	46.5	44.6	43	39.4
13:00	64	67	50.5	54.3	44	48	35	40.5	54	51	47	43	42	39
13:30	62	65	49	53	44.5	47	35	40	54.3	50	45	43	39	37
14:00	60	63	49	52	42.8	47.3	33	38	53	50	45	41	38	37
14:30	58	61	47.5	52	40	44	30	37	50	48	44.2	38	36	35
15:00	54	60	45	50	39	41	29	35	49	47	42	36	34	35
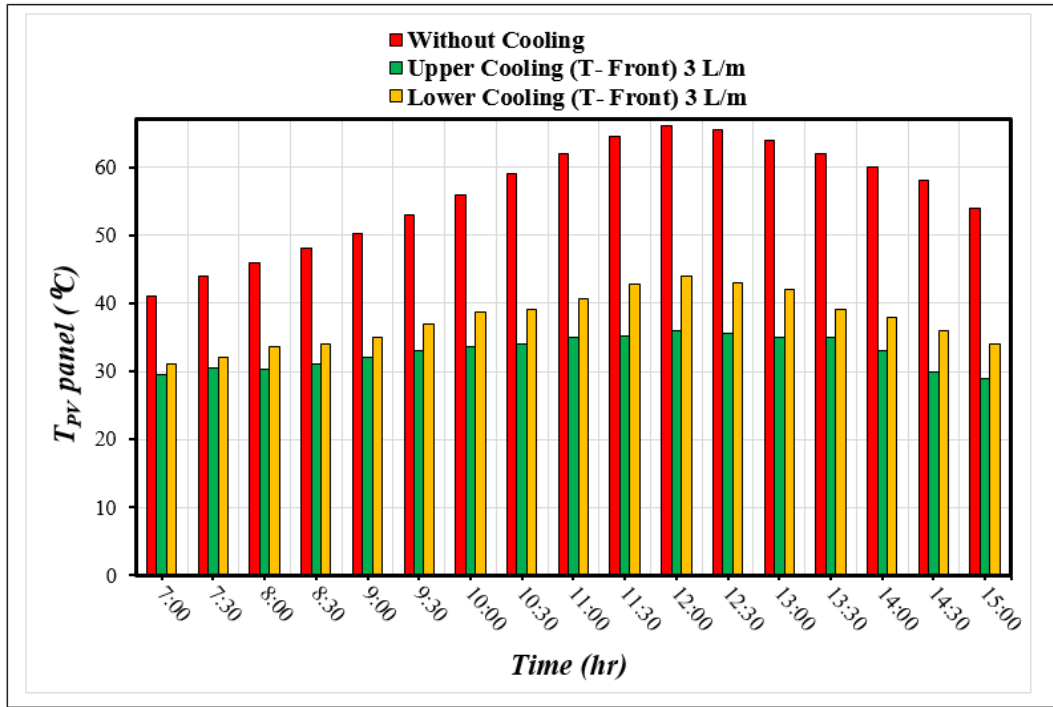
Figure 4.31. Comparison of temperatures on the front surface of cooled and uncooled PV panel at a flow rate of 3 L/m.
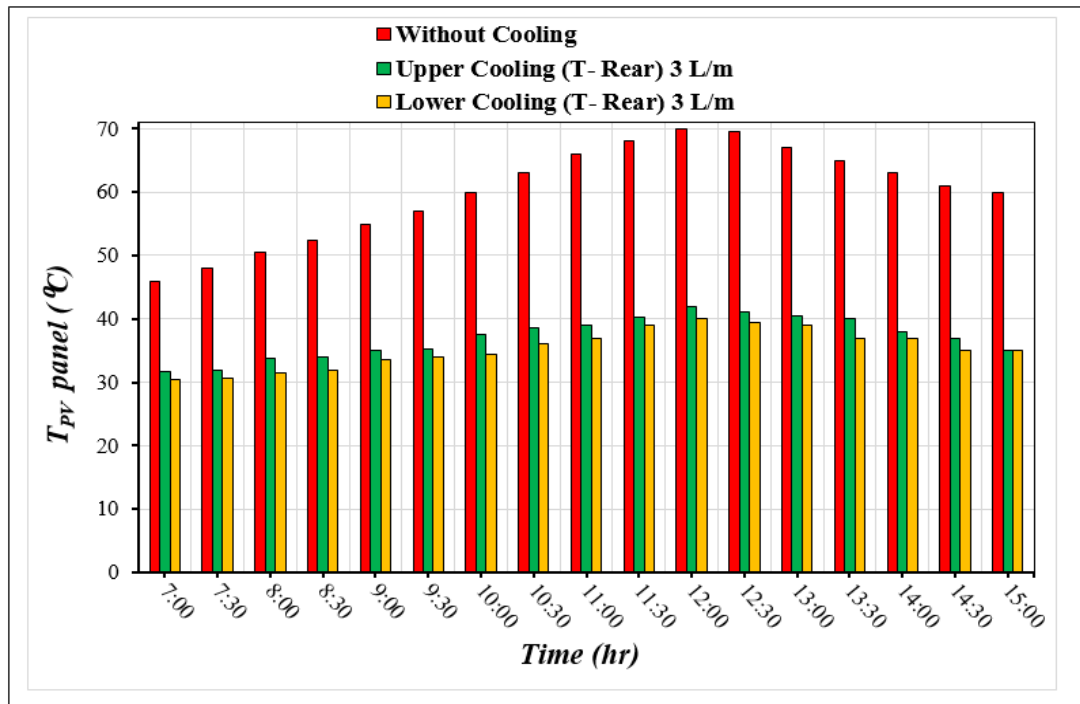
Figure 4.32. Comparison of temperatures on the rear surface of cooled and uncooled PV panel at a flow rate of 3 L/m.

93

4.3.3. Thermographic Analysis

The temperature distribution on all sides and in the center of the front and rear surfaces of the photovoltaic panel must be determined and compared to the Arduino sensor temperature recorder. A visible infrared thermometer camera (FLUKE VT04) with accurate digital and thermal imaging when employed on the visible screen. Every hour on days 8, 9, 10, 11, 12, 13, 19, 20, and 21th, August 2021, we used a visual thermal imager (IR) to capture visual simulation data for the uncooled panel, testing the technique of upper and lower cooling, respectively. Temperature pictures were taken from 7:00 AM to 2:00 PM, with just a flow of 3 L/m, considering this value is the largest flow of experience. We can consider this technique as a substitution for (ANSYS-CFD) simulation in the distribution of the temperature on the panel. The camera sensor was able to track the distribution of solar panel surface temperatures, which were either slightly lower or similar to those of the Arduino data.

We can deduct from the Figures 4.33, 4.34 and 4.35 that the uncooled panel begins to redden because of heat stress, whereas the cold panel appears on the screen in blue. When comparing the uncooled panel images to the Arduino's registered surfaces sensor, it was 66 ºC for the front and 70 ºC for the rear, which glows red, then fades, and disappears. We observe that the panel reaches its peak at 64.8 ºC and 68.7 ºC for the front and back surfaces, respectively, at 12:00 noon. In addition, the Figures 4.36 - 4.41 show the accuracy of the two sensors when their data is converged.

4.3.3.1. Without Cooling

Time				
7:00AM			**8:00AM**	
Front	Rear	Front	Rear
39.8°C 2021:08:09 07:00:11 ε0.95	45.8°C 2021:08:09 07:00:50 ε0.95	45.5°C 2021:08:09 08:00:43 ε0.95	48.1°C 2021:08:09 08:00:57 ε0.95

Time				
9:00AM			**10:00AM**	
Front	Rear	Front	Rear
49.9°C 2021:08:09 09:00:28 ε0.95	53.3°C 2021:08:09 09:00:55 ε0.95	55.4°C 2021:08:09 10:00:28 ε0.95	57.4°C 2021:08:09 10:00:55 ε0.95

Time				
11:00 AM			**12:00 PM**	
Front	Rear	Front	Rear
58.9°C 2021:08:09 11:00:18 ε0.95	64.9°C 2021:08:09 11:00:56 ε0.95	64.8°C 2021:08:09 12:00:25 ε0.95	68.7°C 2021:08:09 12:00:49 ε0.95

Time				
1:00PM			**2:00PM**	
Front	Rear	Front	Rear
62.5°C 2021:08:09 13:00:39 ε0.95	66.9°C 2021:08:09 13:00:47 ε0.95	58.9°C 2021:08:09 14:00:32 ε0.95	61.0°C 2021:08:09 14:00:33 ε0.95

Figure 4.33. Thermal infrared images of the PV panel's without cooling.

4.3.3.2. Upper Cooling
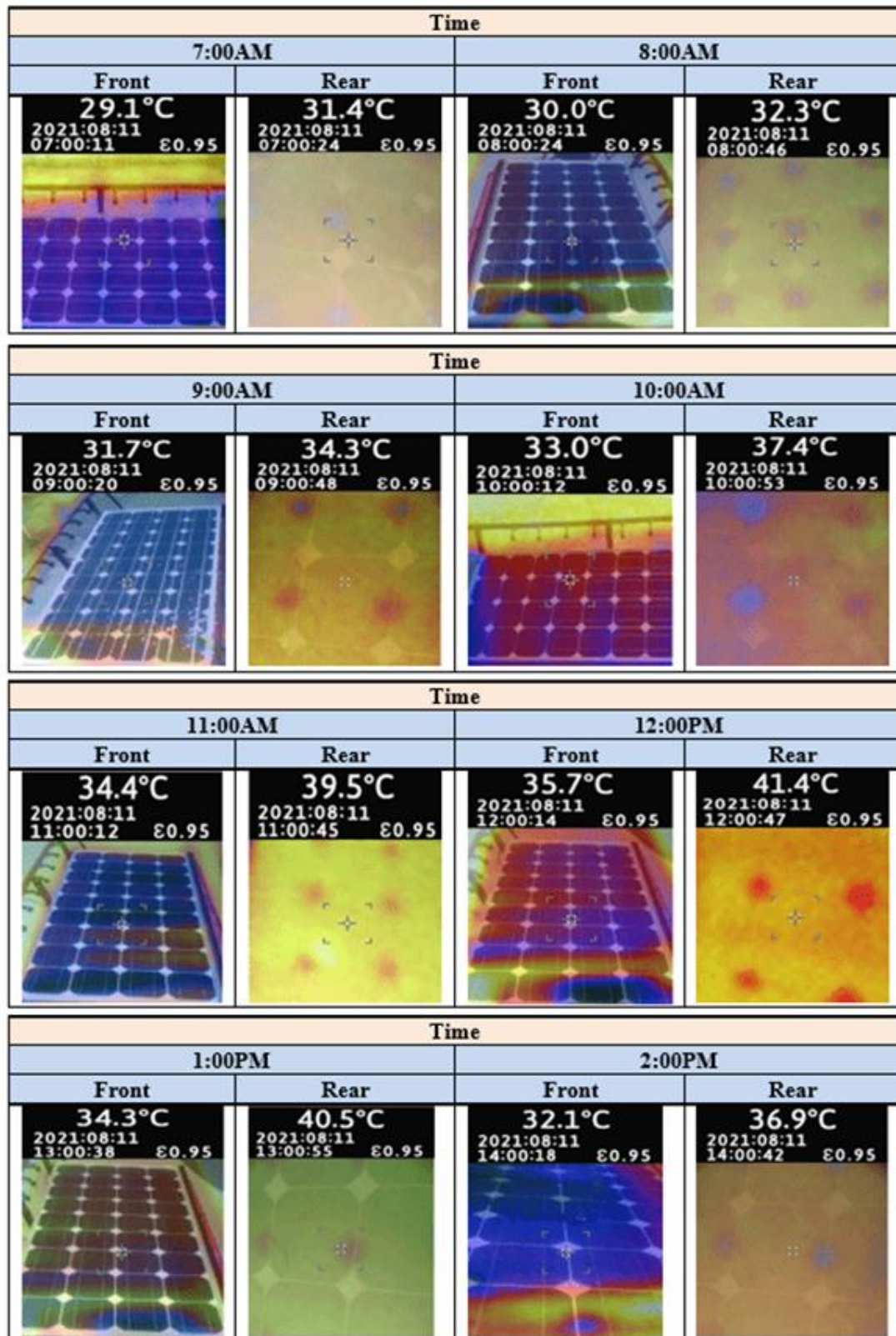
Figure 4.34. Thermal infrared images of the PV panel's upper cooling .

4.3.3.3. Lower Cooling

Time			
7:00AM		8:00AM	
Front	Rear	Front	Rear
30.9°C 2021:08:19 07:00:17 ℇ0.95	29.7°C 2021:08:19 07:00:34 ℇ0.95	33.2°C 2021:08:19 08:00:24 ℇ0.95	31.0°C 2021:08:19 08:00:43 ℇ0.95
Time			
9:00AM		10:00AM	
Front	Rear	Front	Rear
34.5°C 2021:08:19 09:00:28 ℇ0.95	32.4°C 2021:08:19 09:00:34 ℇ0.95	37.4°C 2021:08:19 10:00:22 ℇ0.95	34.3°C 2021:08:19 10:00:43 ℇ0.95
Time			
11:00AM		12:00PM	
Front	Rear	Front	Rear
40.2°C 2021:08:19 11:00:27 ℇ0.95	36.2°C 2021:08:19 11:00:40 ℇ0.95	42.5°C 2021:08:19 12:00:19 ℇ0.95	38.9°C 2021:08:19 12:00:37 ℇ0.95
Time			
1:00PM		2:00PM	
Front	Rear	Front	Rear
41.3°C 2021:08:19 13:00:16 ℇ0.95	38.8°C 2021:08:19 13:00:40 ℇ0.95	38.0°C 2021:08:19 14:00:26 ℇ0.95	36.1°C 2021:08:19 14:00:51 ℇ0.95

Figure 4.35. Thermal infrared images of the PV panel's lower cooling.

Figure 4.36. Comparison of IR and Arduino sensor temperatures for the front PV panel
surface without cooling.
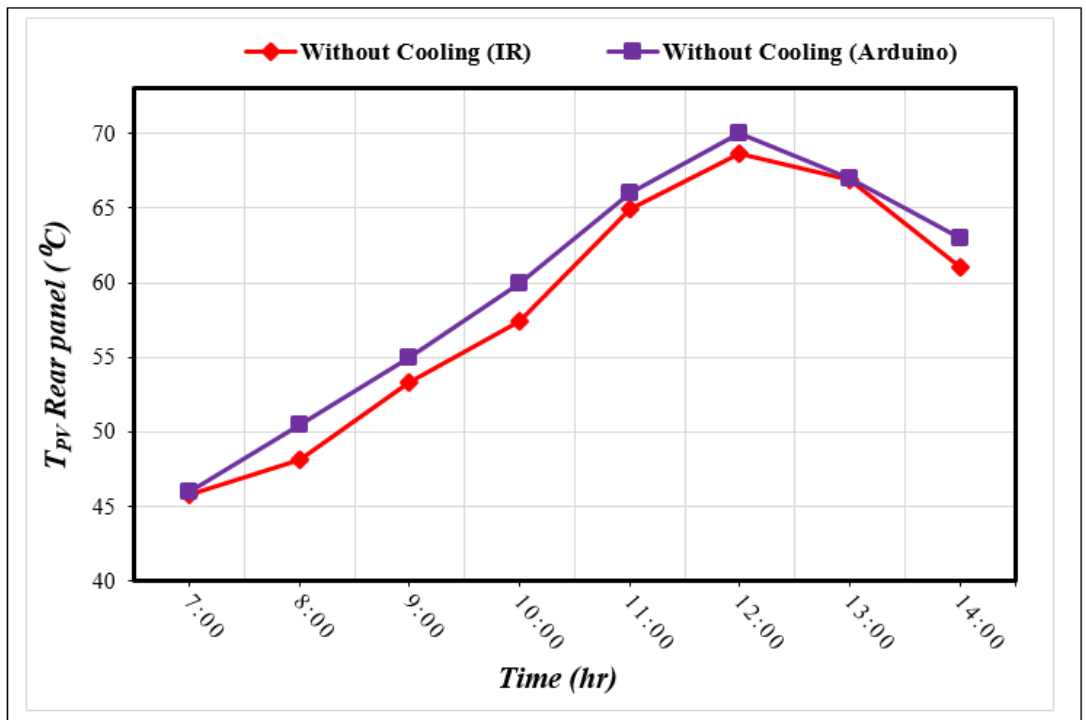
Figure 4.37. Comparison of IR and Arduino sensor temperatures for the rear PV panel
surface without cooling.
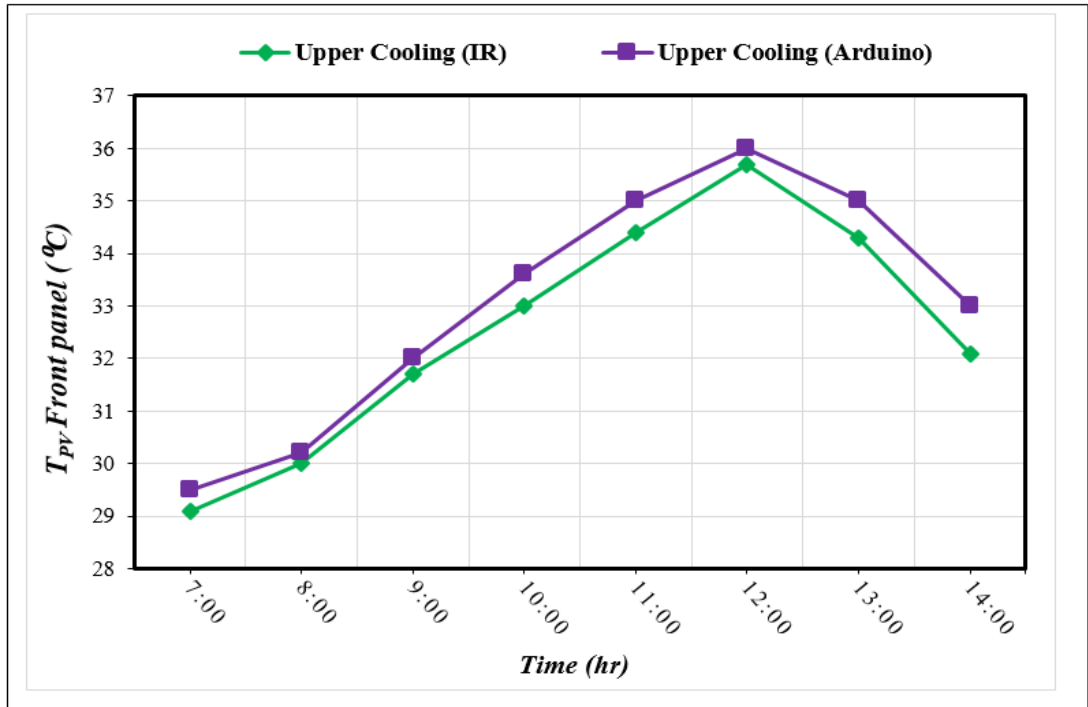
Figure 4.38. Comparison of IR and Arduino sensor temperatures for the front PV panel surface upper cooling.

Figure 4.39. Comparison of IR and Arduino sensor temperatures for the rear PV panel surface upper cooling.

Figure 4 40. Comparison of IR and Arduino sensor temperature for the front PV panel surface lower cooling.

Figure 4.41. Comparison of IR and Arduino sensor temperature for the rear PV panel surface lower cooling.

4.4. ELECTRICAL CHARACTERISTICS

To study the parameters of photovoltaic panels that are important in improving the efficiency of the panel, it is necessary to know the voltage and current, as well as the value of the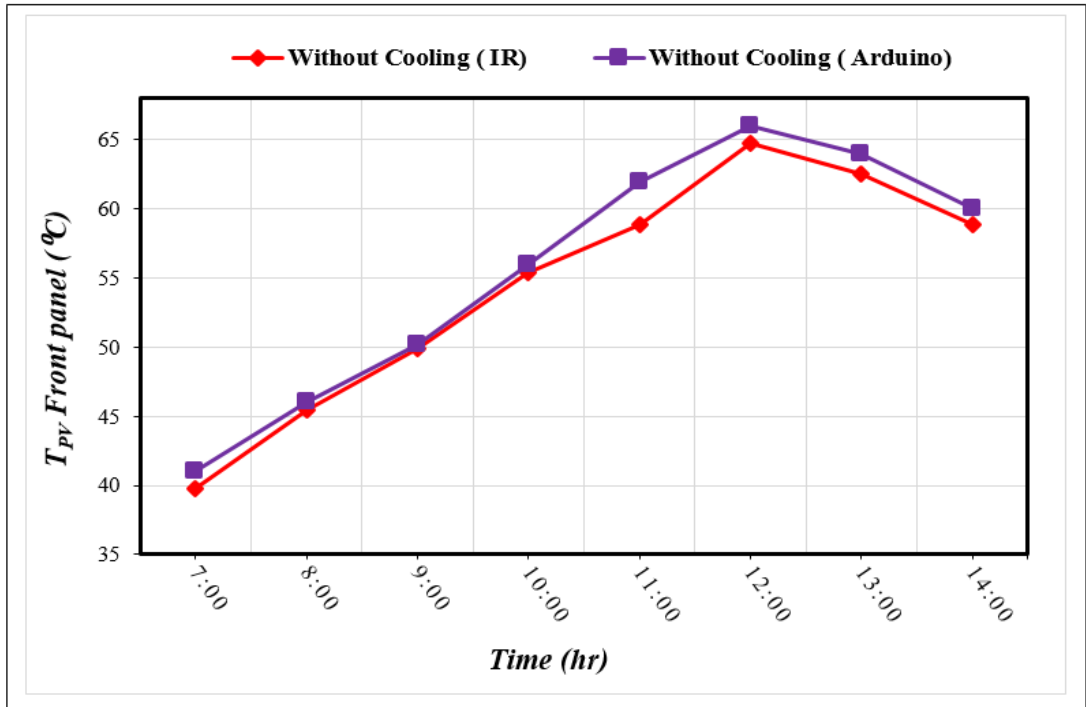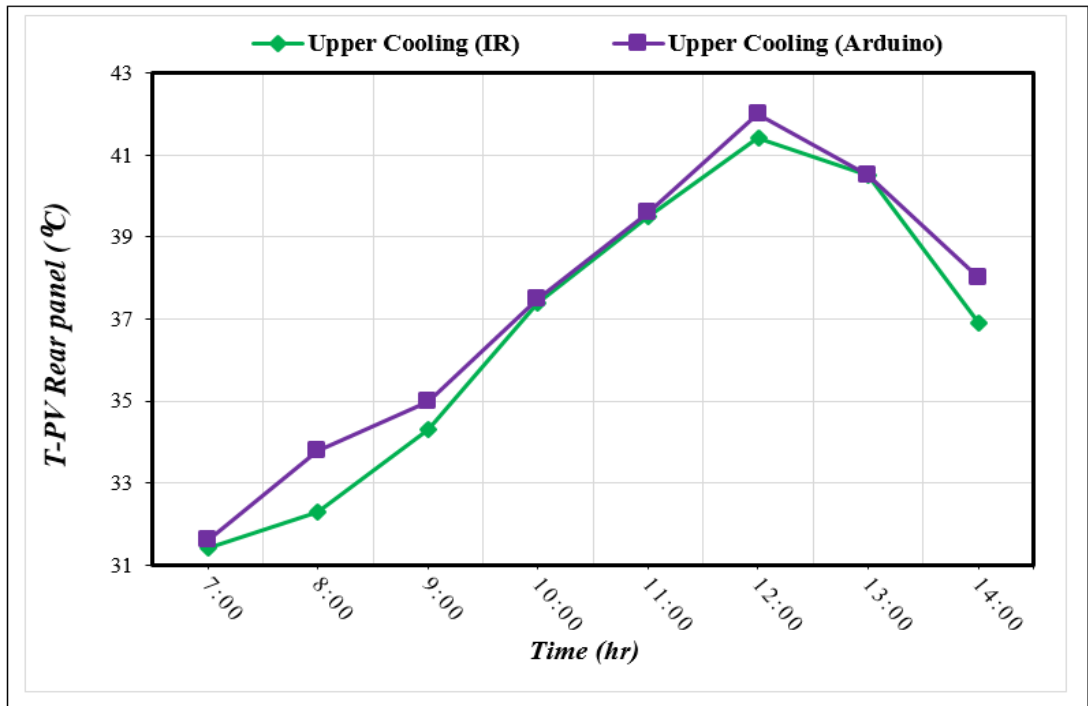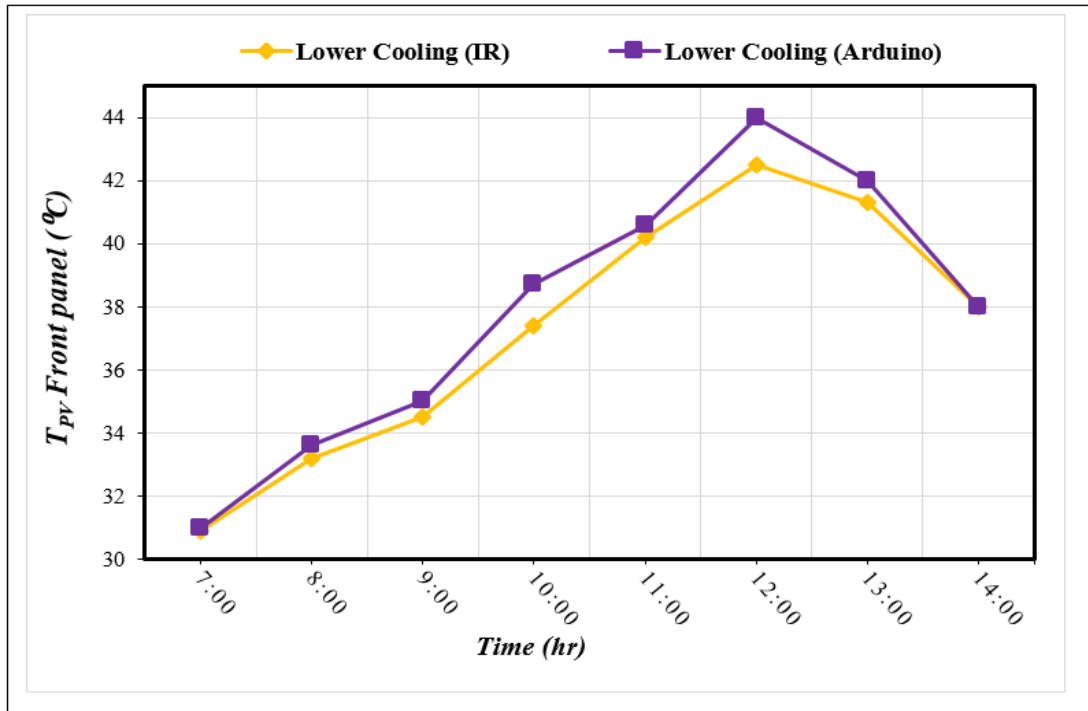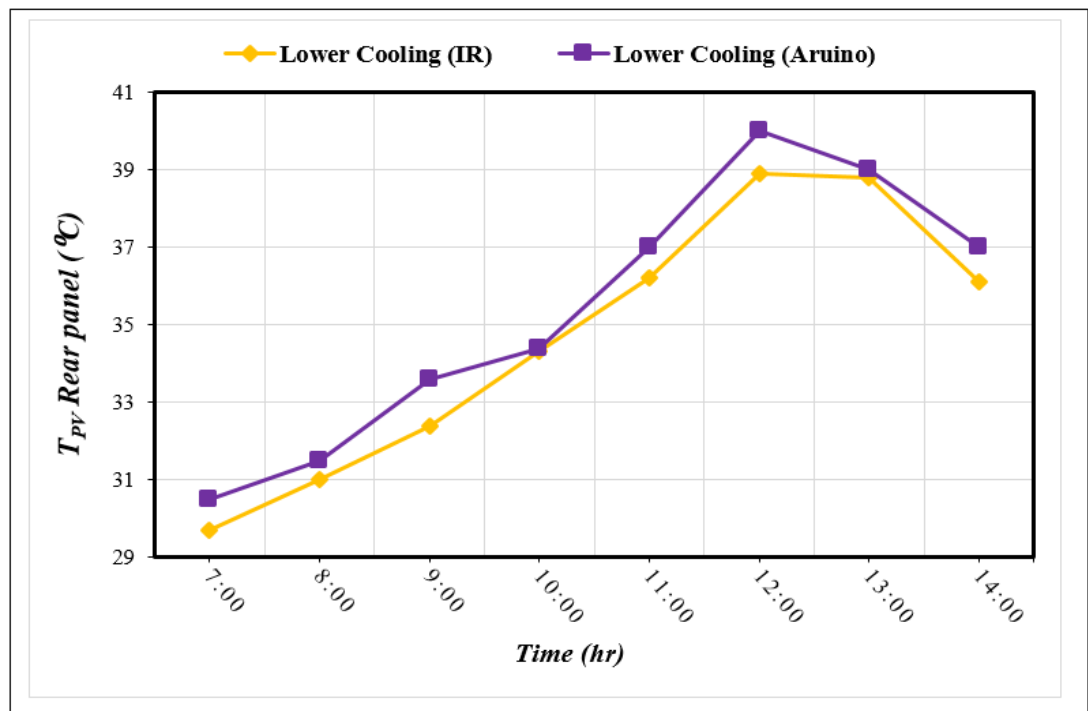 outpot power of the panel. To obtain the greatest power from the photovoltaic panel, the surface heat of the panel must be reduced, as was achieved by applying the flow rates of 1, 2 and 3 L/m, thus reinforcing the efficiency by increasing the flow rate. The following are significant aspects to consider while enhancing the performance of solar panels:

4.4.1. Maximum power point Voltage (Vmp)

According to Ohm's law of power, this factor is very important in improving the performance, depending on the amount of voltage increase as well as the current. The panel voltage reached 14.88 V at a flow rate of 1L/m, and the amount increased by rising the flow (2 L/m) until it reached (16V at 12.00 PM), while the experimental results in August, at radiation 888 W/m^2 and an ambient temperature of approximately 50 °C, revealed an improvement in the voltage of the uncooled panel by 31%, which is considered the largest voltage obtained in the experimental results for water spray nozzle at applying a flow rate of 3 L/m in the upper cooling system that is shown in the Figure 4.42. Likewise, with the lower cooling, the voltage of the cooled panel at the flow of 2 L/m increased by 15.6 V and reached its maximum value of 16.8 V at midday, as shown in the Figure 4.43.

4.4.2. Maximum power point current (Imp)

Current (Imp) is another important parameter in optimizing the performance of a photovoltaic panel. It increases slightly when the panel temperature rises. Because the current of the uncooled panel remained at 3.79 A at 12:00 PM and increased slightly to 4.48 A at a flow of 3 L/m, the rate of voltage increase when cooling the panel is greater than the rate of current decrease in the current, implying that the effect of temperature rise on Imp is negligible. Because in Imp, the values are extremely close to each other, and the current of the uncooled panel occasionally surpasses the current

of the cooled panel, resulting in a higher output power and improved efficiency. As shown in Figures 4.44 and 4.45, temperature affects both Imp and Vmp, although the effect of high temperature on Vmp appears to be greater than it is in Imp.
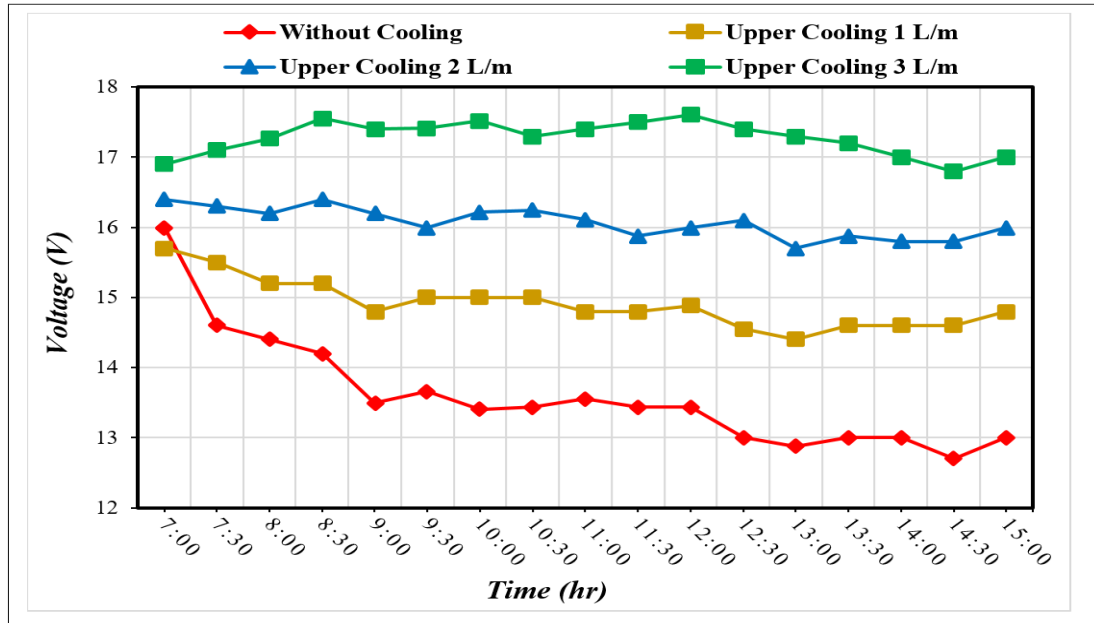

Figure 4.42. Effect of upper cooling on the voltage of the PV panel at flows of 1-3 L/m.
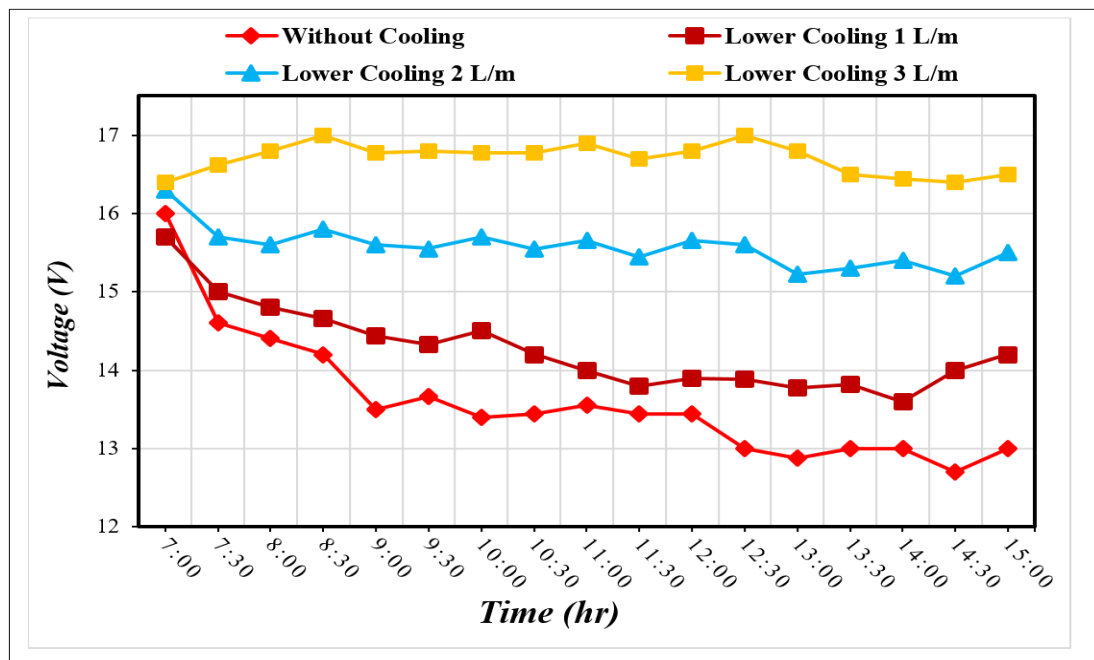

Figure 4.43. Effect of lower cooling on the voltage of the PV panel at flows of 1-3 L/m.
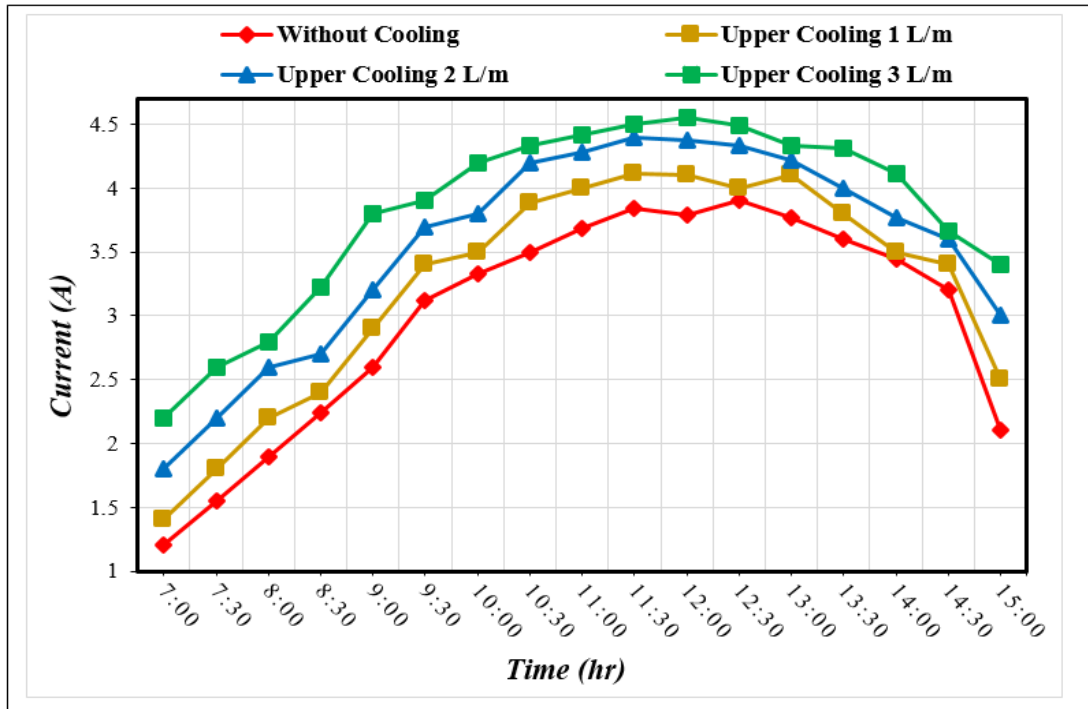
Figure 4.44. Effect of upper cooling on the current of the PV panel at flows of 1-3 L/m.

50
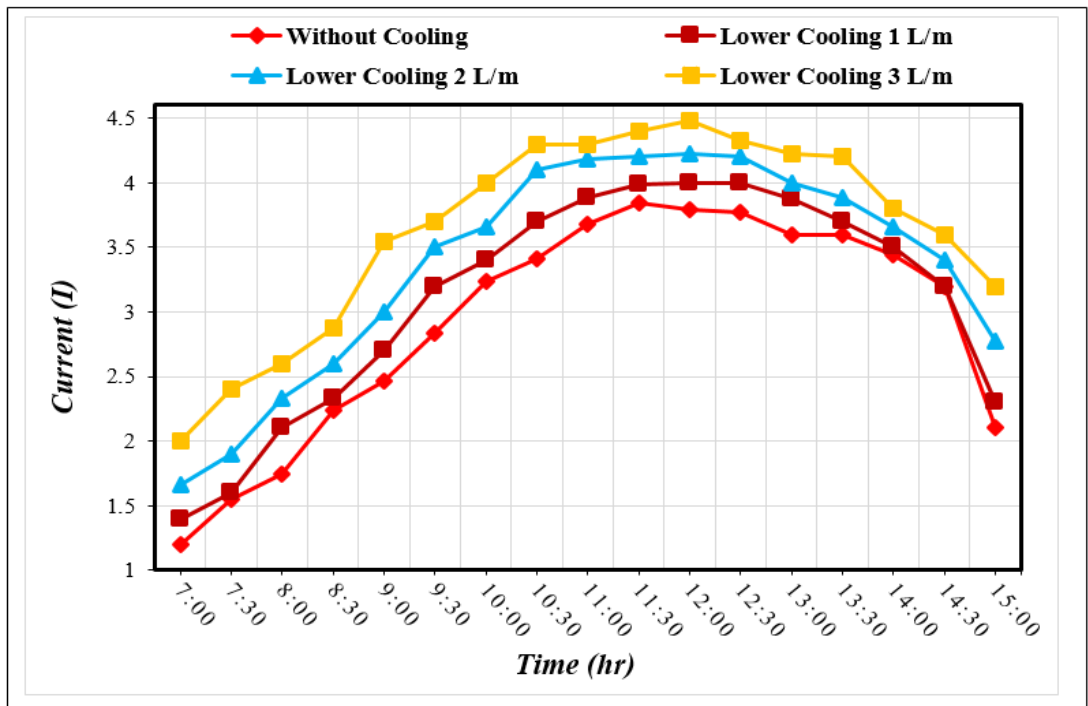
Figure 4.45. Effect of lower cooling on the current of the PV panel at flows of 1-3 L/m.

4.4.3. Power of the Photovoltaic Panel (Pmax)

The net result is that maximum power is increasing in this magnitude of the power equation (Pmax=Imp*Vmp). During the daily test, the temperature of the photovoltaic panel rose in lockstep with the ambient temperature in all cases, resulting in a decrease in both the panel's voltage and a small increase in the value of the current, which resulted in a decrease in the power of the panel in the absence of cooling. However, the cooled panel with an upper or lower technique has a variable flow rate credited with a clear enhancement in the power of the PV module. The working water mass flow rate of 3 L/m provides superior cooling for the photovoltaic panels compared to other mass flow rates. At 12.00 PM, the average power generated by the panel at this flow became 80.08 W, in spite of the fact that the maximum radiation was 888 W/m^2 and the power of the panel in the state without cooling was 50.93 W.

Similarly, for the lower cooling, the panel power at flow of 1 L/m was 55.6 W, but due to the increased cooling of the lower panel, at flow 3 L/m it became 75.26 W, as shown in Figures 4.46 and 4.47. Applying all water spray rates, which are progressively increasing from 1-3 L/m, and obtaining considerable dissipation of surface heat, increases the power of the photovoltaic module. When integrating all the upper and lower water flow scenarios with the uncooled panel, it becomes clear that the upper cooling method saves the most energy for the PV panel, particularly at a flow rate of 3 L/m at 12:00 PM, due to thermal energy dissipation on the panel during this type of cooling. This indicates we got a 57.23% boost in power while using the upper cooling, but less than that when using the lower cooling, which got an increase of 47.77% at the same flow of 3 L/m.
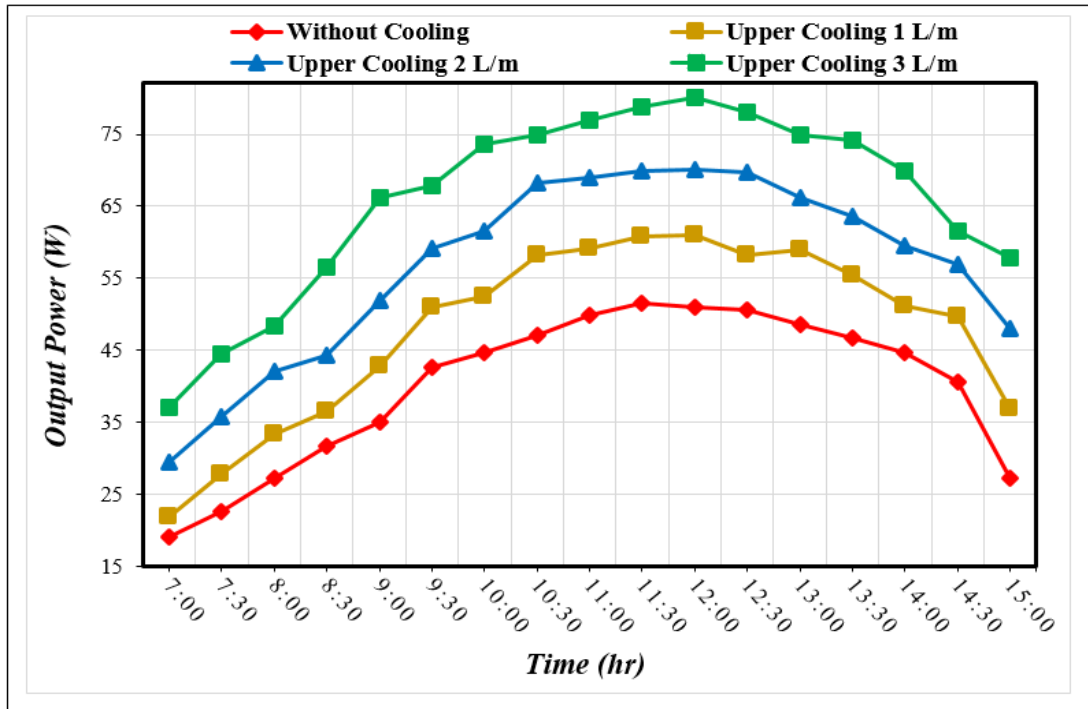
Figure 4.46. Effect of upper cooling on the output power at flows of 1-3 L/m.
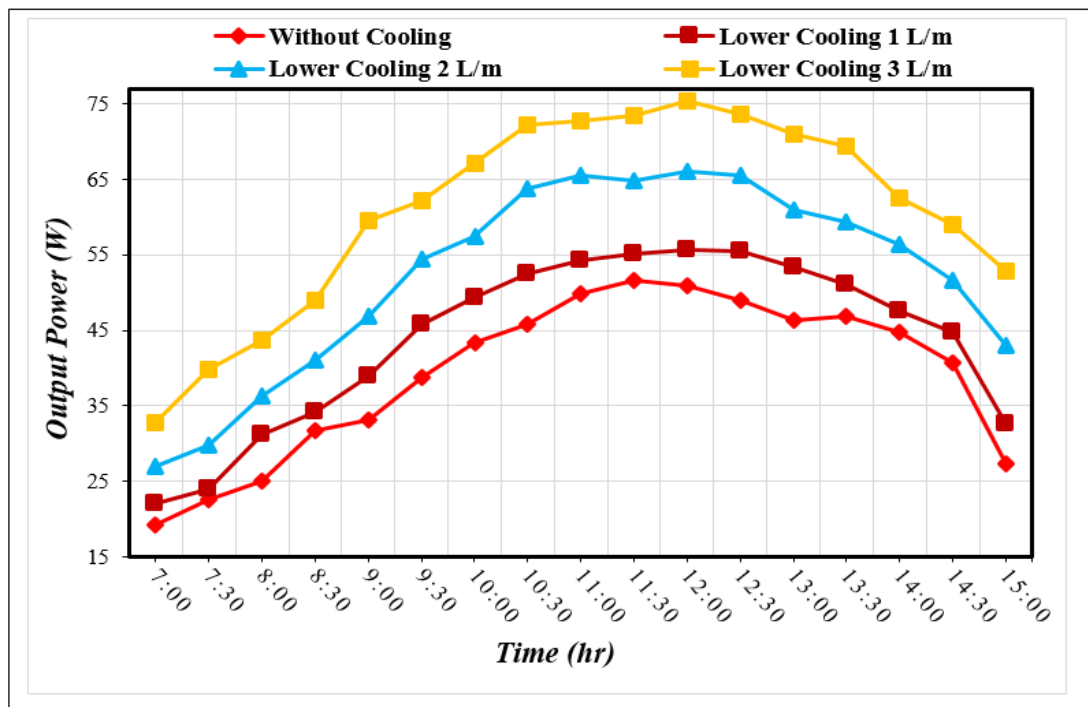
Figure 4.47. Effect of lower cooling on the output power at flows of 1-3L/m.

It was discovered that when cooling processes with improved parameters Imp and Vmp were compared to processes without cooling treatment, all performance had improved, resulting in higher maximum power generation because of lower PV panel temperature as well as a difference in flow rate through the water inlets. The effect of flow rate on the rate of power generated is shown in the Figure 4.48, and this is clear in the 3 L/m spray nozzle, which is the best in our present investigation. It is vital to clarify the influence of radiation on the rise in power created, since the highest power generated occurs when the maximum radiation rate increases during the day, as it did during the test, exactly at 12:00PM, as shown in Figure 4.49. Figure 4.50 demonstrates that the panel generates the most energy at the lowest surface heat, at a flow rate of 3L/m, when the panel power rises from 51 W to 80 W, offset by lowering the surface temperature from 58 ℃ to 41℃. According to the findings, overheating is a primary reason for solar panel energy loss.
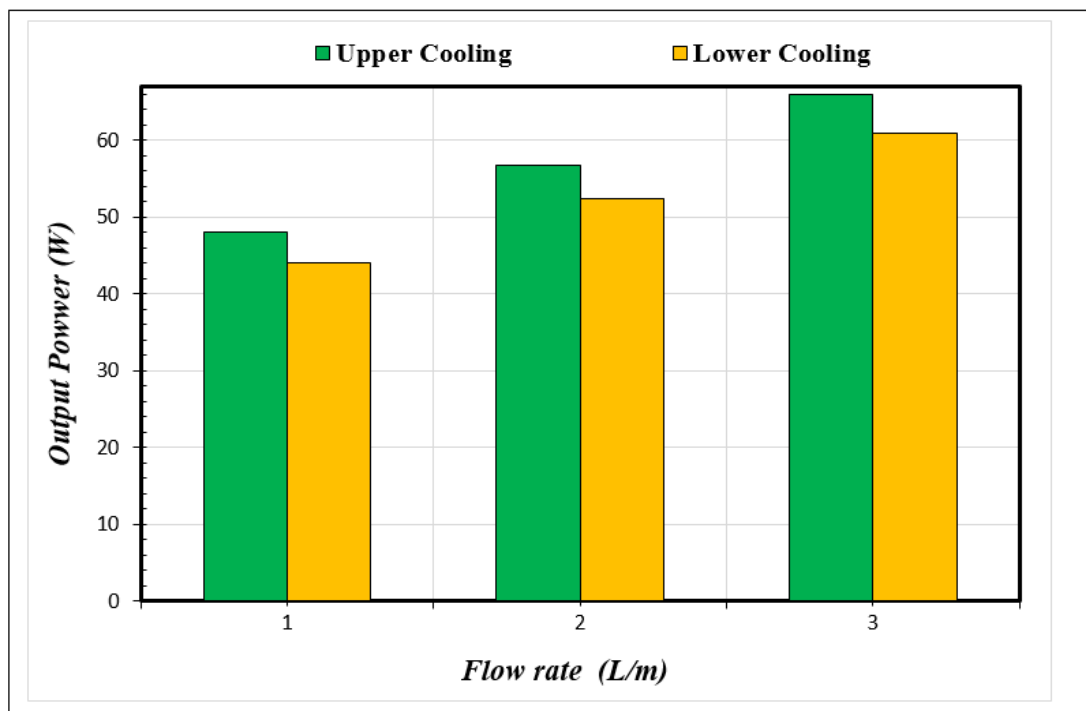
Figure 4.48. Effect of the flow rates on the output power.
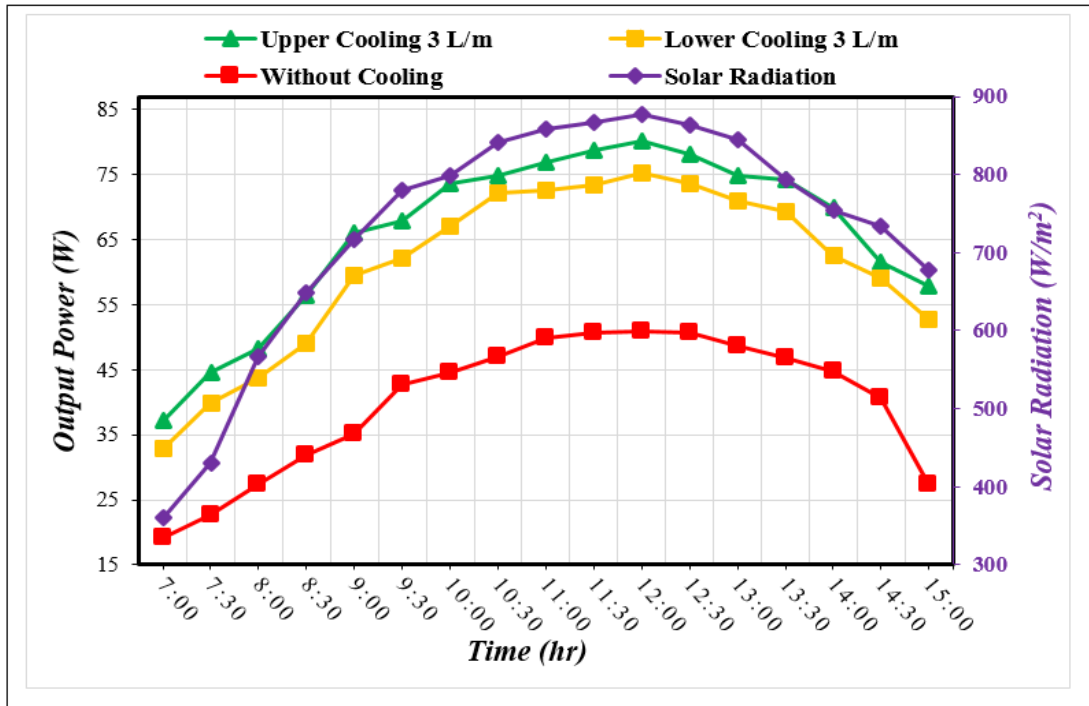
Figure 4.49. Effect of solar radiation and maximum flow on the output power of cooled and uncooled panels.
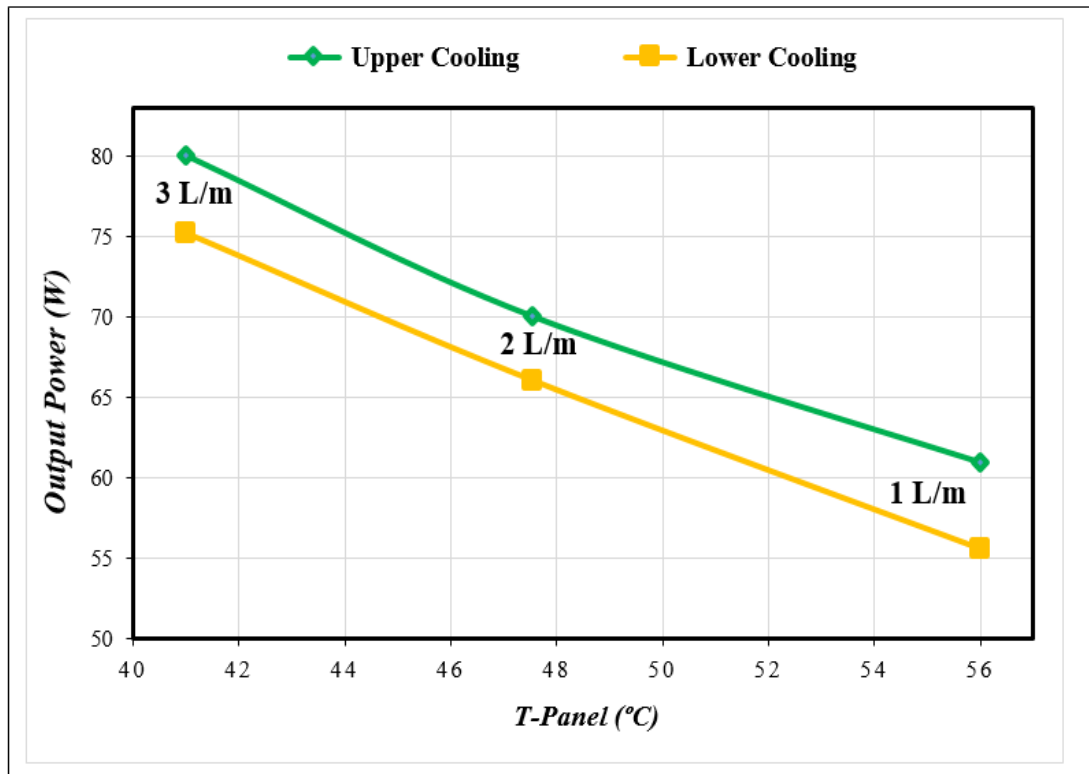
Figure 4.50. Effect of PV panel temperature on output power at flows of 1-3 L/m.

4.4.4. Effeciency of the Photovoltaic Panel

Since the factor of heat affects the factors of power and efficiency, improving performance under the cooling process, as happened in "Imp & Vmp", resulted in an increase in the energy output as compared to the uncooled panel. We previously achieved the highest optimization in power , which is a good sign for improving the electrical power of the PV panel in the context of cooling processes with various water flow rates. Figure 4.51 describes the benefit of upper and lower cooling techniques in raising the efficiency ratio of the photovoltaic panel. The electrical efficiency of the uncooled panel was 9.7%, but by the action of the upper spray at a flow rate of 1 L/m, a decrease in the heat of the panel was achieved, and the efficiency was raised to 11.52% by midday.

Logicaly, the higher the flow rate, the higher the efficiency, so the flow achieved at 2 L/m a significant improvement in efficiency by 13.17%, but the maximum efficiency improvement was at the flow rate 3 L/m by 14.3%.

The same strategy, in Figure 4.52, lower cooling at a flow rate of 3 L/m improved performance as well, albeit less than upper cooling due to rear panel heat. This flow mass provides good cooling for the panel which enhances the performance efficiency by 39.89% which is lower than the upper cooling efficiency by about 7.6% under the same conditions. The effect of varied spray rates on the electrical efficiency of the photovoltaic panel is shown in the bar chart, Figure 4.53 , where the best efficiency was attained at the highest flow rate of 3 L/m. The hypothesis of enhanced efficiency of a PV panel as the surface heat of the panel dissipates is supported by Figure 4.54. Although the efficiency of the uncooled panel was 9.7%, after dispersing heat with a maximum flow of 3 L/m, the efficiency climbed to 14.3%.

Figure 4.51. Effect of upper cooling on the enhancement efficiency.

Figure 4.52. Effect of lower cooling on the enhancement efficiency.
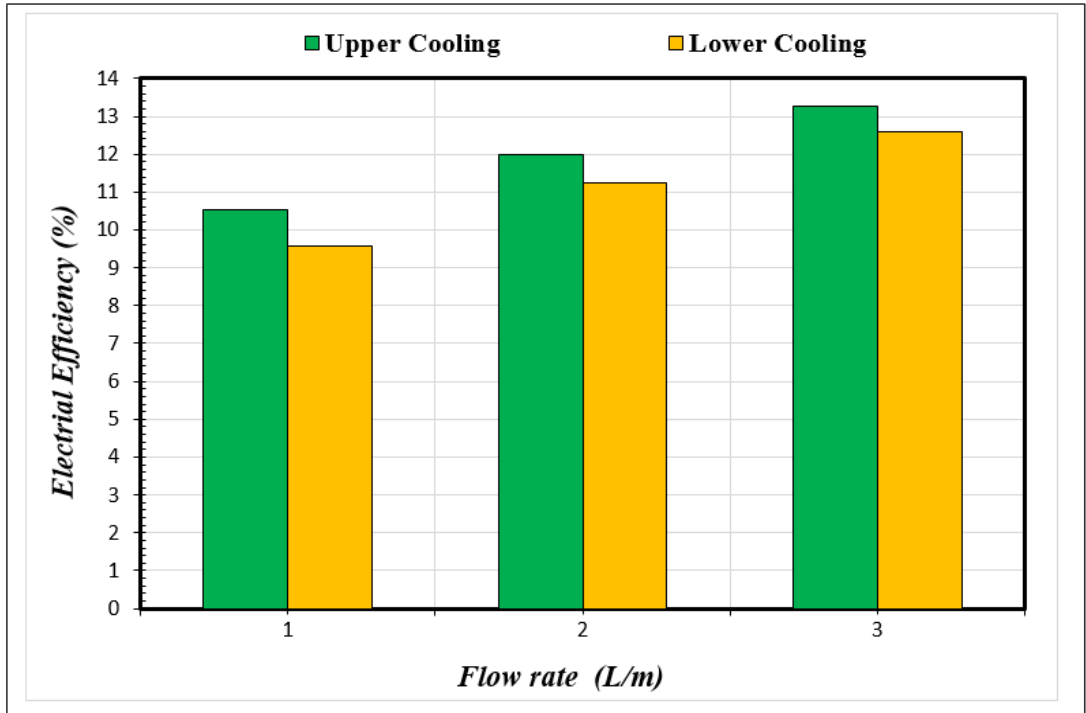
Figure 4.53. Effect of the flow rates on the efficiency.
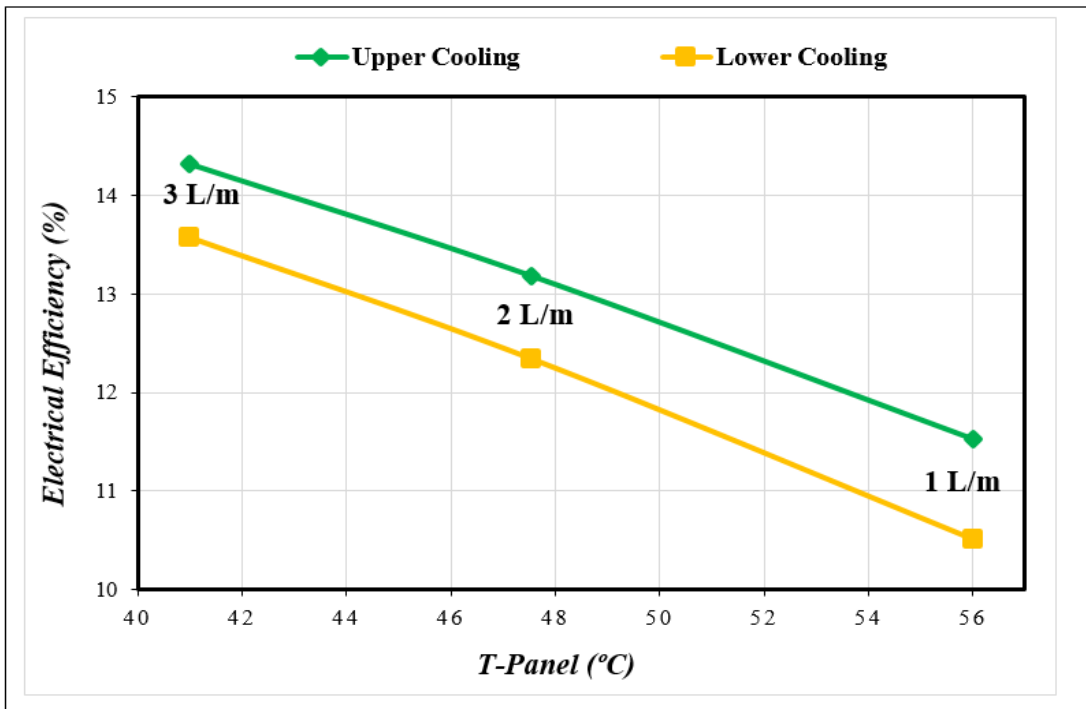
Figure 4.54. Effect of PV panel temperature on efficiency at flows of 1-3 L/m.

4.5. IMPACT OF USING WATER SPRAY NOZZLE TECHNIQUES ON THE PERFORMANCE OF PV PANELS

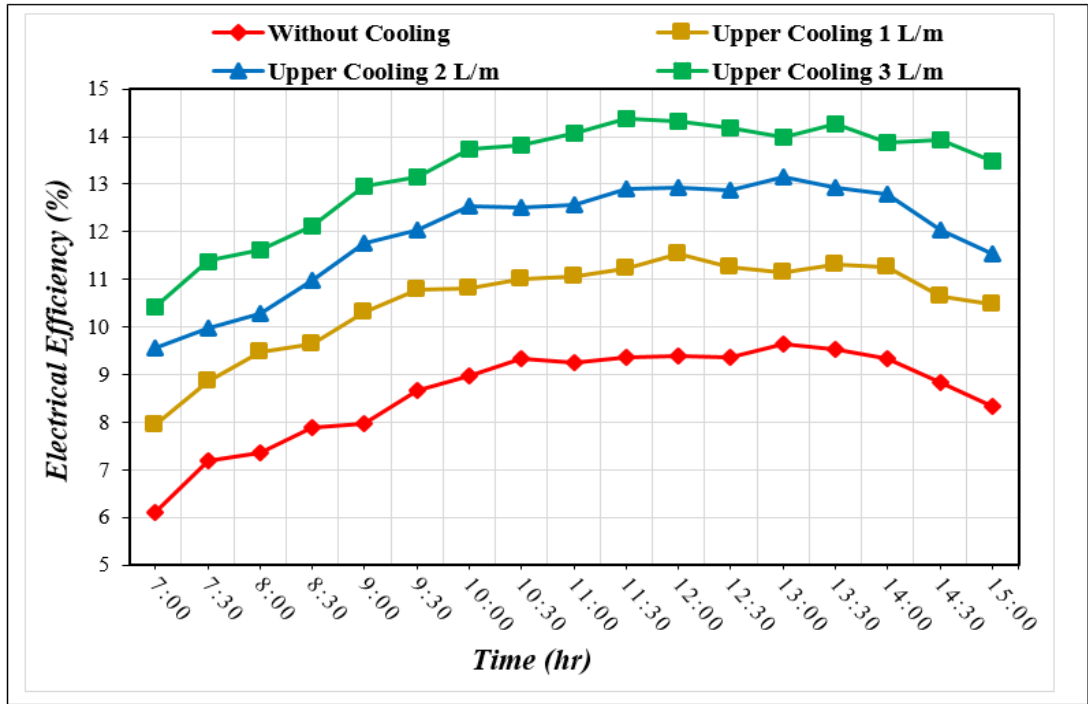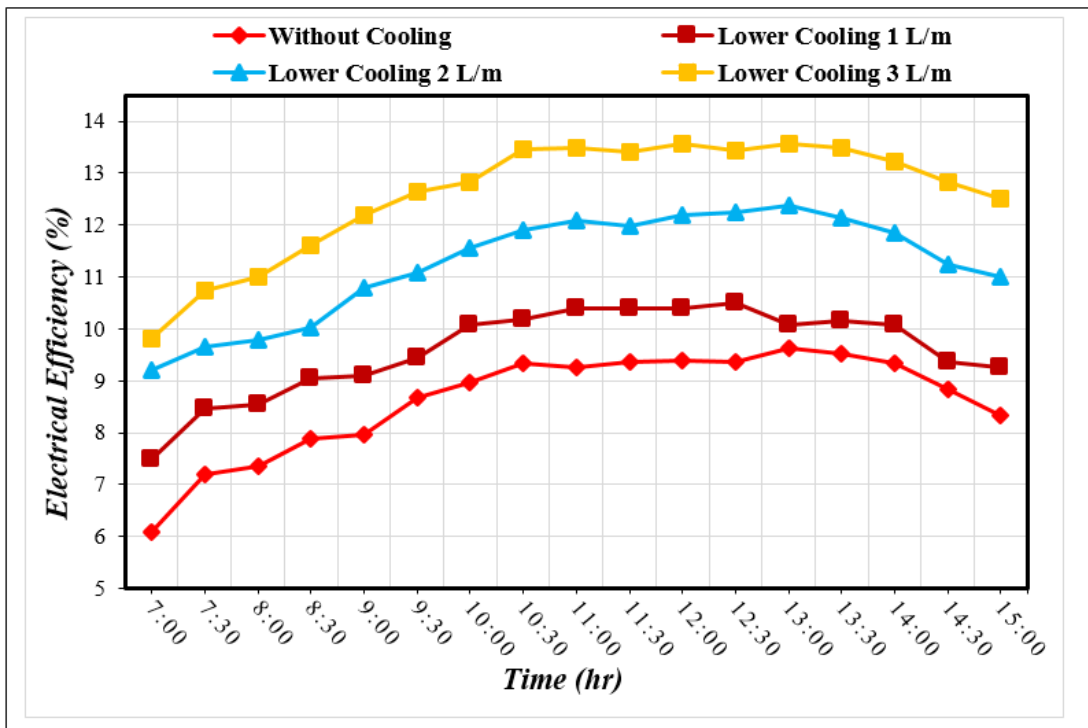Each case of the approach revealed the characteristics and importance of improving the efficiency and performance of solar panels, allowing us to compare the results of the panels without cooling with the data gained from the use of the two cooling systems. The final arithmetic findings generated from the mathematical relationships that were performed and reported in Annex (B3) are summarized in Table 4.2.

4.5.1. Upper Nozzle Cooling Technique

Table 4.2 lists and briefly describes the practical and quantitative results of the nozzle spraying of water on the surfaces of solar panels using cooling technology. Depending on the maximum values derived from the high ambient temperature and high levels of sunlight at 12:00 PM, the two cooling systems are used in extremely hot conditions, based on the heat of the front and rear surfaces of the uncooled panel, which reached 66 °C and 70 °C, respectively. According to the results, the surface heat of the front PV panel was halved when the upper cooling nozzles were used, with the Arduino recording 36 °C for the front surface and 42 °C for the back surface when the maximum flow was applied 3 L/m.

4.5.2. Lower Nozzle Cooling Technique

The results of the lower cooling water spray approach, which were dependent on daily atmospheric conditions, were also discussed and summarized in Table 4.2. The front surface temperature before cooling was 66 ºC, which was reduced to 44 ºC with the help of the lower nozzle, while the rear surface temperature, which reached 70 ºC, decreased to 40 ºC by the same amount as the flow 3 L/m. Because to the water flow nozzle 3 L/m and the lower surface temperature, it was able to achieve improve in the panel's power and efficiency, despite the fact that they were 50.93 W and 9.7%, respectively. The improvement in power as a consequence of the two cooling strategies was 47.52% and 57.23% for the upper and lower, respectively. In addition, the performance efficiency ratio improved by 47.52% and 39.89% respectively. In other words, the difference in performance between the two technologies was rated at 7.6%.

Table 4.2. Improving the performance of photovoltaic panels with the influence of varying water flow

System	Maximum Power output P (W)	Improvement in maximum power output Ṕ (%)	Maximum panel temperature reduction T_{PV} (°C)		Electrical Efficiency η (%)	Improvement in Electrical Efficiency ή (%)
			Front	Rear		
Without Cooling	50.93	——	66	70	9.70	——
Upper Cooling 1 L/m	61	19.77	51	56	11.52	18.76
Upper Cooling 2 L/m	70	37.60	45.2	47	13.17	35.77
Upper Cooling 3 L/m	80.08	57.23	36	40	14.31	47.52
Lower Cooling 1 L/m	55.6	9.16	54.6	52	10.50	8.24
Lower Cooling 2 L/m	66.08	29.74	49	45.5	12.34	27.21
Lower Cooling 3 L/m	75.26	47.77	41	37	13.57	39.89

With the existence of three types of flows, 1, 2, and 3 L/m, it is feasible to turn the data in Table 4.2 into a schematic design by Figures 4.55 and 4.56 to demonstrate the link between the nozzle "flow rate" and its influence on the percentage increase in power and efficiency. As a result, the optimum cooling solution for enhancing solar panel output and efficiency is the water jet spray nozzle top cooling system 3 L/m. Despite the ambient temperature 50 °C, considerable heat dissipation from the front and rear surfaces has happened. As a result, photovoltaic panels have a high efficiency rating. The economic feasibility of cooling the photovoltaic panel in the proposed study can be evaluated through two main advantages, which are: cleaning the surfaces and making use of draining water to irrigate crops in the summer due to the high percentage of drought seasonally.
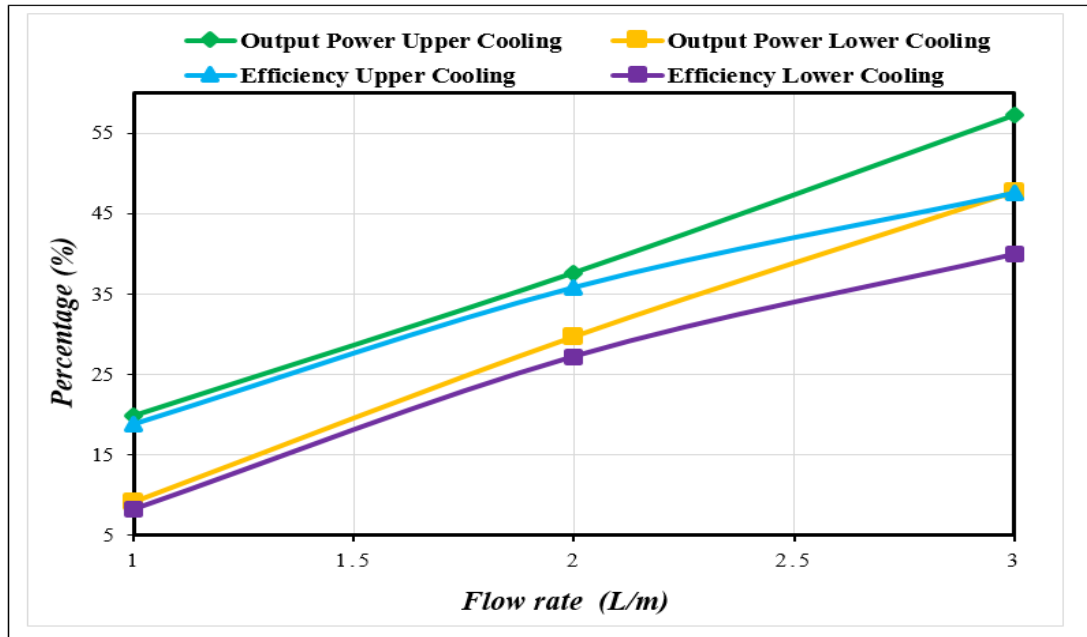
Figure 4.55. Impact of flows on the percentage increase in power and efficiency of the
PV panel.
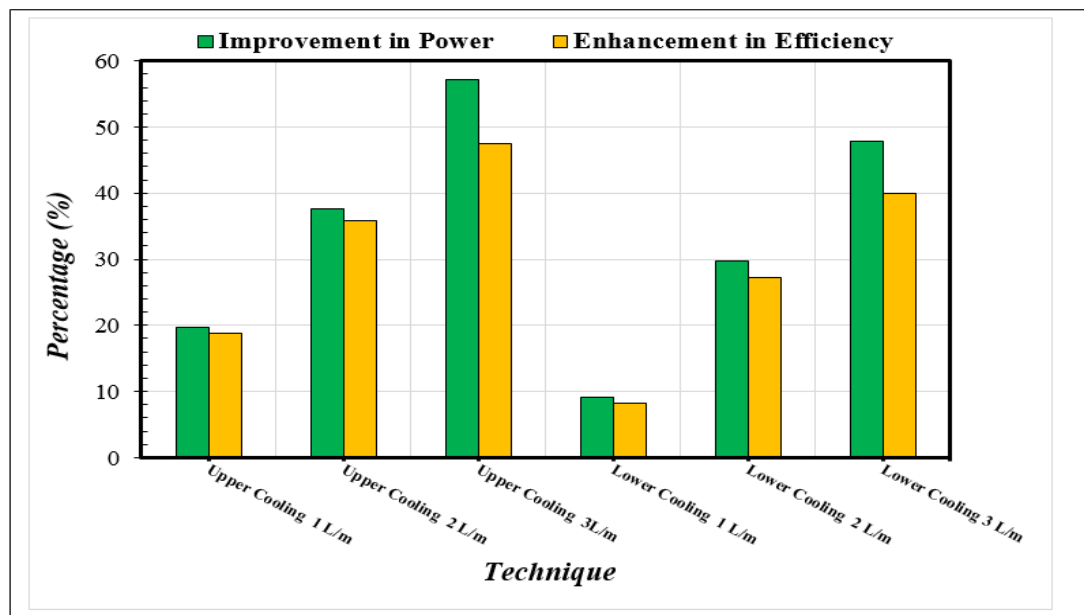
Figure 4.56. Performance comparison of the PV panels by applying cooling techniques

4.6. COMPARISON OF PRIOR WORKS

Sargunanathan et al. (2020), during the treatment of the panel at a flow rate of 1 L/m,
the temperature reduction on the front side was evident. Flooding a water nozzle on
the front roof. The reduction was 35.78%, indicating that our current test is the most

113

effective in terms of lowering temperature by the upper cooling of the front surface, which reached 46%. Despite the fact that evaporative water is exposed to ambient heat via the principle of convective heat transfer, the researcher admitted that upper cooling is one of the best techniques ever used. The power output of the upper panel increased during the test period, reaching 15.33%. Furthermore, the decrease in temperature caused by cooling led to an increase in efficiency of 16.89%. When compared to the results of our investigation, the rate of the efficiency of upper cooling increased by 18.76% [62].

Starting from the principle of improving the efficiency of solar panels, the researchers Ali Bagodaripur et al. (2020), devised a practical experiment that involved spraying non-potable water on the panel's upper side to lower its temperature. The panel's temperature was dropped to 20.19 ℃, resulting in a 5.5% increase in voltage. As a result, the panel's output power was enhanced by 14.5%, and the panel's efficiency was increased by 20% when compared to the spray less panel. The work was similar to our current study, but to varying degrees and close due to climatic variables, such as radiation ratio, wind speed, and ambient temperature, which differed from one country to the next. Aside from the panel's size and characteristics, the researcher concluded that the top nozzle spray approach is quite effective in boosting the photovoltaic panel's performance [63].

In a recent article, Amirhosein Hadipour et al. (2021), revealed his actual experience using three distinct spraying systems with water nozzles that overflowed on the upper photovoltaic panel's surface. The upper spray technique proved the most efficient of the three systems, as it improved the efficiency of the panel by lowering its temperature from 57 ℃ to 27.8 ℃ by applying a flow rate 2 L/m. The panel's highest electrical voltage is 17 V, which contributed to a maximum generated power of 72 W, and all of this contributed to the improved panel's efficiency of 12.1% when compared to the panel without cooling. The system's setup and practical outcomes are identical to our current work. At a radiation rate of 888 W/m^2, our panel reduced the temperature from 70 ℃ to 36 ℃, contributing to a 37.5% increase in the output of generated power, which was reflected in an increase in efficiency, which increased until it reached 13.17%, compared to 9.7% for the uncooled panel [64].

PART 5

CONCLUSION AND RECOMMENDATIONS

The efficiency of the photovoltaic unit deteriorates and its surfaces are damaged because of the high temperature it experiences during its operation, especially in hot climates. It became necessary to conduct a deep empirical investigation dedicated to proving the efficiency of using water spray as the operating fluid of the hybrid system (PV/T) to dissipate the heat of the surfaces up to the standard conditions of the panel (STC), which in turn is a power transformer in the proposed cooling system.

5.1. CONCLUSIONS OF THE EXPERIMENTAL WORK

We highlight the most important conclusions reached as a consequence of comparing the cooled and uncooled panels erected in the outdoor, as well as the effect of Iraq's extreme hot weather as a realistic case study, especially in August of 2021, to be part of the experience.

1. The operation of the PV module is mostly reliant on daily solar irradiation. For panel features to fulfill manufacturer's standards, temperature 25 °C and irradiance 1000 W/m^2 are required (STC). This appears implausible, given that the experiment took place in Iraqi airspace. The monocrystalline glass absorbed a large amount of dangerous incident radiation heat, raising the module temperature to (70 °C) and decreasing all panel parameters, including output power and efficiency. On the summer test days, the high ambient temperature of about (60 °C) made things worse.

2. For the aforementioned reasons, it became necessary to construct an integrated passive cooling and cleaning system (PV/T) that draws its water from an overhead tank that operates according to the theory of gravity. The system does

not consume energy because it does not use any pumps in the harsh climate with its high temperature, as well as its low cost and high performance.

3. The temperature of the uncooled front and rear surfaces of the PV panel was registered 66 °C and 70 °C respectively, and was significantly reduced, thanks to the diversity of the fluxes 1, 2, and 3 L/m. The water mass flow rate 3 L/m from the upper spray nozzles was found to be the most effective in lowering the temperature of the front and rear surfaces by 83.33% and 66.66%, respectively. We should also mention that the heat from the panels won out over the ambient temperature.

4. Despite the fact that the ambient temperature was at its greatest at 12:00 PM, the lower nozzle cooling approach was found to be effective in lowering heat levels. When the flow rate was at its highest, the percentage of temperature decrease for the front and rear surfaces was 50% and 75%, respectively, when compared to the reference panel.

5. When upper and lower cooling methods were used, evidence for thermal drop increased when infrared thermal imaging was applied. This pictorial technology was able to communicate data with values that were quite similar to those received from Arduino sensors during image analysis. This (IR) photo technology has been considered as a replacement for computational fluid dynamics (CFD) simulation and modeling.

6. The maximum power voltage (Vmp) of the panel is impacted by the rise in temperature, and there is no doubt that cooling improves it, especially when the nozzle reaches its maximum flow. As a result, the quantity of voltage has climbed to 17.6 V at upper cooling, although the reference panel recorded 13.44 V. Similarly, the voltage became 16.8 V at the reduced flow, with a tiny drop in current value that may be insignificant. The electrical properties improved significantly when the two cooling strategies were used. Consequently, the output power increased from 50.93 W to 80.08 W at upper cooling and to 75.26 W at lower cooling while spraying the upper and lower water. The two techniques improved the performance rate of the produced power by 57.23% and 47.77%, respectively, at upper and lower cooling.

7. Although the efficiency of the uncooled panel was 9.7%, after dissipating the heat with the maximum flow 3 L/m, the efficiency of the upper and lower cooling panels increased to 14.31% and 13.57%, respectively. Upper and lower cooling efficiency improvement percentage rates of 47.52% and 39.89% were achieved.

8. The upper nozzles were more effective in enhancing the performance of our current investigation than the lower nozzles. The results show a 9.4% difference in the value of power generated at the upper and lower cooling at maximum flow, and show a 7.6% difference in the improvement in efficiency performance between the two techniques.

9. Finally, the (PV/T) model developed in the current intensive study of the passive water nozzle cooling strategy in Iraq is a desirable solution to the problems of hyperthermia, both in terms of its thermal properties of dissipating a large amount of surface heat or its electrical properties of increasing the percentage of energy and improving performance efficiency.

In the same context, it may be economically viable to use the excess drain water from this technique to irrigate crops during the dry summer season, in addition to using hot water for home needs like bathing, cooking, and laundry. It is worth noting that the data gathered from our practical experience agrees with the majority of previous studies' conclusions and suggestions.

5.2. RECOMMENDATIONS AND SUGGESTIONS FOR FUTURE WORK

Despite the existing implemented system's efficiency, there is potential for more improvement by using the following ideas and recommendations as a guideline for advancing solar panels into a better reality.

1. The geometry of the nozzle design, including the degree of inclination and distance from the panel, as well as the number of nozzles, may be changed to optimize efficiency.

2. Improving performance may require mixing a Nano-material with water and spraying it through the nozzle to enhance the heat transfer characteristics of water.

3. Pumps may be used to push the water towards the nozzles and enhance the flow rate, making it an active system instead of being passive system.

4. The framework may be developed by installing any form of radiation tracking device to capture the dispersed energy.

5. We recommend that the experimental work be done indoor by a light source that simulates solar radiation and temperature in order to know the results of numerical modeling and display the behavior of characteristics in programs like (MATLAB) or others and compare them to the experimental work.

REFERENCES

1. Internet: Balasubramanian, A. "Basic energy resources", **https://www.researchgate.net/publication/310021419/**(2021).

2. Shah, S. A. A., Zhou, P., Walasai, G. D., & Mohsin, M., "Energy security and environmental sustainability index of South Asian countries: A composite index approach", *Ecological Indicators*, 10(6): 105-507 (2019).

3. Löf, G. O., Duffie, J. A., & Smith, C. O., "World distribution of solar radiation", *Solar Energy*, *10*(1): 27-37 (1966).

4. Austin, C., Borja, R. and Phillips, J., "Concentrating Solar Power for the Mediterranean Region", *Final Report, German Aerospace Center,* Germany, 21-23 (2005).

5. Al-Kayiem, H. H., & Mohammad, S. T., "Potential of renewable energy resources with an emphasis on solar power in Iraq: An outlook", *Resources*, *8*(1): 42 (2019).

6. Dupré, O., "Physics of the thermal behavior of photovoltaic devices to cite this version : HAL Id : tel-01368592 Physics of the thermal behavior of photovoltaic devices", *Doctoral dissertation, Lyon University,* France, 1–222 (2015).

7. Hamidreza, N. John, B. and Muhammad, A. R., "Evaluation of alternative cooling techniques for photovoltaic panels", *Master Thesis, The University of Alabama*, Albama, USA, 23-45 (2012).

8. Öztürk, H. H., "Güneş enerjisinden fotovoltaik yöntemle elektrik üretiminde güç dönüşüm verimi ve etkili etmenler", *Elektrik Tesisat Ulusal Kongre ve Sergisi Bildirileri*, 1(2): 1-14 (2017).

9. Teo, H. G., Lee, P. S. & Hawlader, M. N. A. "An active cooling system for photovoltaic modules," *Applied Energy*, 90(1): 309–315 (2012).

10. Palumbo, A. "Design and analysis of cooling methods for solar panels", *Doctorate Thesis, Youngstown State University,* USA, 12-45 (2013).

11. Azzouzi, G., "Study of silicon solar cells performances using the impurity photovoltaic effect", *Doctorate Thesis, Ferhat Abbas–Setif University,* Algeria, 23-45 (2014).

12. Dhass, A. D. Lakshmi, P. and Natarajan, E. "Investigation of performance parameters of different photovoltaic cell materials using the lambert-w function", *Energy Procedia*, 9(10): 66–573, 2016.

13. Nižetić, S., Grubišić- Čabo, F., Marinić-Kragić, I. and Papadopoulos, A. M., "Experimental and numerical investigation of a backside convective cooling mechanism on photovoltaic panels", *Energy*, 11(1): 211–225 (2016).

14. Skoplaki, E. & Palyvos, J. A. "On the temperature dependence of photovoltaic module electrical performance: A review of efficiency/power correlations," *Solar Energy*, 83(5): 614–624 (2009).

15. Dubey, S. & Tay, A. A. O. "The theoretical modelling and optimization of a 10 KWP photovoltaic thermal system for a student hostel in Singapore", *International Journal Green Energy*, 11(3): 225–239 (2014).

16. Chow, T. T., "A review on photovoltaic/thermal hybrid solar technology", *Applied Energy*, 87(2): 365–379 (2010).

17. Kandil, K. M., Altouq, M. S., Al-Asaad, A. M., Alshamari, L. M., Kadad, I. M. and Ghoneim, A. A. "Investigation of the performance of cis photovoltaic modules under different environmental conditions", *Smart Grid Renewable Energy*, 2(4): 375–387 (2011).

18. Kaldellis, J. K., Kapsali, M. and Kavadias, K. A. ,"Temperature and wind speed impact on the efficiency of PV installations. Experience obtained from outdoor measurements in Greece", *Renewable Energy*, 6(6): 612–624 (2014).

19. Aish, Q. M., "Temperature effect on photovoltaic modules power drop", *Al-Khwarizmi Engineering Journal*, **11** (2): 62–73 (2015).

20. Zaini, N. H., Ab Kadir, M. Z., Izadi, M., Ahmad, N. I. Radzi, M. A. M. and Azis, N., "The effect of temperature on a mono-crystalline solar PV panel", *IEEE Conference Energy Conversion,* 2(11): 249–253 (2015).

21. Thong, L. W. Murugan, S. Ng, P. K. and Sun, C. C., "Analysis of photovoltaic panel temperature effects on its efficiency", *System*, 18(19): 450-455 (2016).

22. Gedik, E., "Experimental Investigation of Module Temperature Effect on Photovoltaic Panels Efficiency", *Journal of Polytechnic*, 19(4): 569–576 (2016).

23. Pradhan, A. and Panda, B., "Experimental analysis of factors affecting the power output of the PV module", *International Journal of Electrical and Computer Engineering,* 7(6): 3190–3197 (2017).

24. Kumar, T. A., Murthy, C. S. N. and Mangalpady, A., "Performance analysis of PV panel under varying surface temperature", *MATEC Web Conference,* 14(4):1-8 (2018).

25. Khelfaoui, N. Djafour, A., Bouali, K., Danoune, M. B., Gougui, A. and Boutelli, H. "Investigation of the Temperature Effect on the Electrical Parameters of a Photovoltaic Module at Ouargla City", *International Journal of Emerging Electric Power Systems*, 20 (4): 1-14 (2019).

26. Ogbulezie, J. C. Njok, A. O. Panjwani, M. K. and Panjwani, S. K. "The impact of high temperature and irradiance source on the efficiency of polycrystalline photovoltaic panel in a controlled environment", *International Journal of Electrical and Computer Engineering*, 10(4): 3942–3947 (2020).

27. Amar, S. Bahich, M. Bentahar, Y., Afifi, M. and Barj, E., "A Study of the Temperature Influence on Different Parameters of Mono-Crystalline Silicon Photovoltaic Module", *Journal Power Energy Engering*, 9(6): 29-42 (2021).

28. Alsayah, A. M. Aboaltabooq, M. H. K. Majeed, M. H. and Bassam Abed, B. A. S., "CFD study to improve PV cell performance by forced air: Modern design", *Periodicals of Engineering and Natural Sciences*, 7 (3): 1468–1477 (2019).

29. Radziemska, E.. "The effect of temperature on the power drop in crystalline silicon solar cells", *Renewable Energy*, 28(1): 1-12 (2003).

30. Kaiser, A. S., Zamora, B., Mazón, R. García, J. R. and Vera, F., "Experimental study of cooling BIPV modules by forced convection in the air channel", *Applied Energy*, 13(5): 88–97 (2014).

31. Habiballahi, M. Ameri, M., and Mansouri, S. H., "Efficiency Improvement of Photovoltaic Water Pumping Systems by Means of Water Flow Beneath Photovoltaic Cells Surface", *Journal of Solar Energy Engineering*, 137(4): 1-8 (2015).

32. Nižetić, S., Yadav, D., Čoko, A. and Grubišić-Čabo, F., "Water spray cooling technique applied on a photovoltaic panel: The performance response", *Energy Convers,* 10(8): 287–296 (2016).

33. Keron, A. S., Sikder, A. B., Zerin, D. A., & Salam, D. B., "Fabrication and Experimental Analysis of Solar Panel Water Cooling System", *In International Conference on Mechanical Engineering and Renewable Energy,* Indonesia, 12-17 (2018).

34. Hussein, H. A., Numan, A. H. and Abdulrahman, R. A., "Improving the hybrid photovoltaic/thermal system performance using water-cooling technique and Zn-H2O nanofluid", *International Journal Photoenergy*, 20(17): 123-234 (2017).

35. Ömeroğlu, G., "CFD analysis and electrical efficiency improvement of a hybrid PV/T panel cooled by forced air circulation", *International Journal Photoenergy*, 20(18): 323-421 (2018).

36. Ahmad, N., Khandakar, A., El-Tayeb, A., Benhmed, K., Iqbal, A. and Touati, F., "Novel design for thermal management of PV cells in harsh environmental conditions", *Energies*, 11(11): 34-67 (2018).

37. Osma-Pinto, G. and Ordóñez-Plata, G., "Measuring the effect of forced irrigation on the front surface of PV panels for warm tropical conditions", *Energy Reports*, 5(2): 501–514 (2019).

38. Muslim, N. H., Ghadhban, S. A. and Hilal, K. H., "Enhancement of Solar Photovoltaic Module Performance by Using a Water-cooling Chamber for Climatic Conditions of Iraq", *International Journal of Renewable Energy Research* 10(3): 543-578 (2020).

39. Arifin, Z., Tjahjana, D. D., Hadi, S., Rachmanto, R. A., Setyohandoko, G., and Sutanto, B., "Numerical and experimental investigation of air cooling for photovoltaic panels using aluminum heat sinks", *International Journal Photoenergy*, 2(20): 342-367(2020).

40. Kadhim, A. M. and Aljubury, I. M. A., "Experimental evaluation of evaporative cooling for enhancing photovoltaic panels efficiency using underground water", *Journal of Engineering*, 26(8): 14-33 (2020).

41. Benato, A., Stoppato, A ., De Vanna, F. and Schiro, F., "Spraying cooling system for pv modules: Experimental measurements for temperature trends assessment and system design feasibility", *Designs*, 5(2): 654-678 (2021).

42. Jafari, R., "Optimization and energy analysis of a novel geothermal heat exchanger for photovoltaic panel cooling", *Solar Energy*, 22(6): 122-133 (2021).

43. Laseinde, O. T. and Ramere, M. D., "Efficiency Improvement in polycrystalline solar panel using thermal control water spraying cooling", *Procedia Computer Science*, 1(80): 239-248 (2021).

44. Gomaa, M. R., Ahmed, M. and Rezk, H., "Temperature distribution modeling of PV and cooling water PV/T collectors through thin and thick cooling cross-fined channel box", *Energy Reports*, 8(2): 1144-1153 (2022).

45. Kalaiselvan, S., Karthikeyan, V., Rajesh, G., Sethu Kumaran, A., Ramkiran, B., and Neelamegam, P., "Solar PV Active and Passive Cooling Technologies-A Review," *7th IEEE International Conference Computing Power, Energy, Inf. Commun.,* India, 166-169 (2018).

46. Stropnik, R. and Stritih, U., "Increasing the efficiency of PV panel with the use of PCM", *Renewable Energy*, 9(7): 671-679 (2016).

47. Mittelman, G., Alshare, A. and Davidson, J. H., "A model and heat transfer correlation for rooftop integrated photovoltaics with a passive air cooling channel", *Solar Energy*, 83(8): 1150–1160 (2009).

48. Cuce, E., Bali, T. and Sekucoglu, S. A., "Effects of passive cooling on performance of silicon photovoltaic cells", *International Journal of Low-Carbon Technologies,* 6(4): 299-308 (2011).

49. Chandrasekar, M. Suresh, S., Senthilkumar, T. and Ganesh Karthikeyan, M., "Passive cooling of standalone flat PV module with cotton wick structures", *Energy Conversion and Management*, 7(1): 43–50 (2013).

50. Abdulgafar, S. A., Omar, O. S., and Yousif, K. M., "Improving the efficiency of polycrystalline solar panel via water immersion method", *International Journal of Innovative Research in Science, Engineering and Technology*, 32(97): 8127-8132 (2007).

51. Mehrotra, S., Rawat, P., Debbarma, M. and Sudhakar, K., "Performance of a solar panel with water immersion cooling technique", *International Journal of Science, Environment and Technology*, 3(3): 1161-1172 (2014).

52. Chandrasekar, M. and Senthilkumar, T., "Experimental demonstration of enhanced solar energy utilization in flat PV (photovoltaic) modules cooled by heat spreaders in conjunction with cotton wick structures", *Energy*, 9(10): 1401-1410 (2015).

53. Elnozahy, A., Rahman, A. K. A., Ali, A. H. H., Abdel-Salam, M. and Ookawara, S., "Performance of a PV module integrated with standalone building in hot arid areas as enhanced by surface cooling and cleaning", *Energy Buildings*, 8(8): 100-109 (2015).

54. Grubišić-Čabo, F., Nižetić, S., Čoko, D., Marinić Kragić, I. and Papadopoulos, A., "Experimental investigation of the passive cooled free-standing photovoltaic panel with fixed aluminum fins on the backside surface", *Journal of Cleaner Production*, 17(6): 119–129 (2018).

55. Fakouriyan, S., Saboohi, Y. and Fathi, A., "Experimental analysis of a cooling system effect on photovoltaic panels' efficiency and its preheating water production", *Renewable. Energy*, 3(2):1362-1368 (2019).

56. Lubon *et al.*, "Assessing the impact of water cooling on PV modules efficiency", *Energies*, 13 (10): 421-567 (2020).

57. Wongwuttanasatian, T. Sarikarin, T. and Suksri, A., "Performance enhancement of a photovoltaic module by passive cooling using phase change material in a finned container heat sink", *Solar Energy*, 19(5): 47-53 (2020).

58. Chaichan, M. T. and Kazem, H. A., "Environmental conditions and its effect on PV performance", *In Generating Electricity Using Photovoltaic Solar Plants In Iraq, Springer*, 4(5): 83–129 (2018).

59. Internet: "PV Education", **http://pveducation.org/** (2021)

60. Krauter, S., "Increased electrical yield via water flow over the front of photovoltaic panels", *Solar Energy Materials and Solar Cells*, 82(2): 131-137 (2004).

61. Yuva Raju Anand, M. R. and Rudramoorthy, R., "Simulation and Analysis of Thermal Efficiency improvement of Solar PV module by Spectral Absorption using Water", *International Conference on Power and Energy Systems*, Singapore, 34-55 (2012).

62. Sargunanathan, S., Ramanathan, K., Mohideen, S. T. and Suresh, S., "Enhancing

the Performance of the Standalone Rooftop SPV Module during Peak Solar Irradiance and Ambient Temperature by the Active Cooling of the Rear Surface with Spraying Water and the Front Surface with Overflowing Water", *International Journal of Photo Energy,* 2(6): 463-488 (2020).

63. Pagodaripour, A., Ghasemkhani, A., Ghazizade-Ahsaee, H. and Namjo, A., "The assessment and experimental study of photovoltaics panel by spraying water (case study: Kerman, Iran)", *Energy Equipment and Systems,* 8(4): 389-399 (2020).

64. Hadipour, A., Zargarabadi, M. and Rashidi, S., "An efficient pulsed- spray water cooling system for photovoltaic panels: Experimental study and cost analysis", *Renewable Energy***,** 16(4): 867–875 (2021).

65. Kasaeian, A., Khanjari, Y., Golzari, S., Mahian, O. and Wongwises, S., "Effects of forced convection on the performance of a photovoltaic thermal system: An experimental study", *Experimental Thermal and Fluid Science,* 8(5): 13-21 (2017).

66. Haidar, Z. A., Orfi, J. and Kaneesamkandi, Z,. "Experimental investigation of evaporative cooling for enhancing photovoltaic panels efficiency", *Results in Physics***,** 1(1): 690–697 (2018).

67. Moharram, K. A., Abd-Elhady, M. S., Kandil, H. A. and El-Sherif, H. "Enhancing the performance of photovoltaic panels by water cooling", *Ain Shams Engineering Journal***,** 4(4): 869-877 (2013).

APPENDIX A.

FEATURES AND SPECIFICATIONS OF THE GADGETS

A1. SOLAR POWER METER

- Model: CEM DT-1307 Digital Solar meter
- Range: 1999W/m^2, 634 BTU/ (ft^2 * h)
- Resolution: 1W/m^2, 1BTU/ (ft^2 * h).
- Relative humidity: 5ºC to - 40ºC, = < 80%
- Time for sampling: approx. 0.25 second.
- Battery: three AAA
- Display: 3-1/2 digits LCD with maximum reading 1999W/m^2.
- Accuracy: typically, within ±10W/m^2 [±3BTU/ (ft^2 * h)] or ±5%
- Dimensions (L* W *D): 162mm x 63mm x 28mm
- Weight (including battery): about 250g

Figure Appendix 1. Solar Power meter.

A2. WIND SPEED METER (ANEMOMETER)

- Model: PM6252A Digital Anemometer
- Material: ABS+ TPE
- Battery: 1*9V 6F22 battery
- Resolution: 0.01m/s
- Wind Humidity Range: 0-100% R
- Wind Temperature Range: -20 to 60 ºC

- Wind Speed Unit: m/s, ft/s, ft/m, km/h, mil/h, Knots
- Dimensions: 17*8.6*3.9cm /6.68*3.38*1.53inch (L*W*H)
- Weight: 293g/10.34oz

Figure Appendix 2. Wind Speed meter.

A3. FLOW METER

- Model: Z-3001 (0.2-2GPM or 0.5-8 LPM)
- Material: housing (Body) is made of ABS
- Fittings: 1/2" FIP thread size.
- Temperature: limit 4-80 ºC
- Pressure: ≤ 6 Bar
- Fluid: water 1/2" MIP external thread.
- Reading: a floating ball in a plastic rod and numerical level mark.

Figure Appendix 3. Flow Meter.

A4. SOLAR PANEL MULTI METER

- Model: elejoy WS400 A
- Material: ABS
- Power: 0.1~400 W
- Voltage: 12~60 V
- Current: 0~20 A
- Power supply mode: solar panel power supply
- Dimensions: 165 * 80 * 30mm / 6.5 * 3.1 * 1.2in
- Weight: 436g / 1.0lb
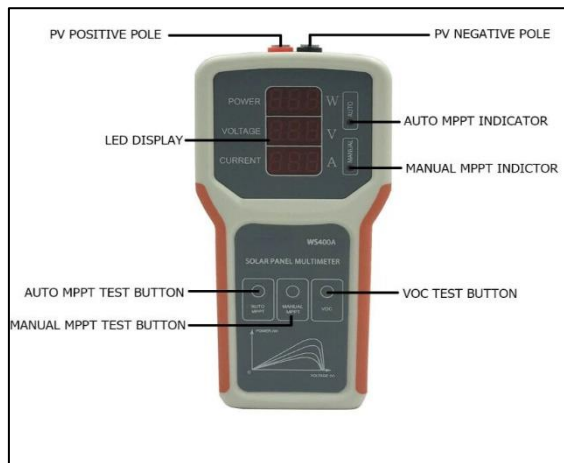
Figure Appendix 4. Solar Panel Multi meter.

A5. IR THERMOMETER IMAGE

- Model: Fluke VT04 visual IR thermometer
- Battery life: Eight (8) hours / weight: < 300 g (10.5 oz.).
- Focus options: NEAR < 23 cm; FAR > 23 cm
- Temperature measurement accuracy: ± 2 °C or ± 2%
- Dimensions: 8.3* 3*2.2 in
- Temperature measurement range: -10 °C to +250°C (14 °F to 482 °F)
- Storage medium: (micro SD card) up to 10000 images per GB
- images (BMP, DIB, GIF, SPE, FIF, SPEG, JPG and PNG)

Figure Appendix 5. IR Thermometer

A6. DIGITAL MULTI METER

- Model: TOLSEN 38031 IEC-61010 CAT III 300 V
- Display: 3-1/2 digits LCD, Maximum 1999
- Voltage DC: 200 m/2/20/200/300 V
- Voltage AC: 2/20/200/300 V
- Current DC: 200 μ/2m/20m/200m/10 A
- Current AC: 2 m/20m/200m/10 A
- Resistance: 200/2k/20k/200k/2M/20M Ω
- Battery Check: 1.5V, 9 V Diode Check
- Battery: 6F22 (9 V) included

Figure Appendix 6. Digital Multi Meter

A7. ARDUINO MEGA 2560

- Microcontroller: mega2560
- Operating Voltage: 5 V
- Analog Input Pins: 16
- DC Current per I/O Pin: 40 m A
- DC Current for 3.3V Pin: 50 m A
- S RAM: 8 KB
- EEPROM: 4 KB
- Clock Speed: 16 MHz
- Flash Memory: 256 KB of which 8 KB used by bootloader
- Digital I/O Pins: 54 (of which 14 provide PWM output)
- Weight: 37g
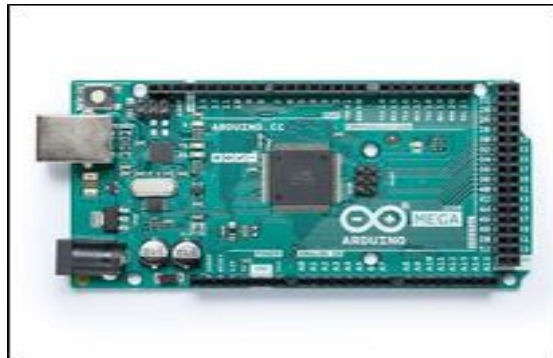
Figure Appendix 7. Arduino Mega 2560.
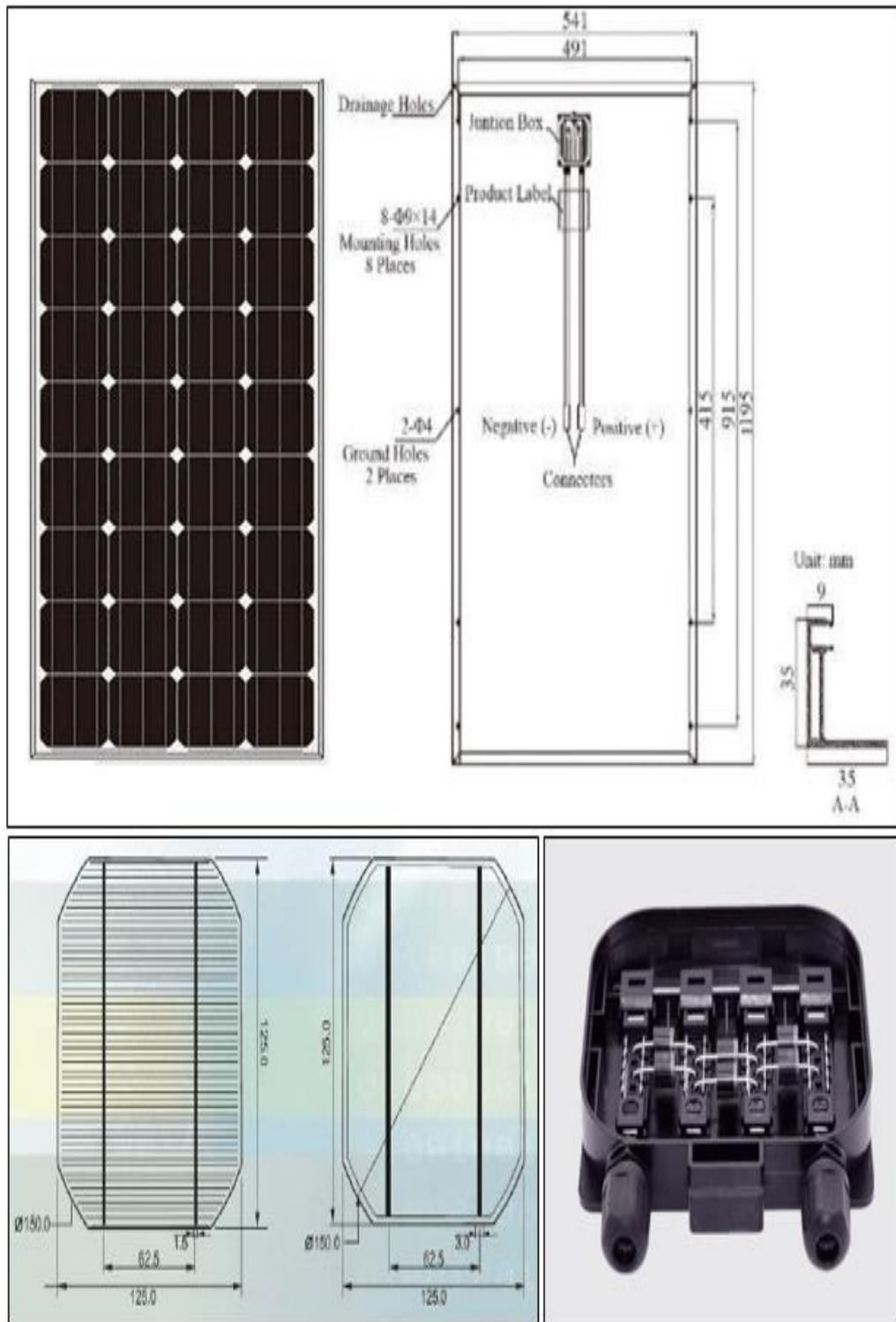
Figure Appendix 8. Photovoltaic panel specifications, dimensions and Fittings used in our study.

APPENDIX B.

MATHEMATICAL EQUATIONS AND CALCULATIONS

This appendix discusses the electrical performance of a basic single-diode mono-crystalline photovoltaic (PV) panel, improvements in power and efficiency, and the nominal operating PV panel temperature (NOPPT).

B1. PERFORMANCE OF PHOTOVOLTAIC (PV) SOLAR PANEL MODULES

The following is a basic formula for calculating the power generated by a photovoltaic PV module:

$$P = I \times V \tag{B.1}$$

Isc, Voc, Imp, and Vmp are the four most important parameters measured under reference conditions:

(Panel temperature (T) = 25 °C, and solar radiation (R) = 1000 W/m^2 and listed in the module's datasheet. The maximal power of the photovoltaic PV module with cooling is:

$$P_{wc} = I_m \times V_m \tag{B.2}$$

The following formula can be used to compute the increase in panel power obtained by the cooling system.

$$\acute{P}\,(\%) = (P_{wc} - P_{woc}) \times 100\%/P_{woc} \tag{B.3}$$

Whereas:

P_{wc}: Panel power with the cooling system.

P_{woc}: Panel power without the cooling system.

To convert light energy into electrical energy, efficient photovoltaic panels must be present [65].

$$\eta = P/(A \times R) \tag{B.4}$$

In addition, maximum cooling efficiency:

$$\eta_{wc} = P_{out}/P_{in} \tag{B.5}$$

Whereas:

A= Surface area of panel

R= Solar radiation

The increase in the panel's conversion efficiency with the cooling system may be estimated as follows [66].

$$\acute{\eta}(\%) = (\eta_{wc} - \eta_{woc}) \times 100\%/\eta_{woc} \tag{B.6}$$

η_{wc}: Panel efficiency with a cooling system.

η_{woc}: Panel efficiency without a cooling system.

B2. Nominal Operating PV Panel Temperature (NOPPT)

Cooling the panels is required to maintain normal functioning at a temperature close to the PV panel's standard working temperature, which is determined using a mathematical formula based on the ambient temperature. This is known as the "nominal operating temperature calculation"[67].

$$NOPPT = 20°C + T_{rise} \tag{B.7}$$

T_{rise}: The ambient temperature at the sunrise 25 ⁰C.

B3. EXAMPLES OF CALCULATIONS

Calculations of case (upper cooling 1 L/m) in Table (4.1)

Table Appendix 1. Example calculations for the upper cooling state at flow 1L/m.

System	Maximal power output $[P_{wc}]$(W) according to Eq. (B.2)	Improvement in maximal power output $\acute{P}$(%) according to Eq. (B.3)	Electrical Efficiency (η_{wc} %) according to Eq. (B.5)	Improvement in Electrical Efficiency $\acute{\eta}$(%) according to Eq.(B.6)
Upper cooling 1L/m	Vm= 14.88V Im= 4.1A P_{wc}= 61W	P_{woc}= 50.93W P_{wc}= 61W $\acute{P}$ = 19.77	P_{wc}= 61W R= 840W/m^2 A= 0.63m^2 η_{wc}=11.52	η_{woc}= 9.7 η_{wc}= 11.52 $\acute{\eta}$ = 18.76

Table Appendix 2. Example calculations for the lower cooling state at flow 1L/m.

System	Maximal power output $[P_{wc}]$(W) according to Eq. (B.2)	Improvement in maximal power output $\acute{P}$(%) according to Eq. (B.3)	Electrical Efficiency (η_{wc} %) according to Eq. (B.5)	Improvement in Electrical Efficiency $\acute{\eta}$(%) according to Eq.(B.6)
Lower cooling 1L/m	Vm= 13.9V Im= 4A P_{wc}= 55.6W	P_{woc}= 50.93W P_{wc}= 55.6W $\acute{P}$ = 9.16	P_{wc}= 55.6W R= 840W/m^2 A= 0.63m^2 η_{wc}=10.50	η_{woc}= 9.7 η_{wc}= 10.50 $\acute{\eta}$ = 8.24

APPENDIX C.

CERTIFICATES

C1. CO-SUPERVISOR'S APPROVAL

Date and Number of Documents: 03.01.2022 - E.93973

REPUBLIC OF TURKEY
KARABUK UNIVERSITY RECTORATE
Graduate Education Institute Directorate

Ref. : E-27105693-302.10.01-93973   03.01.2022
Subject : About AHMED KADHIM
MOHAMMED AL-MAMOORI's
Co-Supervisor

TO WHOM IT MAY CONCERN

Dr. Abdulrahman Th. Mohammad AL ZUHAYRI (Irak- Middle Techinical University Department Mechanical Engineering) has been appointed as a co-supervisor of MSc student AHMED KADHIM MOHAMMED AL-MAMOORI registered in Mechanical Engineering Department of Institute of Graduate Programs for his MSc thesis entitled "An Experimental and Numerical Analysis of High Temperatures Effect on Photovoltaic Cells (PV) Performance: A Case Study of Iraq" under the Supervision of Dr. Mehmet BAKIRCI.

Best regards.

Prof. Dr. İzzet AÇAR
Rektör a.
Vice Rector

This document is signed with secure e-signature.

Document Verification Link :
https://turkiye.gov.tr/ebd?eK=4043&eD=BSFKPHH5R5&eS=93973

Document Verification Code: BSFKPHH5R5
Adress: Demir Çelik Kampüsü Yüksekokullar Binasi Merkez/Karabük
Phone: (370) 418-9393   Fax: (370) 418-7241
e-Mail: iletisim@karabuk.edu.tr   Web Adress: http://www.karabuk.edu.tr
Kep Adress: karabukuniversitesi@hs01.kep.tr

Contact Person: Atakan OZTURK
Title: Tekniker

Figure Appendix 9. Co-Supervisor's approval.

136

C2. PUBLICATION ACCEPTANCE LETTER

Figure Appendix 10. Publication acceptance letter.

RESUME

Ahmed Kadhim Mohammed AL-MAMOORI was born in Diyala, where he attended primary, intermediate, and secondary schools, then enrolling in the College of Engineering/ University of Technology/ Electromechanical Engineering Department in 2001 and graduating in 2005. He worked in the energy field for several years. In 2020, he began his academic career as a graduate student at Karabük University's Institute of Higher Education to obtain a master's degree.